

April 1992 • NREL/TP-253-4279

Thermochemical Cycles for Energy Storage: Thermal Decomposition of ZnSO₄ Systems

Final Topical Report January 1, 1982 – December 31, 1984

W.E. Wentworth
University of Houston
Houston, Texas



National Renewable Energy Laboratory
1617 Cole Boulevard
Golden, Colorado 80401-3393
A national laboratory of the U.S. Department of Energy
Managed by Midwest Research Institute
for the U.S. Department of Energy
under contract No. DE-AC02-83CH10093

Thermochemical Cycles for Energy Storage: Thermal Decomposition of ZnSO₄ Systems

**Final Topical Report
January 1, 1982 – December 31, 1984**

W.E. Wentworth
*University of Houston
Houston, Texas*

NREL technical monitor: R. Gerald Nix



National Renewable Energy Laboratory
1617 Cole Boulevard
Golden, Colorado 80401-3393
A national laboratory of the U.S. Department of Energy
Managed by Midwest Research Institute
for the U.S. Department of Energy
under contract No. DE-AC36-83CH10093

Prepared under Subcontract No. DE-AC03-815F11557

April 1992

This publication was reproduced from the best available copy
Submitted by the subcontractor and received no editorial review at NREL

NOTICE

This report was prepared as an account of work sponsored by an agency of the United States government. Neither the United States government nor any agency thereof, nor any of their employees, makes any warranty, express or implied, or assumes any legal liability or responsibility for the accuracy, completeness, or usefulness of any information, apparatus, product, or process disclosed, or represents that its use would not infringe privately owned rights. Reference herein to any specific commercial product, process, or service by trade name, trademark, manufacturer, or otherwise does not necessarily constitute or imply its endorsement, recommendation, or favoring by the United States government or any agency thereof. The views and opinions of authors expressed herein do not necessarily state or reflect those of the United States government or any agency thereof.



ABSTRACT

The overall objective of our research has been to develop thermochemical cycles that can be used for energy storage. A specific cycle involving ammonium hydrogen sulfate (NH_4HSO_4) has been proposed. Each reaction in the proposed cycle has been examined experimentally. Emphasis has been placed on the basic chemistry of these reactions.

In the concluding phase of this research, reported herein, we have shown that when NH_4HSO_4 is mixed with ZnO and decomposed, the resulting products can be released stepwise ($\text{H}_2\text{O}(\text{g})$ at $\sim 163^\circ\text{C}$, $\text{NH}_3(\text{g})$ at $365\text{--}418^\circ\text{C}$, and a mixture of $\text{SO}_2(\text{g})$ and $\text{SO}_3(\text{g})$ at $\sim 900^\circ\text{C}$) and separated by controlling the reaction temperature. Side reactions do not appear to be significant and the respective yields are high as would be required for the successful use of this energy storage reaction in the proposed cycle. Thermodynamic, kinetic, and other reaction parameters have been measured for the various steps of the reaction.

Finally we have completed a detailed investigation of one particular reaction: the thermal decomposition of zinc sulfate (ZnSO_4). This reaction is involved in the NH_4HSO_4 cycle and also in several other cycles proposed for the thermochemical decomposition of water into hydrogen and oxygen. Typically it proceeds rapidly only at temperatures greater than 850°C .

We have demonstrated that this reaction can be accelerated and the temperature required reduced by the addition of excess ZnO , V_2O_5 and possibly other metal oxides. Further, we have shown that ZnSO_4 can be decomposed from a liquid mixture of ZnSO_4 and Li_2SO_4 , and that this decomposition can be catalyzed by V_2O_5 , aluminum silicate, and possibly other metal oxides.

The work on this project as proposed prior to funding is essentially complete. The results of this research have been and continue to be used in other projects designed to test the overall feasibility of the proposed cycle.

TABLE OF CONTENTS

	PAGE
ABSTRACT	i
TABLE OF CONTENTS	ii
LIST OF FIGURES	iv
LIST OF TABLES	v
I. INTRODUCTION	1-14
General Objective of Research	1
Description of Ammonium Hydrogen Sulfate Cycle	2
Summary of Previous Research	4
II. THERMAL DECOMPOSITION OF $\text{NH}_4\text{HSO}_4/\text{ZnO}$ MIXTURE	15-16
Stoichiometry and Yield for First Reaction Step (Reaction 1c')	15
Kinetics for First Reaction Step (Reaction 1c')	18
Effects of Other Reaction Conditions on First Reaction Step	20
Stoichiometry and Yield for Second Reaction Step (Reaction 1d)	22
Kinetics for Second Reaction Step (Reaction 1d)	23
III. THERMAL DECOMPOSITION OF ZnSO_4	27-56
Preliminary Experiments	27
Improved Method for Measuring SO_2 and SO_3 Simultaneously	29
Evidence for Two Reactions in Decomposition of ZnSO_4	32
Rates of Reaction for Production of SO_2 and SO_3 From ZnSO_4	37
Effect of Excess ZnO on Decomposition of ZnSO_4	37
Effect of Additives on the Decomposition of ZnSO_4	38
Thermal Decomposition of $\text{ZnSO}_4/\text{NaCl}$ Mixtures	38
Thermal Decomposition of Eutectic Mixtures Containing ZnSO_4	40
Thermal Decomposition of $\text{ZnSO}_4/\text{Li}_2\text{SO}_4$ Mixtures	44
Effect of Metal Oxides on Decomposition of $\text{ZnSO}_4/\text{Li}_2\text{SO}_4$ Mixtures	52
IV. GENERAL SUMMARY AND CONCLUSIONS	57
V. RELATIONSHIP OF THIS RESEARCH TO OTHER ENERGY STORAGE AND WATER SPLITTING CYCLES	58
VI. REFERENCES	59-62

APPENDICES

PAGE

A. Thermogravimetric Procedure for Screening Reaction Mixtures	63
B. Analytical Procedure Used for Study of First Step in Decomposition of $\text{NH}_4\text{HSO}_4/\text{M}_2\text{SO}_4$ Mixtures	68
C. Procedure for Measuring the Solubility of Alkali Metal Sulfates in Molten NH_4HSO_4	89
D. Procedure for Calorimetric Measurements For Energy Regeneration Reaction (Reaction 2)	90
E. Evaluation of Reactor Construction Materials	92
F. Analytical Procedures Used For Study of First Step in Decomposition of $\text{NH}_4\text{HSO}_4/\text{ZnO}$ Mixtures	95
G. Analytical Procedures Used for Study of Second Step in Decomposition of $\text{NH}_4\text{HSO}_4/\text{ZnO}$ Mixtures	99
H. Methods Evaluated for Simultaneous $\text{SO}_2(\text{g})$ and $\text{SO}_3(\text{g})$ Analysis . .	105
I. Analytical Procedure Used for Study of $\text{SO}_2(\text{g})$ and $\text{SO}_3(\text{g})$ Yields From Decomposition of ZnSO_4	111
J. Copies of Publications Resulting from this Project	115

LIST OF FIGURES

FIGURE	PAGE
1. X-Ray Diffraction Patterns For Solid Product of Reaction 1c	19
2. SO ₂ and SO ₃ Yield from Thermal Decomposition of ZnSO ₄ at 830°C	28
3. Arrhenius Plot for Rate of SO ₂ Production from Thermal Decomposition of ZnSO ₄	31
4. ZnSO ₄ Decomposition at 945°C	33
5. Two Step ZnSO ₄ Decomposition	34
6. % Decomposition of ZnSO ₄ as a Function of Temperature	35
7. Rate of Product Formation from the Thermal Decomposition of ZnO·2ZnSO ₄ at 920°C, Uncatalyzed and Catalyzed with ZnO	39
8. Liquidus Curve For Mixture ZnSO ₄ /NaCl	41
9. SO ₂ and SO ₃ Yield from Thermal Decomposition of ZnSO ₄ /Li ₂ SO ₄ at 904°C	45
10. Arrhenius Plot for Rate of SO ₂ from Thermal Decomposition of ZnSO ₄ /Li ₂ SO ₄	48
11. Rate of Product Formation from the Thermal Decomposition of ZnSO ₄ at 945°C and of ZnSO ₄ /Li ₂ SO ₄ at 967°C	49
12. Rate of Product Formation from the Thermal Decomposition of ZnSO ₄ /Li ₂ SO ₄ = 0.67 at 969°C	54
13. Rate of Product Formation from the Thermal Decomposition of ZnSO ₄ /Li ₂ SO ₄ at 915°C and of ZnSO ₄ /Li ₂ SO ₄ /V ₂ O ₅ at 900°C	55

LIST OF TABLES

TABLE	PAGE
I Summary of TGA & DTA Results For NH_4HSO_4 /Metal Sulfate Mixtures . . .	6
II Summary of TGA & DTA Results For NH_4HSO_4 /Metal Oxide Mixtures . . .	7
III Experimental Solubility of Alkali Metal Sulfates in NH_4HSO_4 as a Function of Temperature	9
IV Summary of Experimental Results for Mechanism I	11
V Experimental Heat of Reaction at One Atmosphere for The Energy Regeneration Reaction	13
VI Summary of Experimental Results for Mechanism II	16
VII Rate Constants for Decomposition of NH_4HSO_4 / ZnO Mixture	21
VIII Summary of Kinetics for Thermal Decomposition of ZnSO_4 , $\text{ZnO}\cdot 2\text{ZnSO}_4$, and Product of Reaction 1c'	26
IX Summary of SO_2 and SO_3 Yield Rates as a Function of Temperature for Thermal Decomposition of ZnSO_4 - Analysis by Titration . . .	30
X Eutectic Systems Considered for the Thermal Decomposition of ZnSO_4	42
XI Experimental Weight Loss For The Melts Screened for the Decomposition of ZnSO_4	43
XII Summary of SO_2 and SO_3 Yield Rates as a Function of Temperature for Thermal Decomposition of ZnSO_4 / Li_2SO_4 Mixture - Analysis by Tritration	47
XIII Comparison of Data for Thermal Decomposition of Pure ZnSO_4 and Mixture ZnSO_4 / Li_2SO_4	50
XIV Comparison of Data for Thermal Decomposition of ZnSO_4 / Li_2SO_4 and ZnSO_4 / Li_2SO_4 / V_2O_5 Mixtures	56

INTRODUCTION

General Objective of the Research -

If solar insolation is to be of significance in meeting our energy needs, an important aspect of the required technology is the development of methods for storing the energy from this intermittent supply. For applications which require high temperature heat, such as electrical power generation, reversible chemical reaction cycles appear to offer promise for long term energy storage. The selection of an appropriate reaction and the experimental measurement of scientific data for the cycle have been the objectives of research in this laboratory since 1976. This report presents new data which is applicable not only to this cycle but also to other proposed cycles.

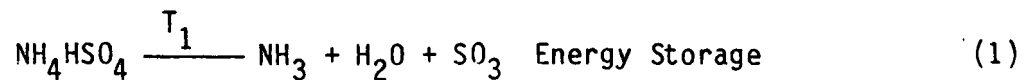
In principle, such cycles would use concentrated solar flux to provide the heat required for a high temperature endothermic decomposition reaction. This converts the thermal input into chemical potential energy in the reaction products which are stored. Heat could be regenerated upon demand by recombining the stored products in the reverse exothermic reaction at some lower temperature.

The maximum temperature available from the solar concentrator (eg. 516°C for Solar One) and the minimum operating temperature of the power generating turbines (eg. ~300°C for Solar One) determine the temperature range within which the chemical reaction must be cycled. A reaction cycle operable within these limits must be identified, and thermodynamic and kinetic data for the various reaction steps measured.

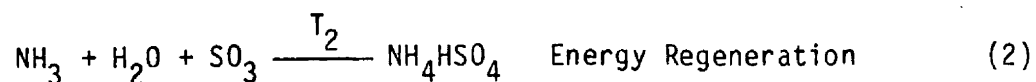
Chemical reaction cycles offer at least two advantages over other methods of storage presently under consideration. First, chemical reaction cycles are potentially capable of storing more energy per unit volume of storage medium than systems based on storage of sensible heat (ie. hot rocks, oil, water, etc.) or as heat of fusion (ie. phase change media). Second, with reaction cycles the storage medium can be at or near ambient temperature during the entire storage period. If the recombination reaction occurs without catalysis, the products must be separated at the decomposition temperature prior to storage. If the recombination reaction requires a catalyst, then it may be possible to store the products together in the absence of the catalyst. This research has focused on a cycle which is uncatalyzed, and considerable effort has been spent on the methods of product separation. Finally, the practical operation of such a cycle depends critically upon a high reaction yield in both directions and long term reversibility for the net reaction, all within a closed system. These features must be demonstrated.

Description of the Ammonium Hydrogen Sulfate Cycle -

Based on general criteria for energy storage reaction cycles,¹ we selected the net thermal decomposition of ammonium hydrogen sulfate (NH_4HSO_4) into ammonia (NH_3), water (H_2O), and sulfur trioxide (SO_3) for the energy storage step:



and the reverse recombination reaction:



for the energy regeneration step in a storage cycle.

Values for the standard enthalpy of reaction, $\Delta H^\circ=336.5 \text{ kJ mole}^{-1}$ (80.4 kcal mole^{-1}) and for the standard entropy of reaction, $\Delta S^\circ=455.8 \text{ J deg}^{-1}$ (108.9 cal deg^{-1}) have been used to calculate the approximate temperature, $T_1=467^\circ\text{C}$, at which the thermodynamic equilibrium constant, K_{eq} , for the reaction is equal to one. The value of T_1 is an approximation of the temperature at which the reaction cycle can be "turned". According to this approximation, reaction 1 will be favored at temperatures in excess of T_1 and reaction 2 will be favored at temperatures below T_1 . The actual temperature required for the energy storage step (T_1) and provided by the energy regeneration (T_2) will depend on the reaction conditions necessary to obtain high yields for each of these reactions.

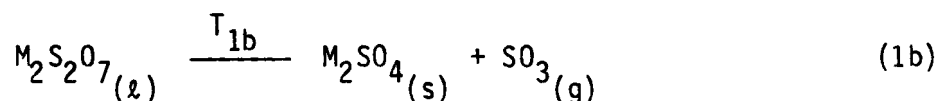
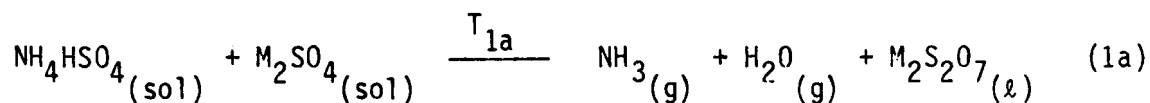
The products of reaction 1 are gases at temperatures in the vicinity of T_1 under standard conditions, but each can be liquified at modest pressures (<10 atm) at ambient temperature (<40°C). Condensation, and thus storage, of these products will be simplified if reaction conditions can be found such that the partial pressure of each product in reaction 1 at equilibrium is in excess of its liquid vapor pressure at ambient temperature. Using thermodynamic data available for reaction 1, calculations indicate that this self condensation can be achieved at $T_1 \sim 500^\circ\text{C}$. The energy storage density provided by this process (storage of H_2O , NH_3 , and SO_3 as liquids at ambient temperature) would be between $3,098 \text{ MJ m}^{-3}$ (740 kcal ℓ^{-1}) and $4,102 \text{ MJ m}^{-3}$ (980 kcal ℓ^{-1}). The lower figure assumes complete loss of the heat of condensation of each product to an ambient heat sink. The higher figure, assumes complete recovery of this heat of condensation from the ambient heat sink or through some co-

generative process.

Summary of Previous Research -

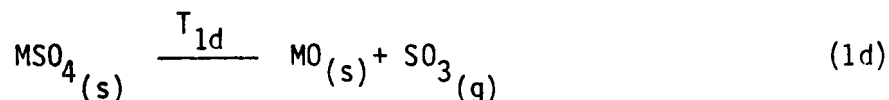
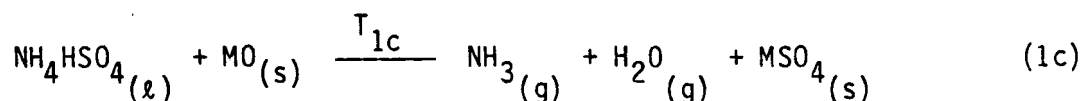
An initial literature survey allowed us to identify two reaction mechanisms which would be equivalent to reaction 1 and which might allow satisfactory separation of SO_3 from NH_3 and H_2O . The use of metal sulfates (M_2SO_4) for forming intermediate pyrosulfates ($\text{M}_2\text{S}_2\text{O}_7$):

MECHANISM I



or the use of metal oxides (MO) to form intermediate sulfates (MSO_4):

MECHANISM II



would in principle provide the desired product separation if large yields from each of the two steps could be achieved by controlling the reaction mixture temperature.

Based on thermodynamic data when available and further assisted by a reaction mechanism model,^{2,3} twenty five different metal oxides and metal sulfates were selected and their reaction with NH_4HSO_4 screened experimentally using dif-

ferential thermal analysis (DTA) and thermogravimetric analysis (TGA). In general, the TGA results proved more useful than the DTA results. The TGA method used is described in Appendix A. The results of this screening have been published,^{4,5} and are summarized in Tables I and II. Only three sulfates (K_2SO_4 , Rb_2SO_4 , Cs_2SO_4) and six metal oxides (ZnO , Cu_2O , NiO , MnO , PbO , MgO), when mixed with NH_4HSO_4 , reacted in two steps with an intermediate weight loss equal to that expected for complete evolution of the available NH_3 and H_2O (30% of the starting weight of NH_4HSO_4).

The first step (reaction 1a) of Mechanism I has been investigated in detail. This investigation required the development of an unconventional procedure for quantitative chemical analysis of the reaction products. This procedure is described in Appendix B. Use of this procedure has shown that with each of the three metal sulfates the principal reaction products are $NH_3(g)$ and $H_2O(g)$. Small amounts of $SO_3(g)$ are also produced. In each case the absolute $NH_3(g)$ yield and the relative $NH_3(g)$ to $SO_3(g)$ yield depends on the reaction temperature and reaction mixture mole ratio (moles of metal sulfate/moles NH_4HSO_4). Quantitative measurements of these yields have been made under various reaction conditions.^{6,7} Optimum reaction conditions in each case require a temperature $\sim 415^\circ C$ and a mole ratio ~ 1.2 . Under these conditions the $NH_3(g)$ yields are $\sim 95\%$ and the $SO_3(g)$ yields are $< 1\%$ in each case. The volatile $NH_3(g)$ yield is greatest for the mixture containing Cs_2SO_4 and lowest for the mixture containing K_2SO_4 . Total recovery of NH_3 and SO_3 is virtually 100% in each case. Preliminary experiments with mixtures containing K_2SO_4 indicate that the $NH_3(g)$ yield can be increased and the $SO_3(g)$ yield reduced when the reaction is carried in the presence of excess water vapor. However, it was not possible to find

TABLE I

SUMMARY OF TGA AND DTA RESULTS FOR MIXTURES OF NH_4HSO_4 WITH EACH OF THE METAL SULFATES SCREENED

<u>Metal Sulfate</u>	<u>Temperature Range 0% to 30% Weight Loss</u>	<u>Corresponding DTA Endotherm</u>	<u>Assumed Reaction</u>	<u>Temperature Range 30% to 100% Weight Loss</u>	<u>Assumed Reaction</u>
Li_2SO_4	does not occur	-----	-----	does not occur	-----
Na_2SO_4	does not occur	-----	-----	does not occur	-----
K_2SO_4	250°C to 350°C	395°C	$\text{K}_2\text{SO}_4 + \text{NH}_4\text{HSO}_4 \rightarrow \text{H}_2\text{O} + \text{NH}_3 + \text{K}_2\text{S}_2\text{O}_7$	400°C to 650°C	$\text{K}_2\text{S}_2\text{O}_7 \rightarrow \text{K}_2\text{SO}_4 + \text{SO}_3$
Rb_2SO_4	~ 250°C to 300°C	390°C	$\text{Rb}_2\text{SO}_4 + \text{NH}_4\text{HSO}_4 \rightarrow \text{H}_2\text{O} + \text{NH}_3 + \text{Rb}_2\text{S}_2\text{O}_7$	350°C to 750°C	$\text{Rb}_2\text{S}_2\text{O}_7 \rightarrow \text{Rb}_2\text{SO}_4 + \text{SO}_3$
Cs_2SO_4	< 250°C to 300°C	345°C	$\text{Cs}_2\text{SO}_4 + \text{NH}_4\text{HSO}_4 \rightarrow \text{H}_2\text{O} + \text{NH}_3 + \text{Cs}_2\text{S}_2\text{O}_7$	450°C to 900°C	$\text{Cs}_2\text{S}_2\text{O}_7 \rightarrow \text{Cs}_2\text{SO}_4 + \text{SO}_3$
CaSO_4	does not occur	-----	-----	does not occur	-----
MgSO_4	does not occur	-----	-----	does not occur	-----
MnSO_4	does not occur	-----	-----	does not occur	-----
Al_2SO_4	does not occur	-----	-----	does not occur	-----
FeSO_4	does not occur	-----	-----	does not occur	-----
NiSO_4	does not occur	-----	-----	does not occur	-----
CuSO_4	does not occur	-----	-----	does not occur	-----
ZnSO_4	does not occur	-----	-----	does not occur	-----
CdSO_4	does not occur	-----	-----	does not occur	-----
HgSO_4	does not occur	-----	-----	does not occur	-----

TABLE II

SUMMARY OF TGA RESULTS FOR MIXTURES OF NH_4HSO_4 WITH EACH OF THE METAL OXIDES SCREENED

<u>Metal Oxide</u>	<u>Temperature Range 0% to 30% Weight Loss</u>	<u>Assumed Reaction</u>	<u>Temperature Range 30% to 100% Weight Loss</u>	<u>Temperature Range For Weight Loss From Pure Metal Sulfate</u>	<u>Assumed Reaction</u>
MgO	<200°C to 400°C	$\text{MgO} + \text{NH}_4\text{HSO}_4 \rightarrow \text{H}_2\text{O} + \text{NH}_3 + \text{MgSO}_4$	900°C to > 1000°C	900°C to > 1000°C	$\text{MgSO}_4 \rightarrow \text{MgO} + \text{SO}_3$
CaO	not observed	-----	not observed	not observed	-----
BaO	<200°C to 300°C	$\text{BaO} + \text{NH}_4\text{HSO}_4 \rightarrow \text{H}_2\text{O} + \text{NH}_3 + \text{BaSO}_4$	not observed	no experiment	-----
Cu ₂ O	<200°C to 400°C	$\text{Cu}_2\text{O} + \text{NH}_4\text{HSO}_4 \rightarrow \text{H}_2\text{O} + \text{NH}_3 + \text{Cu}_2\text{SO}_4$	550°C to 700°C	no experiment	$\text{Cu}_2\text{SO}_4 \rightarrow \text{Cu}_2\text{O} + \text{SO}_3$
ZnO	<150°C to 350°C	$\text{ZnO} + \text{NH}_4\text{HSO}_4 \rightarrow \text{H}_2\text{O} + \text{NH}_3 + \text{ZnSO}_4$	600°C to 900°C	600°C to 900°C	$\text{ZnSO}_4 \rightarrow \text{ZnO} + \text{SO}_3$
NiO	<250°C to 400°C	$\text{NiO} + \text{NH}_4\text{HSO}_4 \rightarrow \text{H}_2\text{O} + \text{NH}_3 + \text{NiSO}_4$	600°C to 900°C	600°C to 800°C	$\text{NiSO}_4 \rightarrow \text{NiO} + \text{SO}_3$
MnO	<250°C to 400°C	$\text{MnO} + \text{NH}_4\text{HSO}_4 \rightarrow \text{H}_2\text{O} + \text{NH}_3 + \text{MnSO}_4$	700°C to 1000°C	700°C to 900°C	$\text{MnSO}_4 \rightarrow \text{MnO} + \text{SO}_3$
PbO	<200°C to 300°C	$\text{PbO} + \text{NH}_4\text{HSO}_4 \rightarrow \text{H}_2\text{O} + \text{NH}_3 + \text{PbSO}_4$	800°C to 1000°C	no experiment	$\text{PbSO}_4 \rightarrow \text{PbO} + \text{SO}_3$
HgO	does not occur	-----	does not occur	no experiment	-----
Al ₂ O ₃	does not occur	-----	does not occur	no experiment	-----

reaction conditions under which any of the three mixtures gave 100% $\text{NH}_3(\text{g})$ yield and negligible $\text{SO}_3(\text{g})$ yield indicating that for these mixtures, temperatures sufficient to drive reaction 1a to completion are also sufficient to initiate reaction 1b. Further, we found some indication that reaction 1a is an incomplete representation of the process taking place in these mixtures at $T_{1a}=250\text{-}350^\circ\text{C}$. Condensable H_2O was repeatedly observed in the reactor at temperatures below those required to produce detectable volatile $\text{NH}_3(\text{g})$. This suggests that decomposition of NH_4HSO_4 in the presence of the metal sulfates forms a nitrogen containing pyrosulfate prior to liberation of free ammonia.

In order to partially characterize the nature of the reaction mixtures ($\text{M}_2\text{SO}_4/\text{NH}_4\text{HSO}_4$) associated with reaction 1a, the solubility of each alkali metal sulfate in molten NH_4HSO_4 ($M_p=145^\circ\text{C}$) was measured as a function of temperature within the range 150 to 250°C . The procedure used is described in Appendix C. The results are presented in Table III, and indicate that the solubilities of Na_2SO_4 , K_2SO_4 , Rb_2SO_4 , and Cs_2SO_4 are the same, within experimental error, at any temperature. The solubility of Li_2SO_4 is somewhat higher at low temperatures, but becomes comparable to that of the other metal sulfates at higher temperatures. The measured solubilities for K_2SO_4 , Rb_2SO_4 , and Cs_2SO_4 are consistent with the observation that the mole ratio $\text{M}_2\text{SO}_4/\text{NH}_4\text{HSO}_4=1.2$ necessary for maximum $\text{NH}_3(\text{g})$ yield via reaction 1a results in a mixture in which the M_2SO_4 is only partially dissolved when reaction begins.

For each of the three reaction mixtures ($\text{K}_2\text{SO}_4/\text{NH}_4\text{HSO}_4$, $\text{Rb}_2\text{SO}_4/\text{NH}_4\text{HSO}_4$, $\text{Cs}_2\text{SO}_4/\text{NH}_4\text{HSO}_4$), thermodynamic and kinetic parameters have been calculated for reaction 1a. Thermodynamic parameters (ΔH , ΔS) were calculated from measurement of the total equilibrium product gas pressure as a function of temperature.^{8,9}

TABLE III

EXPERIMENTAL SOLUBILITY OF THE ALKALI METAL
SULFATES IN AMMONIUM HYDROGEN SULFATE
AS A FUNCTION OF TEMPERATURE

MOLE FRACTION OF METAL SULFATE DISSOLVED

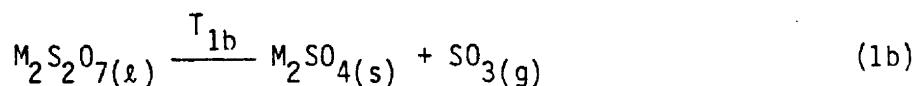
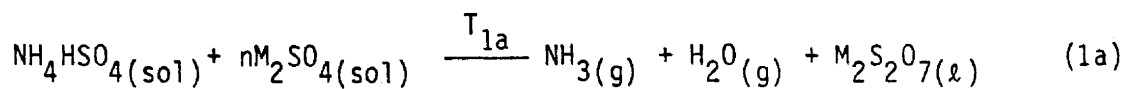
<u>T(°C)</u>	<u>Li₂SO₄</u>	<u>Na₂SO₄</u>	<u>K₂SO₄</u>	<u>Rb₂SO₄</u>	<u>Cs₂SO₄</u>
150	.0233	.0181	.0152	.0087	.0125
175	.0061	.0430	.0417	.0440	.0529
200	.1409	.0492	.0903	.1132	.0855
225	.1655	.1624	.1354	.1544	.1807
250	.1806	.2203	.1977	.2175	.2110

Kinetic parameters (activation energies, rate constants) were calculated from measurement of the rate of $\text{NH}_3(\text{g})$ evolution as a function of temperature.^{8,10} The experimental details have been published elsewhere.^{8,10} The results are summarized in Table IV. Two sets of thermodynamic parameters are given. One pertains to reaction temperatures below $\sim 360^\circ\text{C}$ where the reaction mixture is not homogeneous. At these temperatures the mixture at equilibrium consists of a solution of M_2SO_4 in molten NH_4HSO_4 in contact with undissolved M_2SO_4 . Another set pertains to temperatures above $\sim 360^\circ\text{C}$. At these temperatures the mixture at equilibrium is homogeneous. In either case the thermodynamic state of the reacting species is not well characterized, and the calculation of the respective ΔH and ΔS values required assumptions concerning the nature of the mixture. For this reason the results are not considered definitive. They are, however, considered adequate for the present purposes.

The second step (reaction 1b) was not studied quantitatively. However, qualitative experiments⁹ indicate that this reaction will require a temperature $T_{1b} \sim 900^\circ\text{C}$, that it occurs at a somewhat slower rate than reaction 1a, and that it will yield a mixture of $\text{SO}_2(\text{g})$, $\text{SO}_3(\text{g})$, and $\text{O}_2(\text{g})$.

The energy regeneration step (reaction 2) has been investigated. The heat of reaction was determined by adiabatic calorimetry at atmospheric pressure.⁹ The procedure used is described in Appendix D. The results are summarized in Table V. A net heat of reaction equal to 74-77 kcal/mole was calculated for $T_2 = 310^\circ\text{C}$. In addition, experiments were done in which $\text{NH}_3(\text{g})$, $\text{SO}_3(\text{g})$ and $\text{H}_2\text{O}(\text{g})$ were mixed on a manifold at atmospheric pressure. The reaction is characterized by the formation of a dense mist, and the condensation of a solid product. The reaction temperatures observed ranged from 355°C to 405°C , and the solid product was a mixture of NH_4HSO_4 and $(\text{NH}_4)_2\text{SO}_4$.

TABLE IV
SUMMARY OF EXPERIMENTAL RESULTS FOR MECHANISM I



M_2SO_4	FROM TGA ⁽¹⁾ EXPERIMENTS		FROM EQUILIBRIUM ⁽²⁾ VAPOR PRESSURE EXPERIMENTS
	T_{1a}	T_{1b}	T_{1a}
K_2SO_4	250-350°C	400-650°C	220-480°C
Rb_2SO_4	250-300	350-750	220-480
Cs_2SO_4	<250-300	450-900	220-440

(1) From ref. 4.

(2) From ref. 8.

YIELD DATA FOR REACTION 1a⁽³⁾

M_2SO_4	YIELD $\text{NH}_3(\text{g})$	YIELD $\text{SO}_3(\text{g})$
K_2SO_4	93.6%	0.6 %
Rb_2SO_4	95.4	0.11
Cs_2SO_4	96.1	0.3

(3) Measured at optimum values $\text{T}_{1a} = 415^\circ\text{C}$; $n = 1.2$ and expressed as % of total theoretical yield (see ref. 7).

TABLE IV (Continued)
THERMODYNAMIC PARAMETERS FOR REACTION 1a⁽⁴⁾

M_2SO_4	Below 360°C ⁽⁵⁾		Above 360°C ⁽⁶⁾	
	ΔH	ΔS	ΔH	ΔS
K_2SO_4	49. kcal mole ⁻¹	66. cal deg ⁻¹	43.7 kcal mole ⁻¹	59.2 cal deg ⁻¹
Rb_2SO_4	53.3	74.3	47.	67.
Cs_2SO_4	45.7	65.8	35.8	52.

(4) Thermodynamic data were calculated from equilibrium product gas pressure using assumptions concerning composition of the reactant mixture at equilibrium.

(5) Not all M_2SO_4 in solution (see ref. 8).

(6) Completely liquid reaction mixture (see ref. 8).

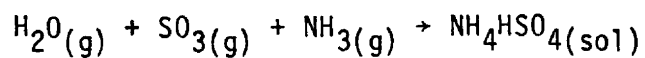
KINETIC PARAMETERS FOR REACTION 1a⁽⁷⁾

M_2SO_4	ACTIVATION ENERGY	PRE-EXPONENTIAL	FORWARD RATE
		FACTOR	CONSTANT (400°C)
K_2SO_4	19.2 kcal mole ⁻¹	$1.6 \times 10^3 \text{ sec}^{-1}$	$1.275 \times 10^3 \text{ sec}^{-1}$
Rb_2SO_4	21.6	1.52×10^4	3.757×10^{-3}
Cs_2SO_4	23.7	1.87×10^5	9.54×10^{-3}

(7) Kinetic data were calculated from measurement of $NH_3(g)$ pressure as a function of time and temperature, and assuming reaction is first order in the forward direction (excess M_2SO_4) and second order on the reverse direction (constant H_2O), (from ref. 10).

TABLE V

EXPERIMENTAL HEAT OF REACTION AT ONE ATMOSPHERE FOR



<u>T</u> <u>(°C)</u>	<u>T</u> <u>(°K)</u>	<u>ΔH</u> <u>(kcal/mole)</u>	<u>Reference</u>
310	583	74-77	1
310	583	76	2

- (1) Chen et al., present work.
- (2) Calculated from data reported by Kelley et al. in "Thermodynamic Properties of Ammonium and Potassium Alums and Related Substances With Reference to Extraction of Alumina From Clay and Aunite," U.S. Dept. of Interior, Technical Paper #688.

Finally, since the reaction mixtures involved in reactions 1a and 1b are potentially very corrosive and since metal reactors would be required to contain these mixtures at the pressures suitable for product condensation, a series of experiments⁹ was carried out to measure the corrosive effects of the mixtures on various metals. The procedure used is described in Appendix E. Of the nine metals tested, Rene 41 and Hastelloy X showed the greatest resistance to corrosion.

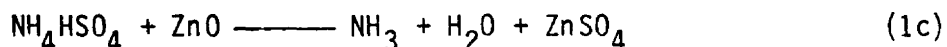
The first step (reaction 1c) of Mechanism II has been examined using mixtures of NH_4HSO_4 with each of the six selected metal oxides. Of these, the mixture $\text{ZnO}/\text{NH}_4\text{HSO}_4$ gave the most complete separation of $\text{NH}_3(\text{g})$ and $\text{SO}_3(\text{g})$ products. Experimental results for this mixture as well as results for reaction 1d are discussed in detail in this report.

II

THERMAL DECOMPOSITION OF THE $\text{ZnO}/\text{NH}_4\text{HSO}_4$ MIXTURE

Stoichiometry and Yield for First Reaction Step (Reaction 1c) -

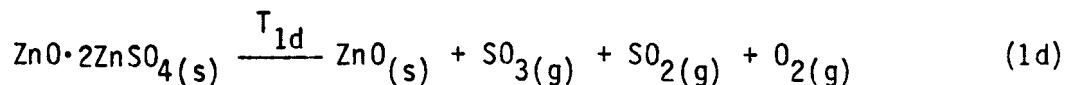
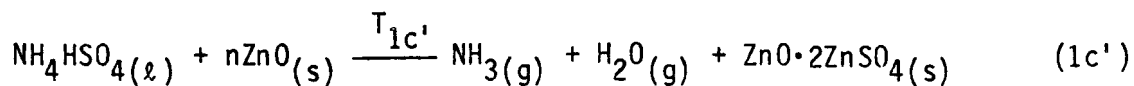
In order to characterize the reaction of NH_4HSO_4 with ZnO , experiments were done to determine the yield of $\text{NH}_3(\text{g})$ evolved as a function of mixture mole ratio ($n=\text{ZnO}/\text{NH}_4\text{HSO}_4$) and reaction temperature over the range 261-459°C. Volatile products from the heated mixture were entrained in an inert gas flow and transferred to a solution of H_2SO_4 which was analyzed. The quantitative chemical analysis procedure used is described in Appendix F. The experimental details and results have been published^{11,12} and are summarized in Table VI. The data showed that: $\text{H}_2\text{O}(\text{g})$ but not $\text{NH}_3(\text{g})$ or $\text{SO}_3(\text{g})$ is evolved at ~163°C; $\text{NH}_3(\text{g})$ but no $\text{SO}_3(\text{g})$ is evolved at temperatures between 365-418°C; maximum $\text{NH}_3(\text{g})$ yield (>99%) is obtained when $n\sim 1.5$ and $T_{1c}=390\text{-}400^\circ\text{C}$; and that at temperatures above 409°C $\text{NH}_3(\text{g})$ begins to decompose. The optimum value for $n=1.5$ is inconsistent with the stoichiometry for reaction 1c.



$$n = \frac{\text{ZnO}}{\text{NH}_4\text{HSO}_4} = 1$$

An oxysulfate, $\text{ZnO}\cdot 2\text{ZnSO}_4$, has been identified in the literature (see refs. 11 and 12 for a more complete discussion of this compound). The value $n=1.5$ suggests that the oxysulfate rather than ZnSO_4 is the end product for the reaction of NH_4HSO_4 with ZnO .

TABLE VI
SUMMARY OF EXPERIMENTAL RESULTS FOR MECHANISM II



REACTION TEMPERATURES

FROM TGA EXPERIMENTS ⁽¹⁾		FROM PRODUCT GAS ANALYSIS ⁽²⁾	
<u>T_{1c'}</u>	<u>T_{1d}</u>	<u>T_{1c'}</u>	<u>T_{1d}</u>
<150-350°C	600-900°C	365-418°C	>800°C

(1) From ref. 4.

(2) From ref. 12.

YIELD DATA FOR REACTION 1c'⁽³⁾

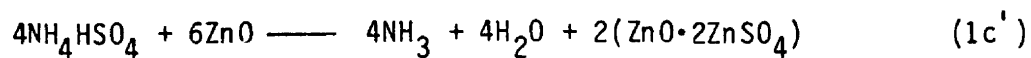
<u>Yield NH₃(g)</u>	<u>Yield SO₃(g)</u>
99.3%	.34%

(3) Measured at optimum values $T_{1c'} = 409^\circ\text{C}$, $n = 1.5$ and expressed as % of total theoretical yield (see ref. 12).

KINETIC PARAMETERS FOR REACTION 1c'⁽⁴⁾

<u>Activation Energy</u>	<u>Pre-exponential Factor</u>	<u>Forward Rate Constant (400°C)</u>
24.7 kcal mole ⁻¹	$1.2 \times 10^7 \text{ min}^{-1}$	$1.331 \times 10^{-1} \text{ min}$

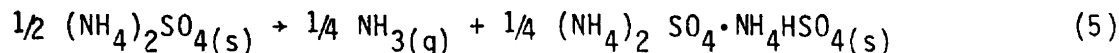
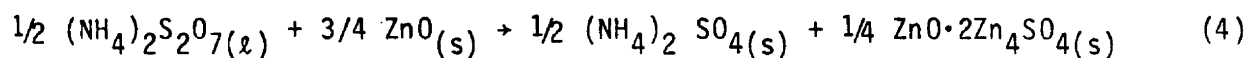
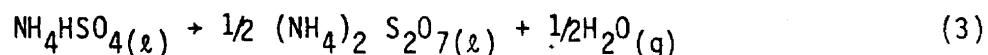
(4) Kinetic data were calculated from measurement of NH₃(g) yield as a function of time and temperature by electrical conductance and assuming reaction is first order in forward direction (from ref. 13).



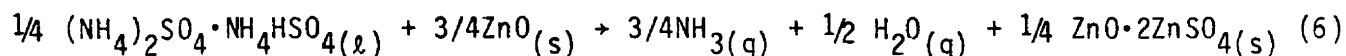
$$n = \frac{\text{ZnO}}{\text{NH}_4\text{HSO}_4} = \frac{6}{4} = 1.5$$

However, the fact that $\text{H}_2\text{O}(\text{g})$ is evolved from the reaction at a temperature much lower than that required for the production of $\text{NH}_3(\text{g})$ indicates that equation 1c is not a complete description of the process. Based on other information from the literature (see ref. 12), it seems likely that the reaction of NH_4HSO_4 with ZnO involves the following sequence of reactions:

At $170^\circ\text{C} < T < 230^\circ\text{C}$



At $230^\circ < T < 400^\circ\text{C}$



The net result of this sequence is consistent with the stoichiometry of reaction 1c' which is used for brevity in discussions which follow.

In order to further characterize the product of reaction 1c', an x-ray powder diffraction spectrum was obtained (see Figure 1) from a sample of this solid and compared to standard diffraction patterns for ZnO , ZnSO_4 , and

$\text{ZnO} \cdot 2\text{ZnSO}_4$. The reaction product pattern showed the main line of pure ZnO at d (interplanar spacing) = 2.48 suggesting excess ZnO in the product. It had only one or two lines in common with $\text{ZnO} \cdot 2\text{ZnSO}_4$, and none of the lines shown in the pure ZnSO_4 pattern. However, this result is considered inconclusive and it is assumed that the reaction product contains a mixture of ZnO, ZnSO_4 and $\text{ZnO} \cdot 2\text{ZnSO}_4$. Evidence for this conclusion is presented in Section II.

Kinetics for First Reaction Step (Reaction 1c') -

The rate of reaction 1c' has been calculated by measuring the rate of $\text{NH}_3(\text{g})$ evolution from the mixture $\text{ZnO}/\text{NH}_4\text{HSO}_4=1.5$. The procedure used was similar to that used to study the reaction stoichiometry^{11,12} (see Appendix F), except that volatile products from the heated mixture were entrained in an inert gas flow and transferred to a solution of HCl rather than H_2SO_4 . The change in electrical conductivity of the solution was related to the amount of $\text{NH}_3(\text{g})$ dissolved and was used to measure $\text{NH}_3(\text{g})$ yield as a function of time at a given temperature. Experiments showed that the measurement of conductivity changes in an HCl solution is more sensitive to dissolved NH_3 concentration changes than is the measurement of pH change when NH_3 is dissolved in H_2SO_4 . Reaction of HCl with NH_3 converts $\text{H}^+(\text{aq})$ which has a high ionic conductance (350 ohm·cm²/equiv) to NH_4^+ which has a relatively low ionic conductance (73.6 ohm cm²/equiv). The experimental details and results have been published.^{11,12} In summary, the results showed that the rate of $\text{NH}_3(\text{g})$ production is first order with respect to NH_4HSO_4 and occurs in two distinct stages. Since the rate associated with the first stage is most likely determined by a combination of processes

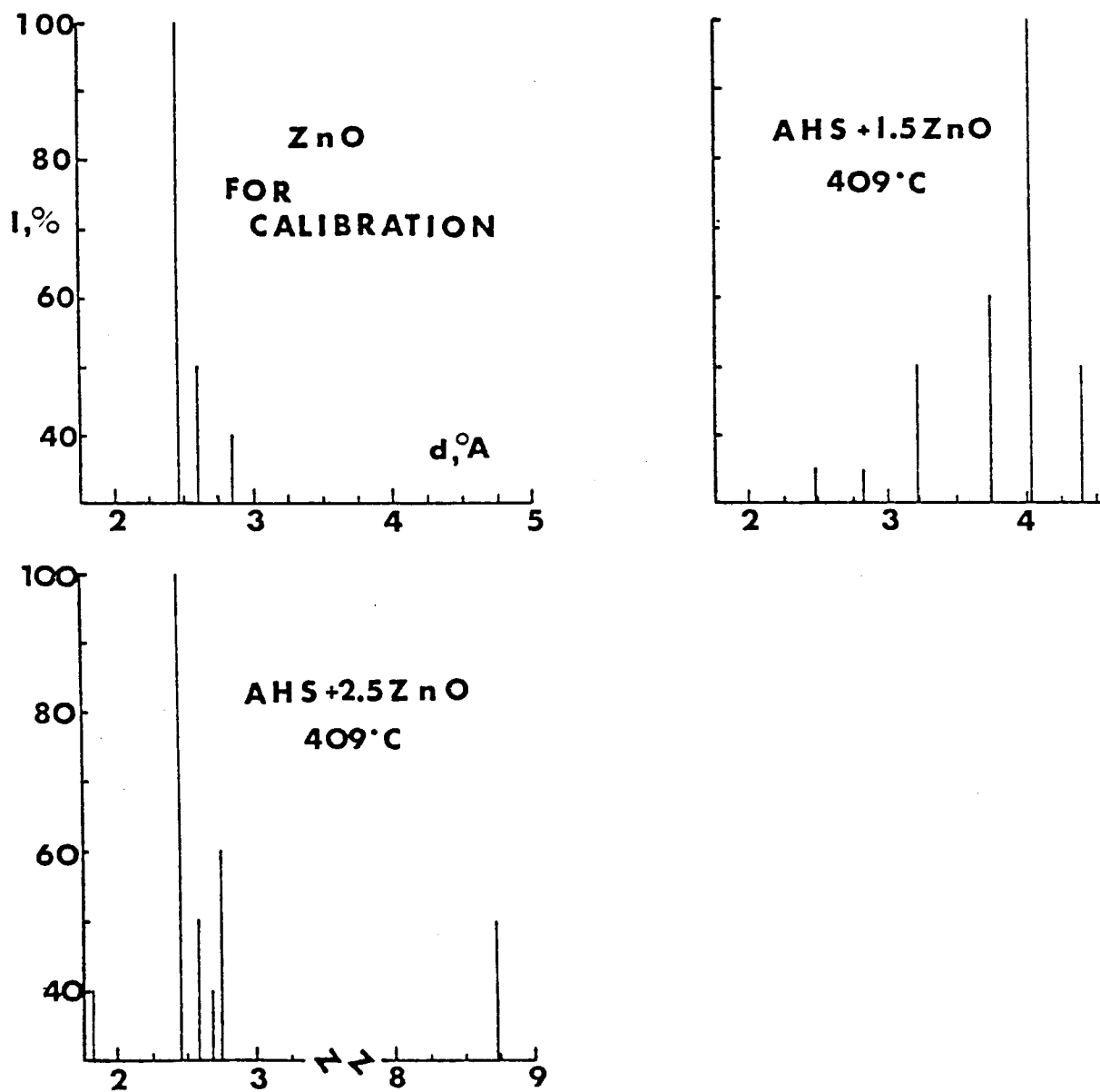


FIG. 1. X-ray Diffraction Patterns for Solid Product of Reaction 1c'.

(reaction 5, the rate of temperature equilibration, and the interaction of $\text{NH}_3(\text{g})$ with condensed droplets of H_2O from reaction 3), only the second stage was studied in detail. Data obtained over the temperature range 340-450°C are associated with reaction 6 and are shown in Table VII.

Effects of Other Reaction Conditions on First Step (Reaction 1c')-

Several experiments were done to determine the effect of water on the thermal decomposition of the $\text{ZnO}/\text{NH}_4\text{HSO}_4$ mixture. No significant change in $\text{NH}_3(\text{g})$ or $\text{SO}_3(\text{g})$ yield was observed when the decomposition at 400°C was done in a water saturated helium atmosphere.¹¹

Since NH_4HSO_4 melts at 145°C and partially decomposes with the release of H_2O at ~170°C, the effect of preheating the $\text{ZnO}/\text{NH}_4\text{HSO}_4$ mixture at 170°C was examined. Preheat times varying from 20 min to 20 hr produced no significant change in the $\text{NH}_3(\text{g})$ and $\text{SO}_3(\text{g})$ yields measured at 400°C.

Since in any application of this chemical cycle the ZnO will be recycled continuously, the effect of such cycling was briefly investigated. ZnO obtained as the product from one $\text{ZnO}/\text{NH}_4\text{HSO}_4$ reaction mixture was used to make a second mixture. The yield of $\text{NH}_3(\text{g})$ obtained at 400°C from the second mixture was virtually the same as that obtained from the first mixture, but the rate of decomposition was faster for the second mixture than for the first.¹¹

Several experiments were done to test the feasibility of increasing the optical absorbtivity of the inherently white $\text{ZnO}/\text{NH}_4\text{HSO}_4$ reaction mixture.¹¹ When charcoal was added to the mixture, decomposition at 400°C produced an increased $\text{SO}_3(\text{g})$ yield (2.3%) and decreased the $\text{NH}_3(\text{g})$ yield. Both effects are

TABLE VII

RATE CONSTANTS OBTAINED AT DIFFERENT TEMPERATURES
FOR THE DECOMPOSITION OF THE $\text{ZnO}/\text{NH}_4\text{HSO}_4$ MIXTURE^{a)}

<u>Temperature</u> <u>(°C)</u>	<u>$K_1 \times 10$</u> <u>(min^{-1})^{b)}</u>	<u>$\sigma_{k_1} \times 10$</u> <u>(min^{-1})^{b)}</u>
340	0.169	0.003
340	0.141	0.004
360	0.381	0.009
380	0.683	0.015
380	0.630	0.010
380	0.510	0.007
400	1.331	0.043
425	2.195	0.060
450	3.315	0.114

a) $\text{ZnO}/\text{NH}_4\text{HSO}_4 = 1.5$

b) Calculated using a rigorous least squares adjustment on the equation
 $\ln(1-x) = -kt$.

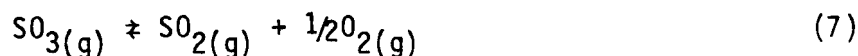
undesirable.

Stoichiometry and Yield for Second Reaction Step (Reaction 1d) -

In order to characterize the decomposition of the solid product from reaction 1c' (assumed to be a mixture of ZnO, ZnSO₄, and ZnO·2ZnSO₄) the yields of SO₂(g) and SO₃(g) produced by this decomposition at ~800°C were measured.¹¹ Volatile products from the heated solid were entrained in an inert gas flow and transferred to a solution of NaOH which was analyzed by potentiometric titration. The analysis procedure used is described in Appendix G.

Complete recovery of the sulfur available in the original ZnO/NH₄HSO₄ mixture was obtained as a mixture of SO₂(g) and SO₃(g). This required more than 4 hours at 815°C. The measured total yields had a mole ratio SO₃/SO₂=3.6.

When the solid was decomposed in a platinum crucible, the rate of decomposition was increased and the total yield ratio SO₃/SO₂ decreased to ~1.35.¹¹ Platinum is known to catalyze the equilibrium:



Apparently this equilibrium influences the net rate of decomposition of the solid.

Results obtained when V₂O₅ was added to the solid were inconclusive due to reaction of the mixture with the quartz sample boat.

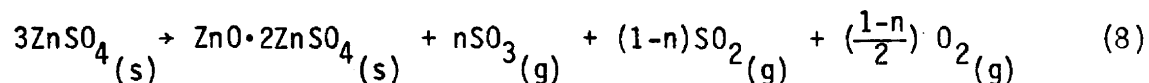
When the solid was decomposed in air rather than helium, the rate of reaction was decreased but the ratio SO₃/SO₂ was not significantly altered.¹¹

Kinetics for the Second Reaction Step (Reaction 1d) -

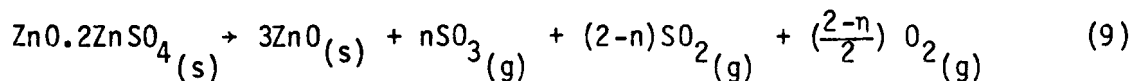
These experiments involved measurement of the rate of weight loss from samples of pure $ZnSO_4$, pure $ZnO \cdot 2ZnSO_4$, and from samples of the solid product of reaction 1c'. Measurements were made as a function of temperature over the range 900-980°C. In each experiment the fraction of the sample decomposed (α) was calculated from weight loss and plotted vs. time. The experimental details and results have been published.^{11,13}

For $ZnSO_4$, the weight loss during thermal decomposition occurred in two distinguishable steps occurring with obviously different rates. Kinetic data were calculated for the second step only. For $ZnO \cdot 2ZnSO_4$ and for samples of reaction 1c' product, weight loss during thermal decomposition occurred in a single step. Kinetic data were calculated for each of these sample types and compared to that for the second step in the thermal decomposition of pure $ZnSO_4$. The comparisons lead to the following conclusions.

The thermal decomposition of $ZnSO_4$ proceeds in two steps: the first occurring when $0 < \alpha < .33$, the second when $.33 < \alpha < 1$. This is consistent with the reaction sequence:



(where $0 \leq n \leq 2$)



(where $0 \leq n \leq 2$)

There is ample evidence in the literature for the formation of an intermediate oxysulfate, although the stoichiometry of this compound has been disputed. The present results support the composition $\text{ZnO} \cdot 2\text{ZnSO}_4$, based on the range of α associated with each of the weight loss steps.

The decompositions of ZnSO_4 and $\text{ZnO} \cdot 2\text{ZnSO}_4$ go essentially to completion at temperatures in the range 900-980°C, and no ZnO decomposition or vaporization was observed up to 980°C.

The decompositions of each of the three solids (ZnSO_4 , $\text{ZnO} \cdot 2\text{ZnSO}_4$, and reaction 1c' product) are best described by the rate equation.

$$\frac{d\alpha}{dt} = kM_0^{-1}$$

Where M_0 is the number of moles of sulfur available in the solid at the start of reaction. This rate equation is derived from the linear law of nuclei formation. Nine alternative rate equations were considered, but none fit the data better.

Rate constants and Arrhenius activation energies were calculated for the decomposition reactions of each of the three solids. The results are given in Table VIII. The rate constants and activation energy for the ZnSO_4 decomposition (second step) are similar to those for the decomposition of $\text{ZnO} \cdot 2\text{ZnSO}_4$, supporting the conclusion that this oxysulfate is an intermediate in the thermal decomposition of ZnSO_4 .

The thermal decomposition of the product from reaction 1c' shows a qualitative similarity to the thermal decompositions of the two pure compounds. A very

fast rate observed at the start of the product decomposition (up to $\alpha = .08$) resembles the fast rate observed during the first stage of the decomposition of pure ZnSO_4 , and the major portion of the product decomposition occurs in a single step which resembles that observed during the decomposition of pure $\text{ZnO} \cdot 2\text{ZnSO}_4$. Although the rate constants and activation energy for the product decomposition in its later stage are rather different from those observed for pure $\text{ZnO} \cdot 2\text{ZnSO}_4$, the integral yield curves used to calculate these parameters are rather imprecise and we suspect the product is either $\text{ZnO} \cdot 2\text{ZnSO}_4$ or a mixture of ZnSO_4 and $\text{ZnO} \cdot 2\text{ZnSO}_4$. In any case it was possible to demonstrate that the product decomposition leads to complete recovery of the sulfur (as SO_2 and SO_3) available in the original $\text{ZnO}/\text{NH}_4\text{HSO}_4$ reactant mixture.

TABLE VIII

SUMMARY OF THE KINETICS OF THE THERMAL DECOMPOSITIONS OF
 $ZnSO_4$, $ZnO \cdot 2ZnSO_4$ AND PRODUCT OF DECOMPOSITION OF ZnO/NH_4HSO_4

<u>COMPOUND</u>	<u>TEMP.</u> <u>(°C)</u>	<u>SO₃ CONTENT</u> <u>(mmoles)</u>	<u>k₀ × 10³</u> <u>(min⁻¹)</u>	<u>k₁^a × 10⁵</u> <u>(min⁻¹ mole)</u>	<u>E_a^b</u> <u>(kcal/mole)</u>
$ZnSO_4$	900	4.669	0.985	0.460	73.2 ± 5.8
	920	4.680	2.534	1.186	
	940	4.670	2.745	1.282	
	940	6.054	3.249	1.967	
	960	5.135	4.110	2.110	
	980	4.846	8.822	4.275	
$ZnO \cdot 2ZnSO_4$	920	4.749	1.728	0.821	76.3 ± 8.3
	940	3.591	3.499	1.256	
	960	4.935	4.141	2.044	
	960	4.805	4.681	2.296	
	960	8.181	2.848	2.330	
	980	4.182	8.991	3.760	
Res AHS + 1.5 ZnO	860	3.672	0.467	0.172	60.3 ± 2.7
	880	3.649	1.140	0.416	
	900	3.714	1.273	0.473	
	920	3.655	1.953	0.714	
	920	2.449	4.377	1.072	
	940	3.569	3.359	1.199	
	960	2.686	5.926	1.592	
	960	3.660	4.760	1.742	
	980	2.282	12.766	2.913	

- Notes: a. Calculated using a standard least squares fit. $k_1 = k_0 M_0$.
- b. Calculated using the individual Probable Errors for each k_1 ($\sigma_{k_1} = \sigma_{k_0} \cdot M_0$, since σ_{M_0} is very small), and a rigorous least squares adjustment procedure.
- c. Experiments involved measurement of rate of weight loss from sample during decomposition (see ref 13).

III

THERMAL DECOMPOSITION OF PURE ZnSO_4

Since the thermal decomposition of the product of reaction 1c' produces a mixture of $\text{SO}_2(\text{g})$ and $\text{SO}_3(\text{g})$, it was considered important to examine the rate and relative ratio at which these two gases are evolved. Since the product of reaction 1c' is apparently a mixture of ZnSO_4 and $\text{ZnO} \cdot 2\text{ZnSO}_4$, it was considered expedient to use the thermal decomposition of pure ZnSO_4 to develop and test methods for making these measurements.

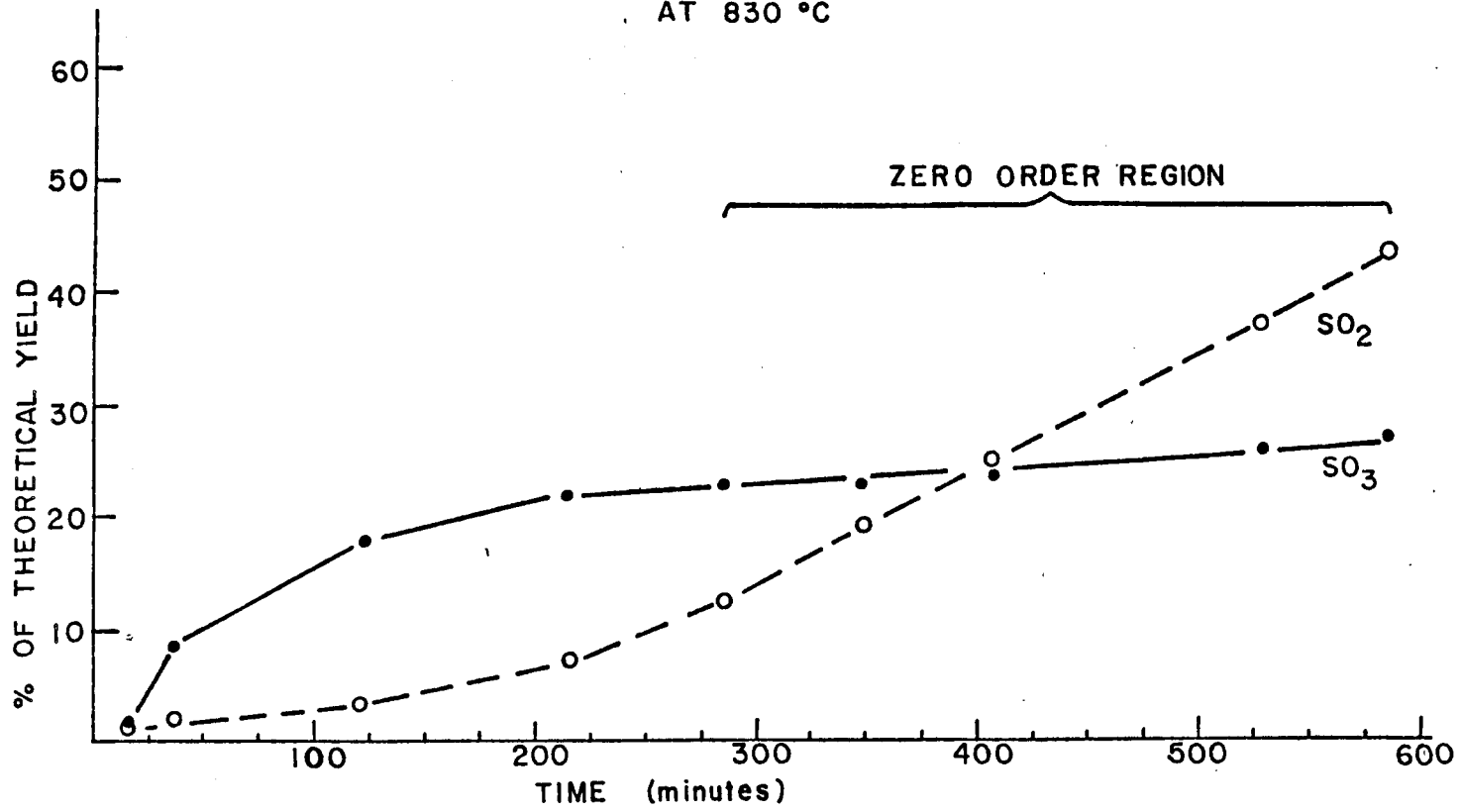
Preliminary Experiments -

The method used for studying the net stoichiometry of reaction 1d (see Appendix G) can also be used to provide a measure of separate $\text{SO}_2(\text{g})$ and $\text{SO}_3(\text{g})$ yields at any time after initiation of the reaction. To obtain yields as a function of time, the test solution was changed at regular intervals and each solution analyzed separately. As a practical matter, sampling was limited to a maximum frequency of ~20 minutes. This method was used to obtain preliminary results for the decomposition of pure ZnSO_4 .¹⁴

Yields of $\text{SO}_2(\text{g})$ and $\text{SO}_3(\text{g})$ were measured as a function of reaction time and temperature. A typical set of data is shown in Figure 2 for decomposition at 830°C. Similar results were obtained at temperatures within the range 830-950°C. These results showed: that at all temperatures the decomposition of ZnSO_4 produces mostly $\text{SO}_3(\text{g})$ during its early stages and mostly $\text{SO}_2(\text{g})$ during its later stages; and that the rate of $\text{SO}_3(\text{g})$ production is approximately zero

FIGURE 2.

SO₃ AND SO₂ YIELD FROM THE THERMAL DECOMPOSITION OF ZnSO₄
AT 830 °C



order over a significant portion of the decomposition. The zero order rate constants calculated for the rate of $\text{SO}_2(\text{g})$ production at each temperature are given in Table IX. These were used to calculate an Arrhenius activation energy (see Figure 3) of 50.34 kcal/mole.

This activation energy (50.34 kcal/mole) is somewhat different from the activation energy (73.2 kcal/mole) obtained previously for the zero order decomposition of ZnSO_4 as calculated from weight loss data (see Table VIII). However, in both experiments (weight loss and product gas measurement) rather large (~1g) samples of ZnSO_4 were used, and the removal of product gases from the surface of the decomposing solid was inefficient and not necessarily comparable. The rate data from each experiment and thus the activation energies calculated are most likely pertinent only to the respective reaction conditions.

Improved Method for Measuring $\text{SO}_2(\text{g})$ and $\text{SO}_3(\text{g})$ Simultaneously -

The development of a method for measuring simultaneously and continuously the $\text{SO}_3(\text{g})$ and $\text{SO}_2(\text{g})$ produced in the thermal decomposition of ZnSO_4 and related compounds involved a major research effort. Several methods described in the literature were tested and found inadequate (see Appendix H for a discussion of methods evaluated). An entirely new method has been developed and its description published.¹⁵

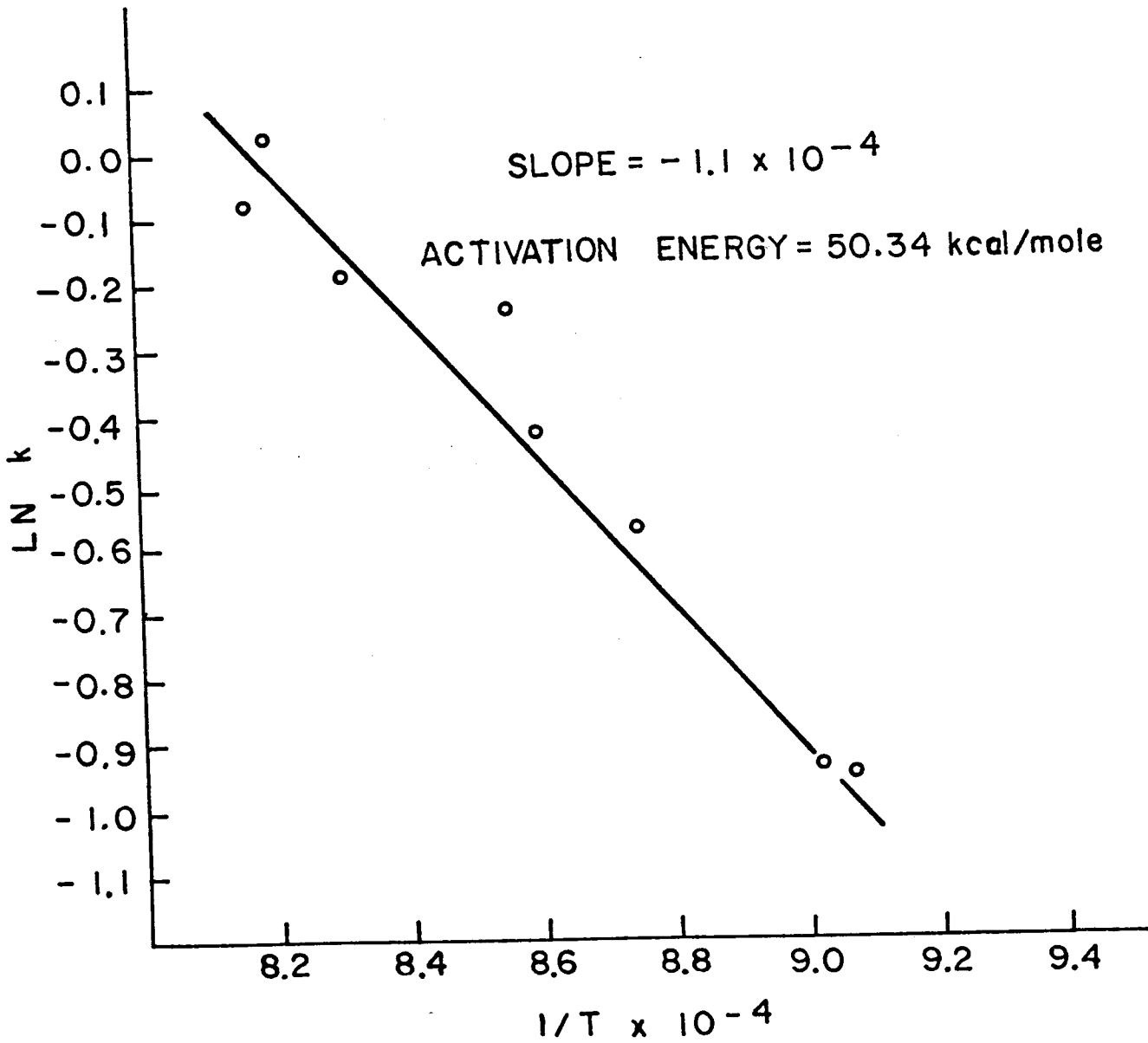
In this method, the product gases are entrained in an inert gas flow and swept first through a heated tube containing calcium oxalate (CaC_2O_4) and thence through two optical cells in series. The CaC_2O_4 serves to convert any $\text{SO}_3(\text{g})$ present in the carrier flow to CO_2 but does not react with the $\text{SO}_2(\text{g})$. $\text{SO}_2(\text{g})$

TABLE IX
 SUMMARY OF SO₂ YIELD RATE AS A FUNCTION OF TEMPERATURE
 FOR THERMAL DECOMPOSITION OF ZnSO₄- ANALYSIS BY TITRATION

Reaction Temperature (°C)	ZnSO ₄ Sample (millimoles)	Zero Order Rate Constant K _{SO₂}
830	5.801	0.113 %/min
850	5.490	0.269
870	10.723	0.265
888	7.121	0.373
895	7.725	0.570
931	7.121	0.643
947	6.875	1.063
950	14.276	0.833

FIGURE 3.

ARRHENIUS PLOT FOR RATE OF SO₂ FROM
THERMAL DECOMPOSITION OF ZnSO₄



is measured at the first optical cell which is part of a nondispersive ultraviolet monitor set to detect SO_2 absorption. CO_2 is measured at the second optical cell which is part of a nondispersive infrared monitor set to measure CO_2 absorption. A more complete discussion of the method is given in Appendix I.

The apparatus designed allows the use of smaller ZnSO_4 samples (~ 0.1 g) and faster carrier gas flows (up to 300 cc/min) than were possible in the experiments described previously. It has been shown¹⁶ that the rate of reaction can be determined directly from the measured absorbance curves, and that the area under each curve is directly proportional to the respective product yield.

A typical set of curves observed for the decomposition of ZnSO_4 at 945°C is shown in Figure 4. The sum of the $\text{SO}_3(\text{g})$ and $\text{SO}_2(\text{g})$ yields measured by integration of the area under each curve consistently equals 100% of the SO_4^{2-} present in the initial ZnSO_4 sample. The observed absorbance intensity at any point on a curve is directly proportional to reaction rate at that time, and the curve itself reflects the way the reaction rate changes as a function of extent of reaction.

This method has been used to study the thermal decomposition of ZnSO_4 as a function of various reaction conditions.

Evidence of Two Reactions in the Decomposition of ZnSO_4 -

Data obtained using the method described above confirm that the decomposition of pure ZnSO_4 involves two separate reactions.¹⁶ (see Figure 5) A low temperature process becomes significant at $\sim 740^\circ\text{C}$ yielding ~ 7 mole percent total

FIGURE 4.

ZINC SULFATE DECOMPOSITION AT 945 °C

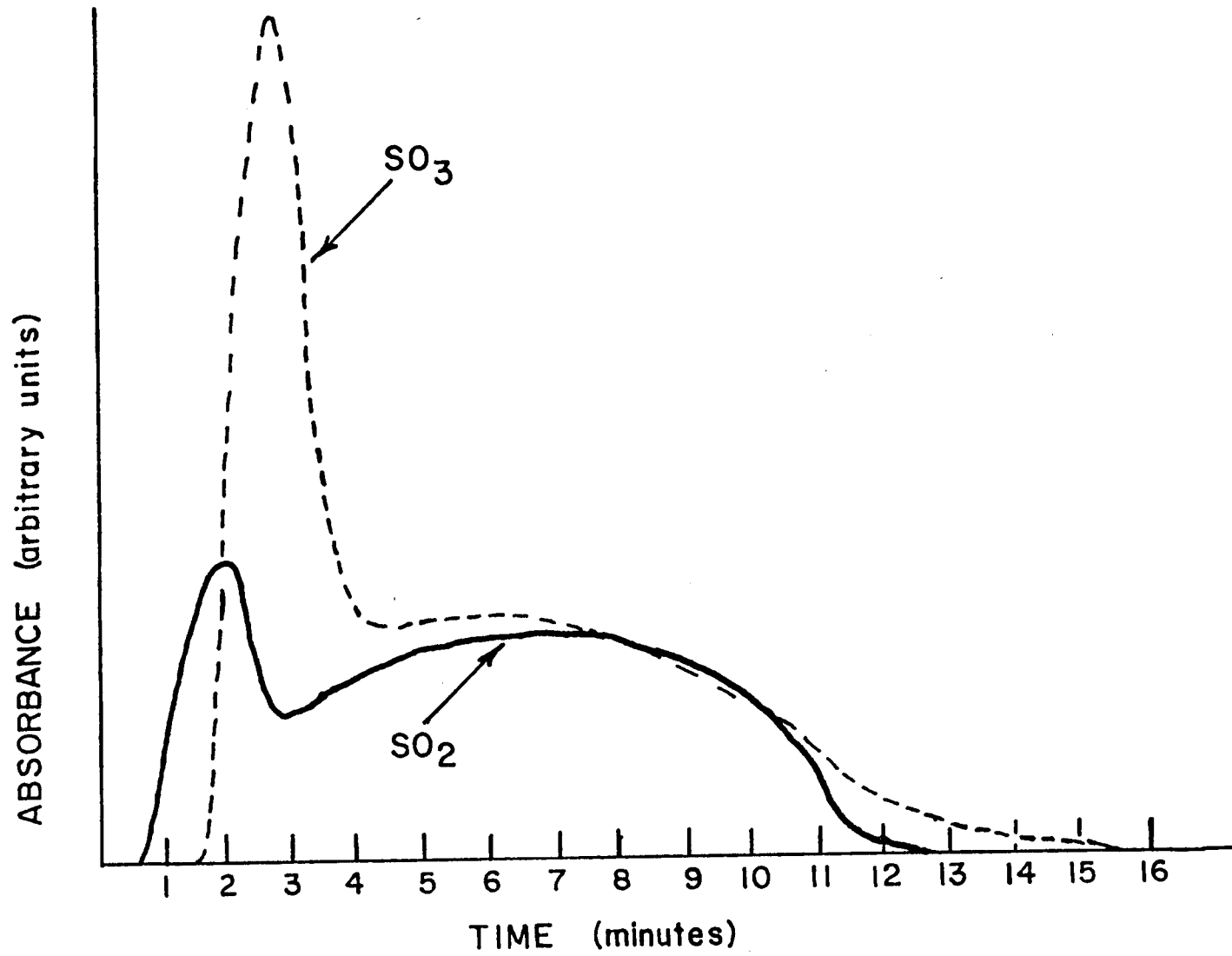


FIGURE 5.

ZINC SULFATE DECOMPOSITION

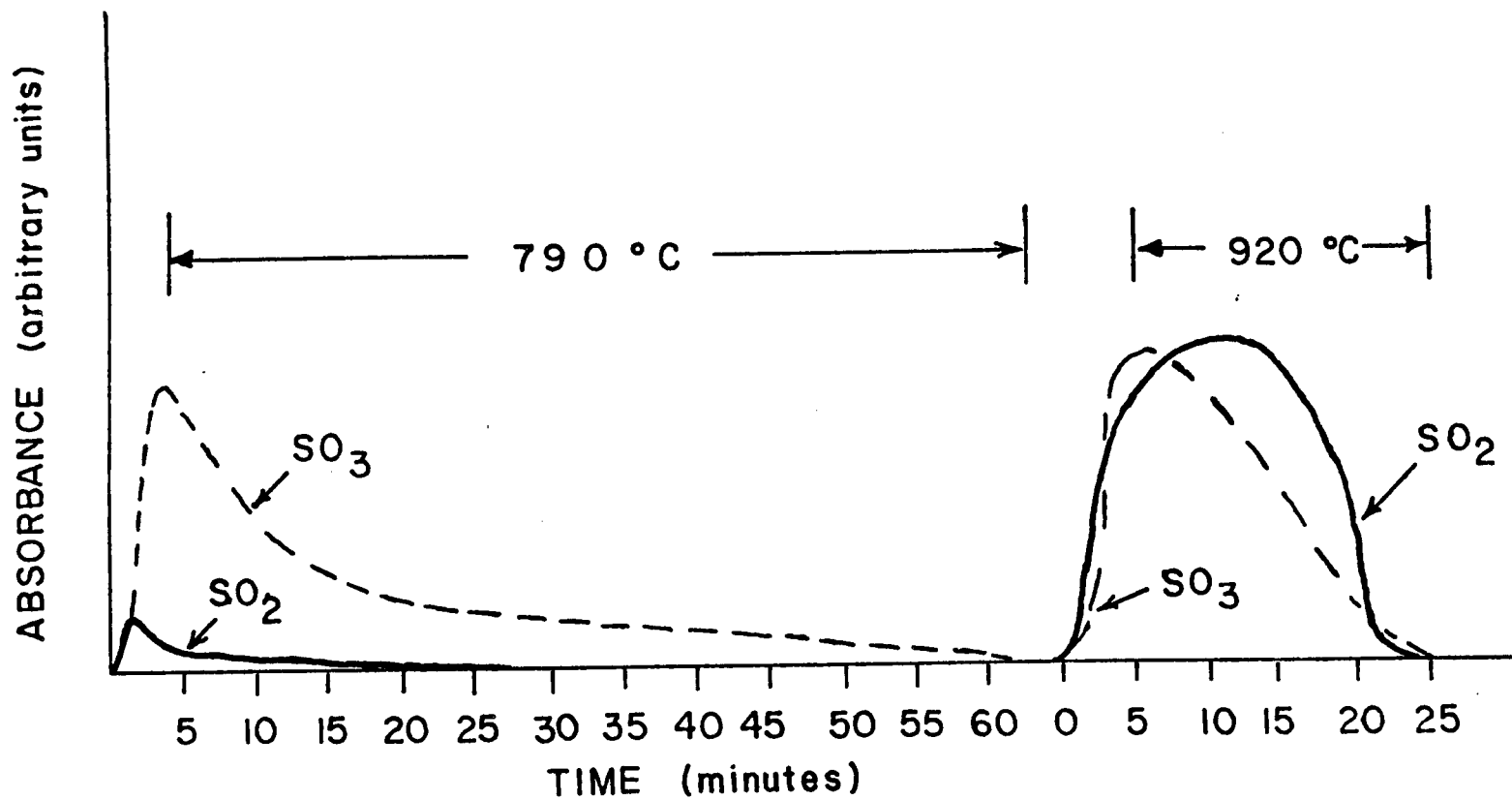
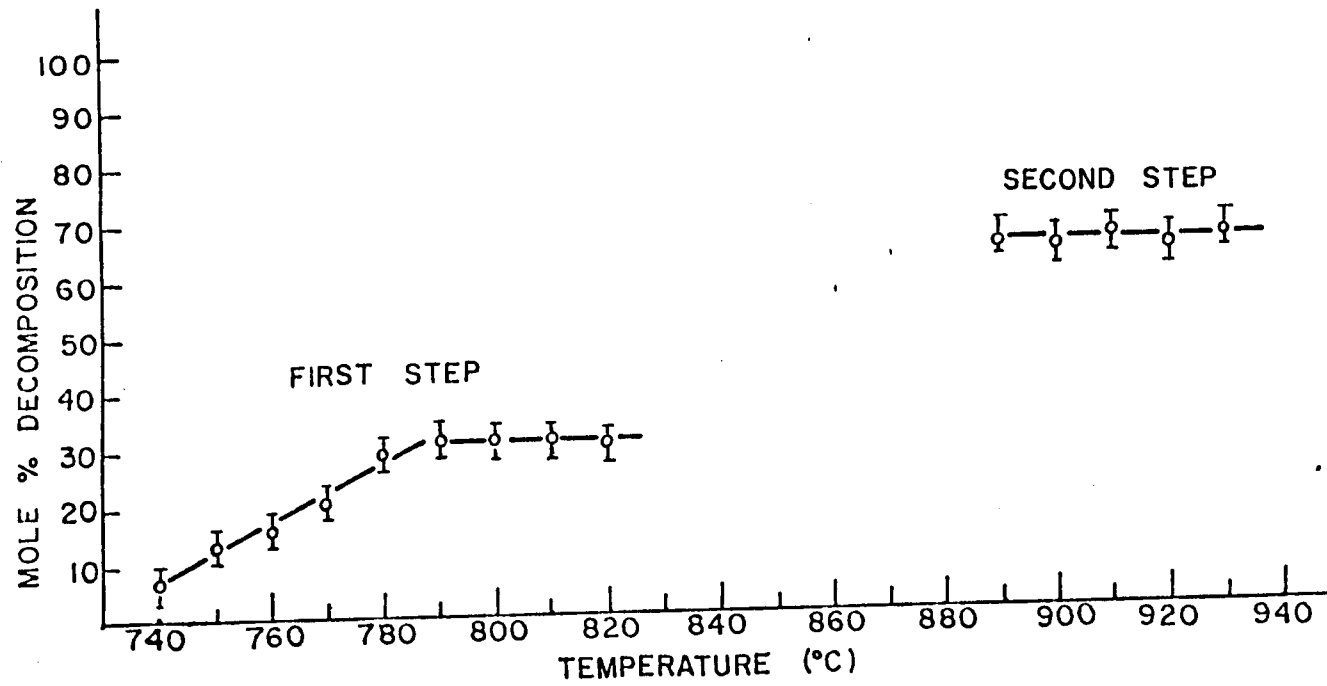
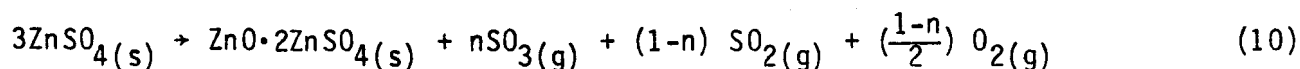


FIGURE 6.

% DECOMPOSITION OF $ZnSO_4$ AS A FUNCTION OF TEMPERATURE

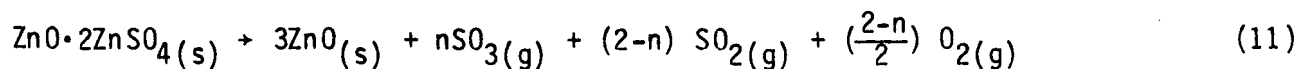


conversion of the available sulfur to SO_2 and SO_3 before reaction becomes undetectable. The extent of decomposition via this reaction increases as reaction temperature is increased from 740 to 780°C. At temperatures between 780 to 820°C the extent of reaction remains constant. (see Figure 6) Within this temperature range the average value for the net decomposition as measured by the sum of the $\text{SO}_3(\text{g})$ and $\text{SO}_2(\text{g})$ yields is 30.1 mole percent. The mole ratio SO_3/SO_2 has an average value of 3.9, indicating that $\text{SO}_3(\text{g})$ is the major product for this reaction step, and is independent of flow rate over the range 150-300 cc/min. The data are consistent with the stoichiometry represented by:



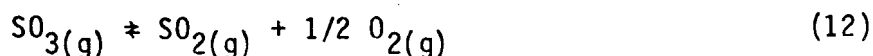
Where $0 < n < 1$. Our experiments give an average value $n = .80$.

A high temperature process was observed over the range 890-930°C. This reaction consistently completes conversion of all sulfur initially present in the ZnSO_4 sample to SO_2 or SO_3 . The extent of decomposition has an average value of 65 mole percent. The data are consistent with the stoichiometry represented by:



Where $0 < n < 2$. Our experiments give an average value of $n = .79$ indicating that this reaction step produces slightly more $\text{SO}_2(\text{g})$ than $\text{SO}_3(\text{g})$.

The values of n for reactions 10 and 11 may be a function of experimental conditions other than temperature, but our results indicate they are not significantly influenced by the gas phase equilibrium:



In general reaction 12 favors the formation of SO_2 as temperature is increased,

and equilibrium is catalyzed by contact with platinum. In these experiments the ratio SO_3/SO_2 remained constant as carrier gas flow rate was varied over the range 150-300 cc/min. Lower ratios were observed only at lower flow rates and when the gases were passed over platinum before detection.¹⁶ The ratios reported above are most likely the nonequilibrium ratios in which the products leave the decomposing solid.

Rates of Reaction for Production of SO_2 and SO_3 from ZnSO_4 -

Although the rates of $\text{SO}_3(\text{g})$ and $\text{SO}_2(\text{g})$ production can be measured directly from the respective absorbance curves obtained during the decomposition of ZnSO_4 samples, attempts to calculate rate constants as a function of temperature gave irreproducible results, and data suitable for calculating an activation energy have not yet been obtained. The measured rates depend to some extent on sample size and surface area. However, it is important to note that the overall rate of reaction observed in these experiments is considerably faster than that observed in previous experiments. It was also possible to compare qualitatively the rate of decomposition of pure ZnSO_4 to the rate of decomposition of a mixture containing excess ZnO .¹⁶

Effect of Excess ZnO on Decomposition of ZnSO_4 -

When a mixture of ZnSO_4 and excess ZnO is heated, no low temperature (<800°C) decomposition is observed.¹⁶ Apparently $\text{ZnO}\cdot 2\text{ZnSO}_4$ is formed efficiently without release of sulfur oxides from the bulk of the sample. When the

mixture is heated to 920°C both $\text{SO}_2(\text{g})$ and $\text{SO}_3(\text{g})$ are observed indicating decomposition of the oxysulfate. The presence of excess ZnO, however, increases dramatically the rate at which these products are formed. Figure 7 shows a comparison of the rate of decomposition of $\text{ZnO}\cdot 2\text{ZnSO}_4$ obtained from pure ZnSO_4 with the rate of decomposition of $\text{ZnO}\cdot 2\text{ZnSO}_4$ obtained by heating ZnSO_4 with excess ZnO. Since ZnO does not catalyze reaction 12 efficiently, the catalytic effect of ZnO on reaction 11 must occur within the bulk of the sample mixture.

Effect of Additives on the Decomposition of ZnSO_4 -

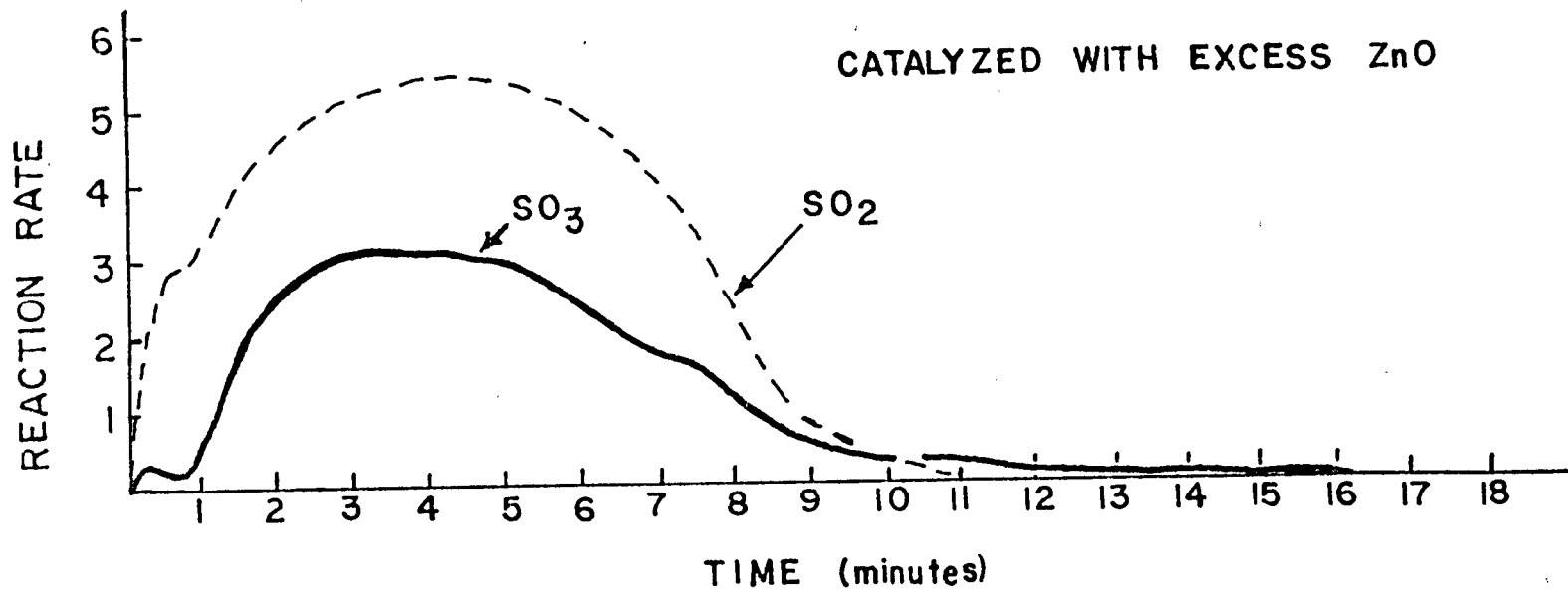
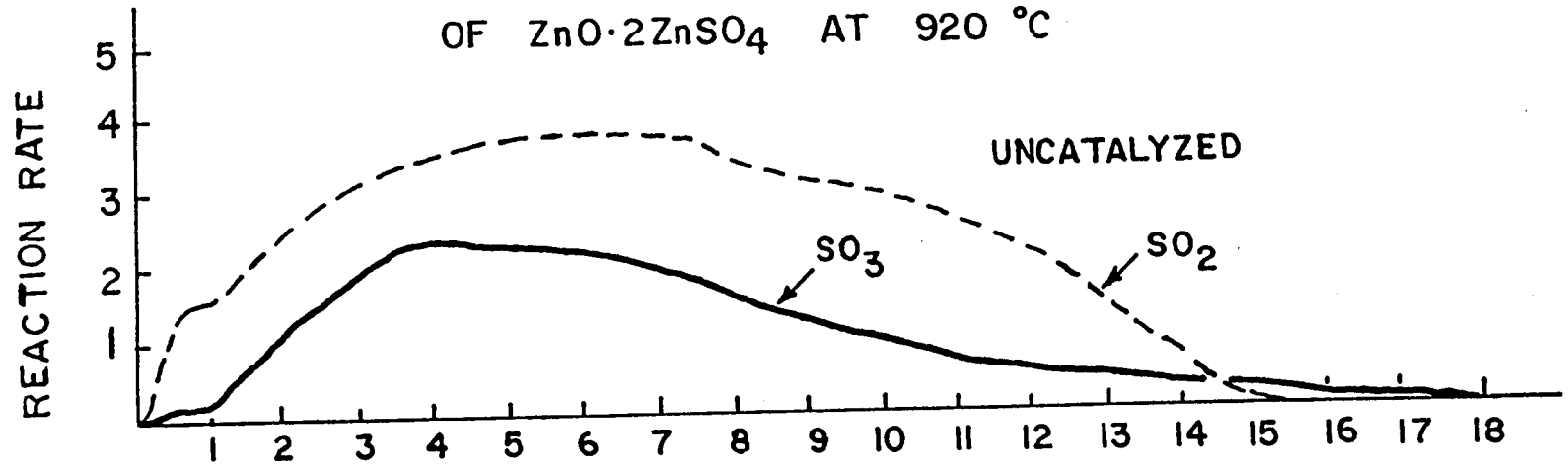
Since the temperature required to decompose ZnSO_4 completely to ZnO is rather high with respect to the temperature currently available from solar power facilities (ie. Solar One) an attempt was made to identify catalysts which might be used to lower the decomposition temperature. In addition, since the reactions of solids are more difficult to control in large scale reactors than those of fluids, an attempt was made to identify substances which, when mixed with ZnSO_4 and heated, would form a liquid solution or melt without significantly altering the decomposition chemistry.

Thermal Decomposition of $\text{ZnSO}_4/\text{NaCl}$ Mixtures -

Mixtures of $\text{ZnSO}_4/\text{NaCl}$ were known to be fluid at temperatures well below the melting point of either solid, and decomposition at ~500°C has been reported in the literature. A series of experiments were carried out to further characterize this system.

FIGURE 7.

RATE OF PRODUCT FORMATION FROM THE THERMAL DECOMPOSITION
OF $ZnO \cdot 2ZnSO_4$ AT $920^\circ C$



Experiments were done to define at what temperatures and compositions the mixture was fluid.¹¹ Mixtures having a mole fraction of $ZnSO_4$ (X_{ZnSO_4}) in the range 0.1 to 0.8 were heated until a clear liquid formed. The rate of cooling was monitored, and the appearance of the sample observed. Changes in cooling rate considered indicative of thermal events were recorded as was the temperature at which precipitation first occurred. These data are shown in Figure 8 as a liquidus curve. The results indicate that the mixture $ZnSO_4/NaCl$ does not form a simple eutectic system. This was confirmed by conventional Differential Thermal Analysis experiments which also indicated multiple thermal events which could not be readily interpreted.

Weight loss from samples of $ZnSO_4/NaCl$ mixtures was measured as a function of time, temperature, and composition.¹¹ The results could not be interpreted in terms of a simple conversion of the available sulfur to sulfur oxides. This was confirmed by additional experiments in which the volatile products were analyzed. A significant amount of $ZnCl_2$ was evolved at $200^\circ C$, and at this temperature less than 30% of the available sulfur was evolved as $SO_2(g)$ or $SO_3(g)$.

Thermal Decomposition of Eutectic Mixtures Containing $ZnSO_4$ -

Some eutectic mixtures which include $ZnSO_4$ per se or as a reciprocally formed compound are listed in Table X. A number of these were prepared and the weight loss produced by thermal decomposition measured.¹¹ The weight loss was calculated as a percentage of the available SO_4 in the mixture as prepared. Results are summarized in Table XI.

In general the mixtures containing alkali halides decomposed to a greater extent than could be explained by simple conversion of the available SO_4 to

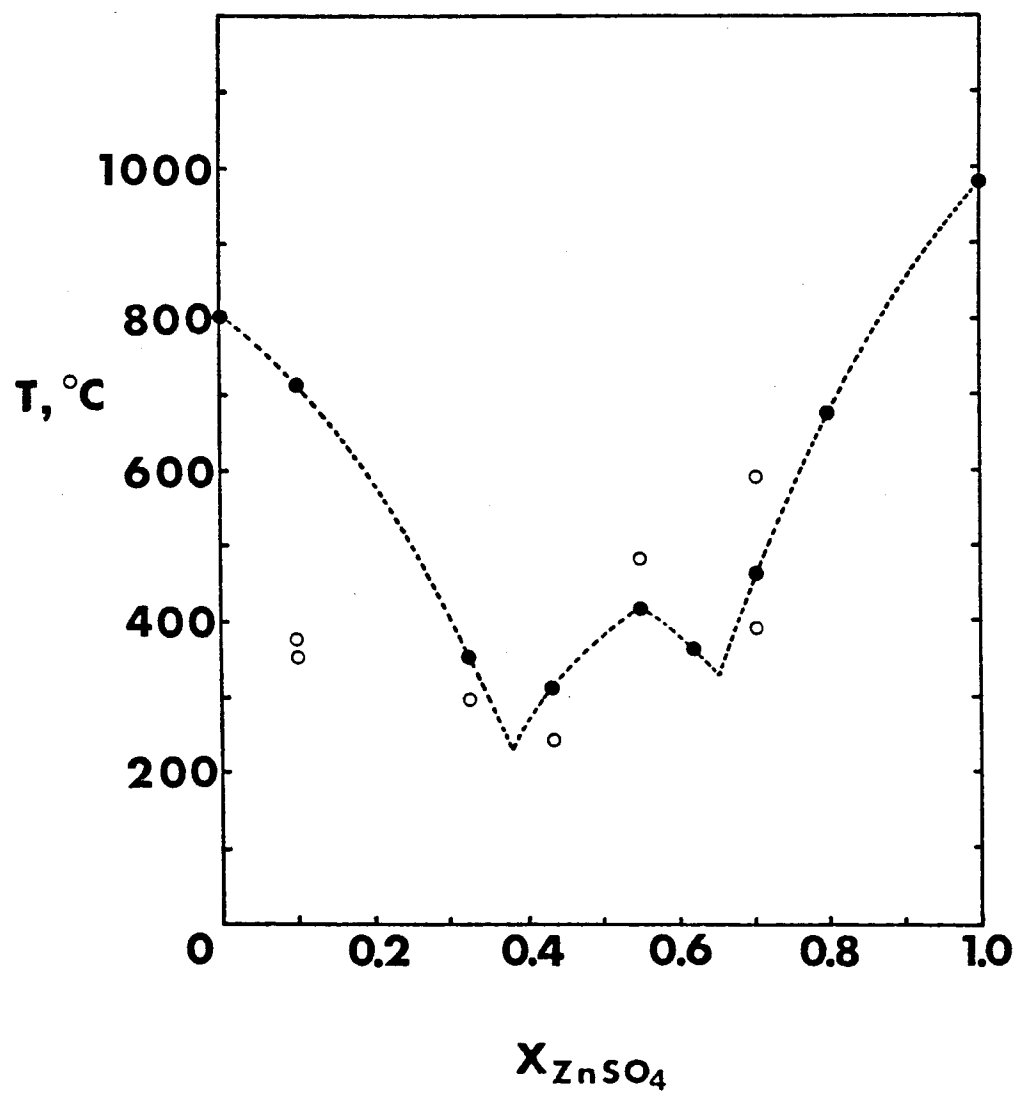


FIGURE 8. Liquidus curve for mixture ZnSO₄/NaCl
 ● Temperature at which precipitation first occurs
 ○ Unidentified change in rate of cooling

TABLE X

EUTECTIC SYSTEMS CONSIDERED FOR THE THERMAL DECOMPOSITION OF ZnSO_4 .

System	Xa, Xb, Xc	Melting Point, °C
$\text{Na}_2\text{SO}_4/\text{ZnSO}_4$	0.450, 0.550	472.0
	0.575, 0.425	478.0
$\text{K}_2\text{SO}_4/\text{Na}_2\text{SO}_4/\text{ZnSO}_4$	0.190, 0.258, 0.552	385.0
	0.302, 0.291, 0.407	384.0
	0.245, 0.334, 0.421	388.0
	0.340, 0.225, 0.435	392.0
$\text{K}_2\text{SO}_4/\text{ZnSO}_4$	0.570, 0.430	450.0
	0.230, 0.770	475.0
	0.430, 0.570	440.0
$\text{Li}_2\text{SO}_4/\text{ZnSO}_4$	0.600, 0.400	459.0
$\text{Li}_2\text{SO}_4/\text{Na}_2\text{SO}_4/\text{ZnSO}_4$	0.400, 0.240, 0.320	366.0
$\text{Li}_2\text{SO}_4/\text{ZnCl}_2/\text{ZnSO}_4$	0.007, 0.930, 0.090	293.0
$\text{Li}_2\text{SO}_4/\text{ZnCl}_2$	0.010, 0.990	310.0
$\text{ZnCl}_2/\text{ZnSO}_4$	0.900, 0.100	300.0
$\text{LiCl}/\text{Li}_2\text{SO}_4/\text{ZnCl}_2$	0.230, 0.005, 0.765	285.0
KCl/ZnSO_4	0.344, 0.656	466.0
	0.666, 0.334	295.0
$\text{KCl}/\text{NaCl}/\text{ZnSO}_4$	0.330, 0.335, 0.335	290.0
	0.250, 0.200, 0.550	290.0
KBr/ZnSO_4	0.675, 0.325	395.0
	0.413, 0.587	470.0
KI/ZnSO_4	0.473, 0.527	435.0
	0.658, 0.342	360.0

TABLE XI
 EXPERIMENTAL WEIGHT LOSS DATA FOR THE MELTS SCREENED FOR
 THE DECOMPOSITION OF $ZnSO_4$

<u>System of $ZnSO_4$ plus:</u>	<u>X ($ZnSO_4$)</u>	<u>Time (hours held at 700°C)</u>	<u>Weight loss^a (at 700°C)</u>	<u>Time(hours held at 900°C)</u>	<u>Weight loss (cumulative)</u>
LiCl	0.495	16	83	25	126
NaCl ^c	0.358	18	136	0	136 ^c
KCl	0.360	11	43	35	132
$ZnCl_2$ ^d	0.493	8	194	0	194 ^d
Li_2SO_4	0.560	12	10	4	35
Na_2SO_4	0.680	20	1	5	10
Na_2SO_4/K_2SO_4 ^e	0.208	1	0	18	4 ^e
Rb_2SO_4	0.508	15	9	50	91
Cs_2SO_4	0.508	14	5	17	25

- Notes:
- a) The weight losses are given as percent of the initial SO_3 available as sulfate in the $ZnSO_4$.
 - b) All the samples were liquids with yellowish spots at the end of the experiments (except where otherwise specified).
 - c) See also the section on sodium chloride effect.
 - d) This system was tested in the flow apparatus, rather than in the weight loss analyzer at a temperature of 790°C and a N_2 flow of 111 cc/min. Also, it was a liquid only during the first few minutes of the test.
 - e) $X(Na_2SO_4) = 0.374$, $X(K_2SO_4) = 0.418$. This system was a liquid at the beginning of the experiment, but no observation was made on the nature of the residue.

$\text{SO}_3(\text{g})$ and $\text{SO}_2(\text{g})$. The mixtures containing alkali metal sulfates all formed melts, but in general decomposed at rates slower than that observed for pure ZnSO_4 . Only the mixture containing Li_2SO_4 decomposed at a rate comparable to that of pure ZnSO_4 . The heavier alkali metal sulfates are known to form stable pyrosulfates, whereas Li_2SO_4 does not form such a compound. The $\text{Li}_2\text{SO}_4/\text{ZnSO}_4$ mixture was selected for further investigation.

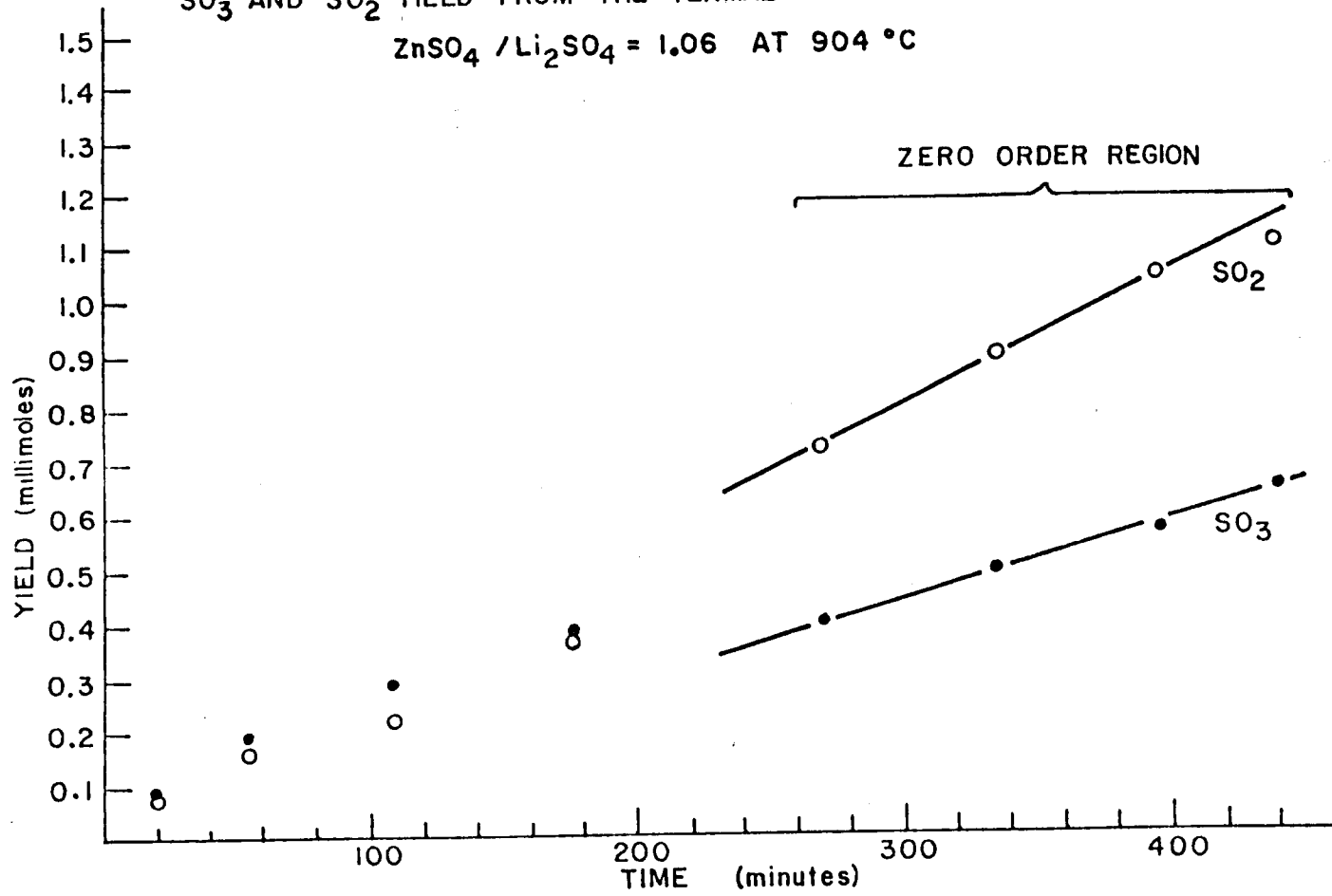
Thermal Decomposition of $\text{ZnSO}_4/\text{Li}_2\text{SO}_4$ Mixtures -

A preliminary experiment was done using a mixture of ZnSO_4 and Li_2SO_4 having a mole ratio $\text{ZnSO}_4/\text{Li}_2\text{SO}_4 = 1.27$. This was decomposed in a quartz sample boat at 920°C , and the separate $\text{SO}_2(\text{g})$ and $\text{SO}_3(\text{g})$ yields determined as a function of time at regular intervals using the apparatus and titration procedure described in Appendix G. The sample was liquid at 920°C initially, but solidified before the decomposition was complete. The sum of the $\text{SO}_2(\text{g})$ and $\text{SO}_3(\text{g})$ yields at the point where further decomposition became unobservable was equal to 103.5% of the sulfur initially present as ZnSO_4 .

Additional experiments were done with a mixture having a mole ratio $\text{ZnSO}_4/\text{Li}_2\text{SO}_4 = 1.06$ using the same procedures (Appendix G). The $\text{SO}_2(\text{g})$ and $\text{SO}_3(\text{g})$ yields from this mixture were measured at regular intervals as a function of time and temperature.¹⁷ A typical set of data is shown in Figure 9 for decomposition at 904°C . Similar results were obtained at 946°C . The results showed that both the rate of $\text{SO}_2(\text{g})$ production and the rate of $\text{SO}_3(\text{g})$ production are zero order over a significant portion of the decomposition. The zero order rate constants calculated from the rate of $\text{SO}_2(\text{g})$ production are given in Table

FIGURE 9.

SO₃ AND SO₂ YIELD FROM THE THERMAL DECOMPOSITION OF MIXTURE
ZnSO₄ / Li₂SO₄ = 1.06 AT 904 °C



XII. These were used to calculate an Arrhenius activation energy (see Figure 10) of 66.15 kcal/mole. This is larger than the activation energy (50.34 kcal/mole) calculated for $\text{SO}_2(\text{g})$ production from pure ZnSO_4 under similar conditions. Although the rate data from these two experiments, and thus the activation energies calculated, are most likely pertinent only to the reaction conditions used, the conditions were similar in both experiments and the activation energies (50.34 kcal/mole for ZnSO_4 , and 60.15 kcal/mole for $\text{ZnSO}_4/\text{Li}_2\text{SO}_4$) provide a reasonable kinetic comparison of the two chemical systems.

Finally,¹⁶ a sample of a mixture having a mole ratio $\text{ZnSO}_4/\text{Li}_2\text{SO}_4 = 0.67$ was decomposed at 969°C using the apparatus and procedures described in Appendix I, and the yields of $\text{SO}_2(\text{g})$ and $\text{SO}_3(\text{g})$ measured separately and continuously as a function of time. The mixture was prepared by combining weighed amounts of ZnSO_4 and $\text{Li}_2\text{SO}_4 \cdot \text{H}_2\text{O}$ and heating at 600°C until a homogeneous mixture was obtained. This was cooled and the recrystallized solid ground and mixed. Samples were decomposed in a quartz boat. Representative experimental absorbance curves for $\text{SO}_2(\text{g})$ and $\text{SO}_3(\text{g})$ production are shown in Figure 11. Similar results for the decomposition of pure ZnSO_4 are also shown in this figure for comparison. Significant data are compiled in Table XIII.

For the mixture ($\text{ZnSO}_4/\text{Li}_2\text{SO}_4$) the sum of the $\text{SO}_2(\text{g})$ and $\text{SO}_3(\text{g})$ yields at the point where further decomposition becomes unobservable is equal to 99.2% of the sulfur available from the ZnSO_4 initially present in the mixture. The mole ratio of the total yields (SO_3/SO_2) is 0.82 which is slightly less than that obtained (1.1) for the decomposition of pure ZnSO_4 under similar conditions.

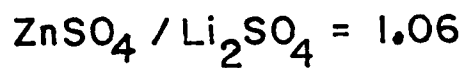
The decomposition from the mixture ($\text{ZnSO}_4/\text{Li}_2\text{SO}_4$) appears to occur with an overall rate which is considerably slower than the decomposition of pure ZnSO_4 .

TABLE XII
 SUMMARY OF SO₂ and SO₃ YIELD RATES AS A FUNCTION OF TEMPERATURE FOR
 THERMAL DECOMPOSITION OF ZnSO₄/Li₂SO₄-ANALYSIS BY TITRATION

<u>Reaction Temperature (°C)</u>	<u>ZnSO₄/Li₂SO₄ Sample (mole ratio)</u>	<u>Zero Order Rate Constant KSO₂</u>
904	1.05	1.58 x 10 ⁻³ mmole/min
946	1.06	4.21 x 10 ⁻³

FIGURE 10.

ARRHENIUS PLOT FOR RATE OF SO₂ FROM
THERMAL DECOMPOSITION OF MIXTURE



SLOPE = -3.34×10^{-4}

ACTIVATION ENERGY = 66.15 kcal/mole

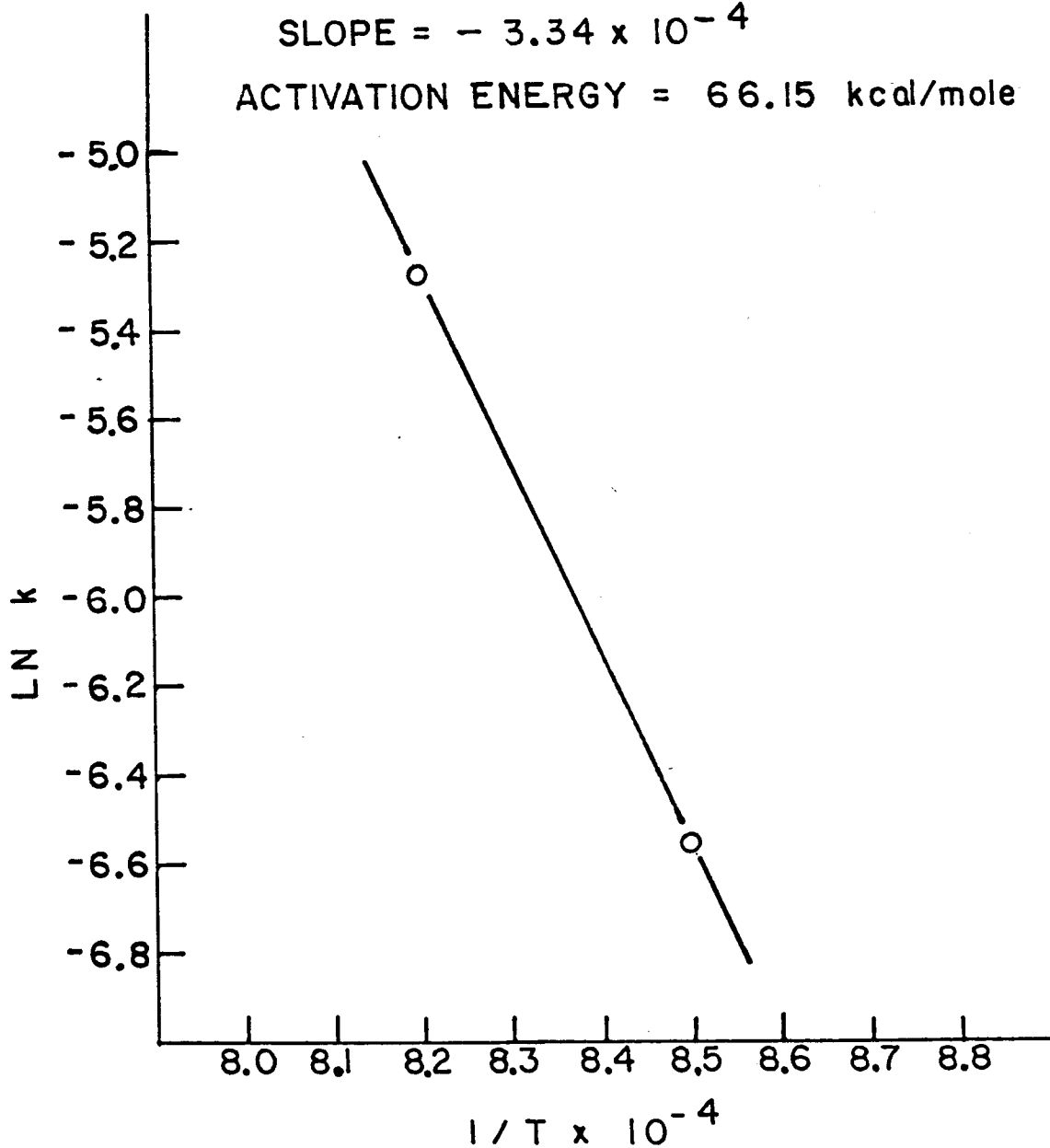


FIGURE 11

RATE OF PRODUCT FORMATION FROM
THE THERMAL DECOMPOSITION OF

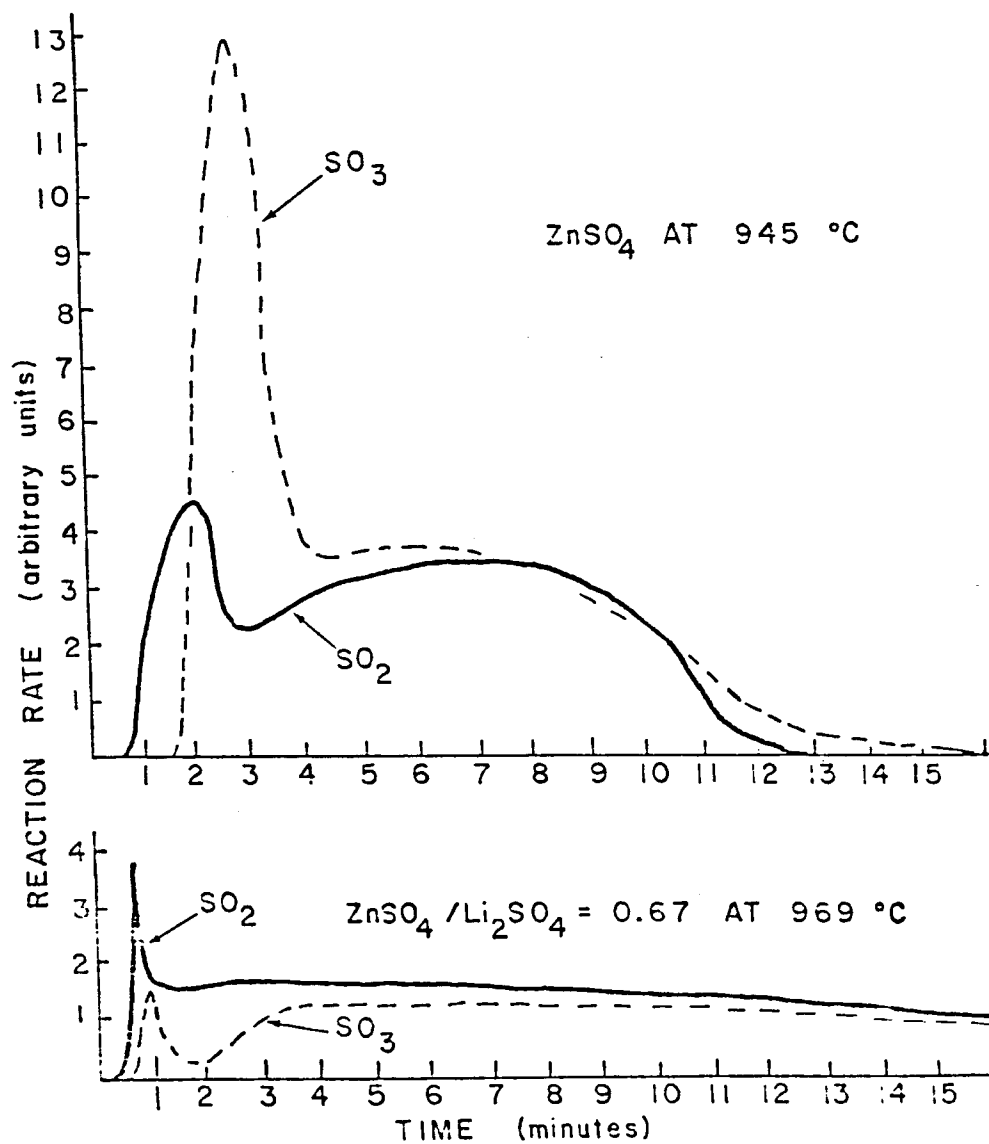


TABLE XIII
 COMPARISON OF DATA FOR THERMAL DECOMPOSITION OF PURE $ZnSO_4$ AND MIXTURE
 $ZnSO_4/Li_2SO_4$

SAMPLE MOLE RATIO		TEMP. (°C)	TOTAL YIELDS			MOLE RATIO SO_3/SO_2	RXN TIME (min)
$ZnSO_4$	Li_2SO_4		% SO_2	% SO_3	SUM		
1	-	945	47.5	52.7	100.6	1.1	16
40	60	969	54.4,	44.8,	99.2	0.82	>50

- 1) Expressed percentages of the sulfur available from the $ZnSO_4$ initially present.
- 2) Quartz boat used in all experiments.
- 3) Flow rate was 150 cc/min in both experiments.

Complete decomposition of pure ZnSO_4 (.63 mmoles) occurred in only 16 min at 945°C . Decomposition of the mixture (.75 mmoles ZnSO_4) to the point at which all of the $\text{SO}_2(\text{g})$ and $\text{SO}_3(\text{g})$ yields were equal to $> 99\%$ of the sulfur available from the ZnSO_4 initially present in the mixture required > 50 min.

The shapes of the $\text{SO}_2(\text{g})$ and $\text{SO}_3(\text{g})$ absorbance curves obtained during the decomposition of the mixture ($\text{ZnSO}_4/\text{Li}_2\text{SO}_4$) indicate that two different kinetic processes are involved. Two processes are also involved in the decomposition of pure ZnSO_4 . However, the decomposition of the mixture differs from that of the pure ZnSO_4 in that the ratio SO_3/SO_2 remains nearly constant throughout the entire decomposition of the mixture, while in the decomposition of pure ZnSO_4 the ratio SO_3/SO_2 is higher during the early stages of reaction then decreases and remains nearly constant through the later stages of reaction (see Figure 11). The first process in the decomposition of pure ZnSO_4 has been associated with the formation of $\text{ZnO}\cdot 2\text{ZnSO}_4$ and the second process with the subsequent decomposition of this oxysulfate (see previous discussion). An explanation of the two processes occurring during the decomposition of the mixture, however, is not obvious.

In summary, it appears that while the decomposition kinetics may vary somewhat, both pure ZnSO_4 and a mixture of $\text{ZnSO}_4/\text{Li}_2\text{SO}_4$ can be decomposed to produce a mixture of $\text{SO}_2(\text{g})$ and $\text{SO}_3(\text{g})$. The decomposition of pure ZnSO_4 goes readily to completion at temperatures greater than 850°C , while the decomposition of the mixture ($\text{ZnSO}_4/\text{Li}_2\text{SO}_4$) at temperatures $< 970^\circ\text{C}$ appears to stop when an amount of sulfur equal to that present as ZnSO_4 has been converted to $\text{SO}_2(\text{g})$ and $\text{SO}_3(\text{g})$. The $\text{ZnSO}_4/\text{Li}_2\text{SO}_4$ mixture can be decomposed as a liquid as long as the extent of decomposition is not too great, and the temperature

required to decompose the liquid mixture is not significantly different from that required to decompose solid ZnSO_4 .

Effect of Metal Oxides on Decomposition of $\text{ZnSO}_4/\text{Li}_2\text{SO}_4$ Mixtures -

Since the $\text{ZnSO}_4/\text{Li}_2\text{SO}_4$ mixture is fluid during part of its decomposition, this reaction is more amenable to catalysis than is the decomposition of solid ZnSO_4 . Several potential catalysts were investigated using the apparatus and procedure described in Appendix G. The addition of platinum powder to the reaction mixture produced no measurable effect on the time required to complete the decomposition to $\text{SO}_2(\text{g})$ and $\text{SO}_3(\text{g})$ at 920°C , but decreased the ratio SO_3/SO_2 .¹¹ The addition of V_2O_5 powder to the reaction mixture ($\text{ZnSO}_4/\text{Li}_2\text{SO}_4$) clearly increased the rate of decomposition without changing significantly the SO_3/SO_2 ratio.¹¹

The effects of other metal oxides were investigated using the apparatus and procedure described in Appendix I. The addition of either NiO or MnO powder to the mixture ($\text{ZnSO}_4/\text{Li}_2\text{SO}_4$) lowered appreciably the temperature at which decomposition commenced, while the oxides CdO , Fe_2O_3 , and ZrO each produced only a slight lowering of the reaction onset temperature.¹⁸

It was not possible to evaluate these catalytic effects quantitatively because the mixtures all reacted with the quartz sample boat used. Containers made of stainless steel, inconel, Hasteloy-C, zirconium, nickel, and boron nitride were each tried. All were corroded or otherwise destroyed by contact with the fluid reaction mixtures containing a metal oxide. Several ceramic containers were also evaluated. Glazed porcelain was attacked severely, but Alundum (alumina) and Combax (aluminum silicate) containers proved satisfactory.

Figure 12 gives a comparison of the rate of decomposition of the mixture $\text{ZnSO}_4/\text{Li}_2\text{SO}_4$ when decomposed in a quartz boat with that observed when the decomposition is done in a Combax boat.

The shapes of the $\text{SO}_2(\text{g})$ and $\text{SO}_3(\text{g})$ absorbance curves obtained during the decomposition of the mixture ($\text{ZnSO}_4/\text{Li}_2\text{SO}_4$) in the Combax boat indicate that the decomposition occurs by several different kinetic processes. At least one, and at some temperatures two, inflection points were observed. The nature of these processes has not been studied. The sum of the $\text{SO}_2(\text{g})$ and $\text{SO}_3(\text{g})$ yields at the point where decomposition becomes negligible is typically greater than the amount of sulfur present initially as ZnSO_4 but less than the total sulfur present initially (as ZnSO_4 plus Li_2SO_4). Thus, the net decomposition of the mixture is clearly enhanced by contact with the Combax boat.

The decomposition is enhanced even more when V_2O_5 powder is added to the mixture prior to decomposition (see Figure 13 and Table XIV). In this case the net decomposition is extensive (typically equal to conversion of 75% of the total sulfur present in the initial mixture) at a temperature as low as 827°C . At 900°C complete conversion of the available sulfur to $\text{SO}_2(\text{g})$ and $\text{SO}_3(\text{g})$ was achieved. The total yield mole ratio (SO_3/SO_2) was typically equal to 0.2 which is only slightly higher than that (0.1) observed for the $\text{ZnSO}_4/\text{Li}_2\text{SO}_4$ mixture alone.

The nature of the effect of the aluminum silicate boat and of V_2O_5 on the decomposition of $\text{ZnSO}_4/\text{Li}_2\text{SO}_4$ was not investigated in detail. However it was obvious that both the molten mixture and the molten V_2O_5 permeate the porous boat. This should produce a very large reactive surface area.

FIGURE 12

RATE OF PRODUCT FORMATION FROM THE THERMAL DECOMPOSITION OF $ZnSO_4 / Li_2SO_4 = 0.67$ AT $969^\circ C$

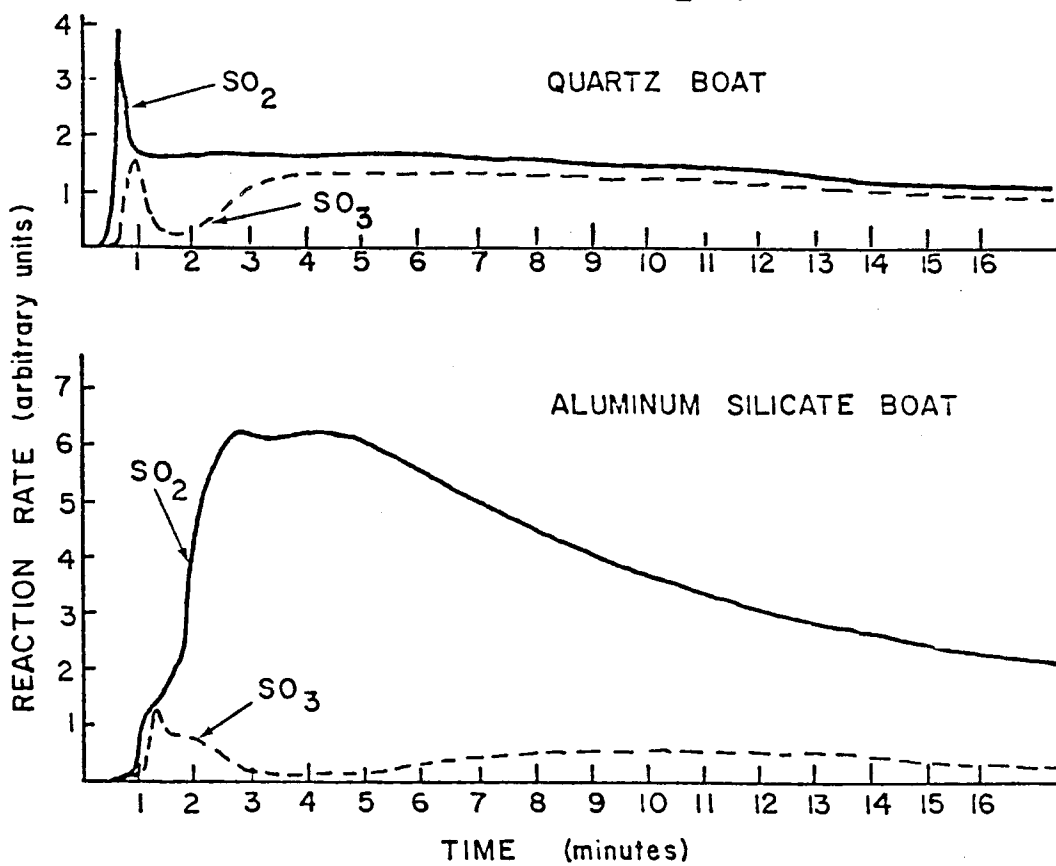


FIGURE 13

RATE OF PRODUCT FORMATION FROM
THE THERMAL DECOMPOSITION OF

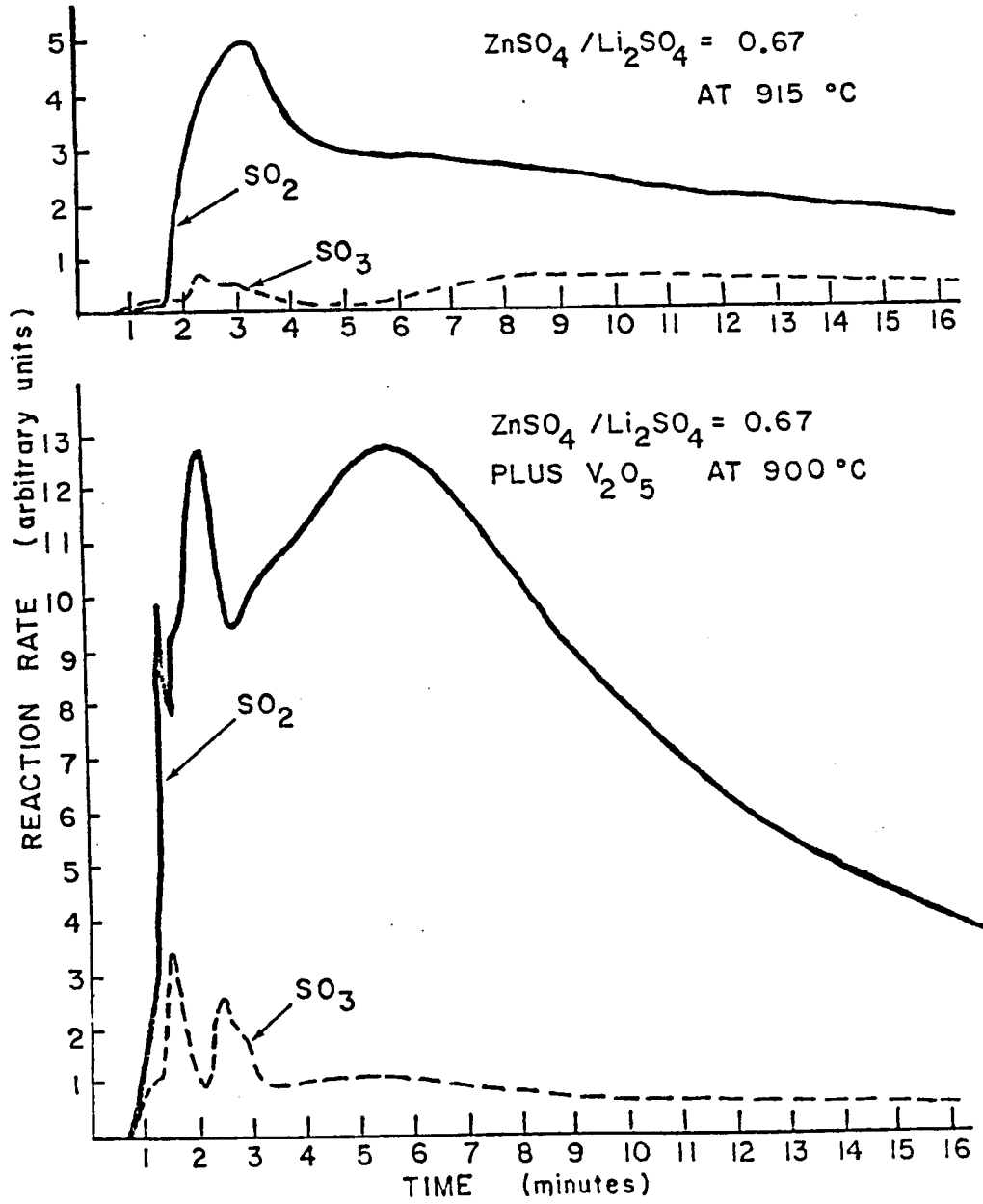


TABLE XIV

COMPARISON OF DATA FOR THERMAL DECOMPOSITION OF $\text{ZnSO}_4/\text{Li}_2\text{SO}_4$
AND $\text{ZnSO}_4/\text{Li}_2\text{SO}_4/\text{V}_2\text{O}_5$ MIXTURES

SAMPLE ZnSO_4	MOLE RATIO		TEMP (°C)	TOTAL YIELDS ⁽¹⁾			TOTAL YIELDS ⁽²⁾			MOLE RATIO SO_3/SO_2
	Li_2SO_4	V_2O_5		% SO_2	% SO_3	SUM	% SO_2	% SO_3	SUM	
1	1.5	-	915	108.0	13.6	121.6	43.6	5.5	49.1	.12
1	1.5	-	935	155.0	8.7	163.7	63.0	3.5	66.5	.06
1	1.5	-	969	159.9	15.7	175.6	64.8	6.3	71.2	.10
1	1.5	-	990	169.0	14.4	183.0	68.4	6.0	74.4	.09
1	1.5	1	827	157.1	28.2	185.3	63.6	11.4	75.0	.18
1	1.5	1	850	172.0	32.6	204.6	70.0	13.0	83.0	.20
1	1.5	1	877	214.0	32.6	246.6	86.6	13.2	99.8	.15
1	1.5	1	900	233.0	28.0	261.0	94.3	11.3	105.6	.12

1) Expressed as percentages of the sulfur available only from the ZnSO_4 initially present.

2) Expressed as percentages of the total sulfate available from both the ZnSO_4 and Li_2SO_4 initially present.

3) Combax boat used in all experiments.

4) Flow rate was 150 cc/min in all experiments.

IV

General Summary and Conclusions

Each reaction in the proposed NH_4HSO_4 energy storage cycle has been examined experimentally. Emphasis has been placed on the basic chemistry of these reactions. This has required the development of unconventional experimental methods, particularly as related to the simultaneous and continuous measurement of $\text{SO}_2(\text{g})$ and $\text{SO}_3(\text{g})$.

In this concluding phase of research we have shown that when NH_4HSO_4 is mixed with ZnO and decomposed, the resulting products can be released stepwise ($\text{H}_2\text{O}(\text{g})$ at $\sim 163^\circ\text{C}$, $\text{NH}_3(\text{g})$ at $365\text{--}418^\circ\text{C}$, and a mixture of $\text{SO}_2(\text{g})$ and $\text{SO}_3(\text{g})$ at $\sim 900^\circ\text{C}$) and separated by controlling the reaction temperature. Side reactions do not appear to be significant and the respective yields are high as would be required for the successful use of this energy storage step in the proposed cycle. Thermodynamic, kinetic, and other reaction parameters have been measured for the various reaction steps. The final step in this sequence involves the decomposition of ZnSO_4 (or a mixture of ZnSO_4 and $\text{ZnO}\cdot 2\text{ZnSO}_4$). This reaction has been studied in detail. We have demonstrated that this reaction can be accelerated and the temperature required reduced by the addition of excess ZnO , aluminum silicate, V_2O_5 and possibly other metal oxides.

The work on this project as proposed prior to funding is essentially complete. The results of this research have been and continue to be used in other projects designed to test the overall feasibility of the proposed cycle.^{20,21}

Relationship of This Research to Other Energy Storage and Water Splitting Cycles

The results of our research which pertain to the thermal decomposition of pure ZnSO_4 and $\text{ZnSO}_4/\text{Li}_2\text{SO}_4$ mixtures have significance beyond their application to the ammonium hydrogen sulfate cycle.

Other proposed energy storage cycles also involve ZnSO_4 .²² Further, the thermal decomposition of ZnSO_4 is directly involved in the ZnSe thermochemical water splitting cycle²³, and it can be substituted for the decomposition of H_2SO_4 which is involved in several other cycles suggested for the production of H_2 from water.²⁴⁻²⁸ In each of these applications, a major concern is the high temperature required to decompose ZnSO_4 to $\text{SO}_2(\text{g})$ and ZnO . We have shown that this reaction can be accelerated and the temperature required reduced by the addition of excess ZnO , aluminum silicate V_2O_5 and possibly other metal oxides which appear to act as catalysts. Further, we have shown that ZnSO_4 can be decomposed from a liquid mixture of ZnSO_4 and Li_2SO_4 . This may provide a means for improving heat transfer in a practical system provided that incomplete decomposition of the ZnSO_4 can be tolerated.

VI

References

References to Previous Work on this Project*

1. Wentworth (W.E.), Chen (E.C.M.) - Solar Energy, 1976, 18, 205-214.
2. Wentworth (W.E.), Batten (C.F.), Corbett (G.E.) and Chen (E.C.M.) - "An Ionic Model for the Systematic Selection of Chemical Decomposition Reactions for Energy Storage," in Proceedings of the 1977 Annual Meeting (published by the American Section of the International Solar Energy Society) p 18-1.
3. Wentworth (W.E.), Hildebrandt (A.F.), Batten (C.F.), Corbett (G.E.), and Chen (E.C.M.) - Rev. Int. Hautes Temper. Refract., Fr., 1978, 15, 231-236.
4. Ray, Jr. (J.C.) - "Chemical Storage of Solar Energy: A Survey of Inorganic Sulfates and Oxides Which Separate Sulfur Trioxide from the Decomposition Gases of Ammonium Bisulfate," Masters Degree Thesis, University of Houston - CLC, 1978.
5. Wentworth (W.E.), Batten (C.F.), Schuler (T.), Ibanez (J.), Lopez (L.), Cook (C.J.), Chen (E.C.M.), and Ray (J.) - "The Storage and Regeneration of High Temperature Thermal Energy By Means of Reversible Chemical Reactions. The Ammonium Hydrogen Sulfate System," in Proceedings of the 1978 Annual Meeting (published by the American Section of the International Solar Energy Society) pp. 985-989.
6. Wentworth (W.E.), Batten (C.F.), Merrill (J.), Schuler (T.), Ibanez (J.G.), Cook (C.J.), Chen (E.C.M.), Ray (J.) - A.S.M.E. Publ. 79-Sol-20 (published by the American Society of Mechanical Engineers) 1979.

7. Final Report ALO/3974-11 for the year May 1, 1977-April 30, 1978 - unpublished.
8. Schuler (T.) - "The Kinetics and Thermodynamics of the Thermal Decomposition of Ammonium Bisulfate in the Presence of Alkali Metal Sulfates," Masters Degree Thesis, University of Houston - UP, 1979.
9. Final Report HCP/3947/17 for the year May 1, 1978 - April 30, 1979 - unpublished.
10. Wentworth (W.E.), Batten (C.F.), Schuler (T.), Osborne (K.) and Chen (E.C.M.) - Rev. Int. Hautes. Temper. Refract., Fr., 1980, 17, pp. 99-119.

References for Present Work on This Project**

11. Ibanez (J.G.) - "Thermal Energy Storage Using NH_4HSO_4 Decomposition with ZnO ", Ph.D. Thesis, University of Houston - UP, 1982.
12. Ibanez (J.G.), Wentworth (W.E.), Batten (C.F.), and Chen (E.C.M.) - Rev. Int. Hautes Temper. Refract. Fr., 1984, accepted.
13. Ibanez (J.G.), Wentworth (W.E.), Batten (C.F.) and Chen (E.C.M.) - Rev. Int. Hautes Temper. Refract., Fr., 1984, accepted.
14. Goodwin, (E.) - "Kinetic Study of the Decomposition of Zinc Sulfate", Undergraduate research project, University of Houston - UP, 1982 - unpublished.
15. Batten (C.F.), Wentworth (W.E.), and Ibanez (J.I.) - Anal. Chem., (in preparation).
16. Batten (C.F.), Wentworth (W.E.), - J. Phys. Chem. (in preparation).

17. Goodwin (E.) - "The Effect of Li_2SO_4 on the Decomposition of ZnSO_4 ", undergraduate research project, University of Houston - UP, 1983 - unpublished.
18. Rice (H.) - undergraduate research project, University of Houston - UP, 1983 - unpublished.
19. Sanh Dieu - Senior thesis, University of Houston - UP, 1984 - unpublished.

References to Other Related Research Projects

20. Prengle, H.W. Jr., Hunt, J.C., Mauk, C.E., and Sun, E.G.H., - Solar Energy, 1980, 24, 373.
21. Lee, Maw-Chwain - "Chemical Storage of Solar Energy - Reaction Engineering of the Ammonium Hydrogen Sulfate Cycle", Ph.D. Thesis, University of Houston - UP, 1983.
22. Rocket Research Co., Chemical Energy Storage for Solar Thermal Conversion, Final Report to Sandia Lab, Livermore, CA., RRC-80-R-678, SAND 79-8198.
23. Otsuki, P.K. and Krikorian, O.H., U.S. Department of Energy W-7405-ENG048, UCRL-52546 (1978).
24. Hosmer, P.K. and Krikorian, O.H., Solar Furnace Decomposition Studies of ZnSO_4 , presented at the Users Assoc. Solar Fuels Workshop, Albuquerque, NM (November. 28-29, 1979).
25. Krikorian, O.H. and Hosmer, P.K., The Utilization of ZnSO_4 Decomposition in Thermochemical Hydrogen Cycles, in Third World Hydrogen Energy Conference, Tokyo, June 23-26, 1980.

26. Norman, J.H. et al. "Chemical Studies of the General Atomic Sulfur-Iodine Thermochemical Water-Splitting Cycle", in Hydrogen Energy System, Proc. 2nd World Hydrogen Energy Conference, Zurich, Switzerland, 21-24 August 1978, Vol. 2, Pergamon Press., Oxford.
27. Farbman, G.H., The Westinghouse Sulfur Cycle Hydrogen Production Process, Ibid. Vol. 5.
28. Van Velzen, D., et al., Development, Design and Operation of a Continuous Laboratory - Scale Plant for Hydrogen Production by the Mark-13 Cycle, Ibid, Vol. 2.

*Work funded under contracts EG-77-C-04-3974 (1977-1978) and DOE-77-C-01-3974 (1978-1979).

**Work funded under contract DE-AC03-815F11557.

APPENDIX A

THERMOGRAVIMETRIC PROCEDURE FOR SCREENING REACTION MIXTURES

Thermogravimetric experiments were done batchwise according to the following procedure. Weighed amounts of dried NH_4HSO_4 and metal oxide or metal sulfate in an arbitrary mole ratio (metal oxide or metal sulfate always in excess) were placed in dried crucibles and the combined weight determined. The crucibles and contents were then inserted in a muffle furnace which had been previously equilibrated at a fixed temperature (normally 250°C). The crucibles were left in the furnace at this temperature for 2 hours, removed, cooled in a desiccator, and reweighed. The temperature of the furnace was raised 50°C and allowed to re-equilibrate during the time required for reweighing. The crucibles were then returned to the furnace and held there for another 2 hour period. This process was repeated in 50°C increments to 900°C . Control crucibles containing samples of the pure metal oxide or metal sulfate were treated in the same manner. After each heating, the control crucible weight loss was converted to a fractional metal sulfate or metal oxide weight loss. In general this was a very small number, as expected, and is a measure more of experimental technique rather than actual weight loss. This fraction was multiplied by the weight of the metal sulfate or metal oxide used to prepare the corresponding mixture sample and the result subtracted from the total weight lost from the mixture crucible. The reduced weight loss from the reaction mixture crucible was then converted to a percentage of the initial weight of NH_4HSO_4 in the reaction mixture. Percent weight losses were then plotted as a function of temperature for each mixture.

These experimental percent weight loss plots (thermographs) were examined to determine if weight loss was continuous or discontinuous as a function of temperature. Discontinuities were presumed to indicate the occurrence of different

decomposition reactions which occur with measurable yield of volatile products over non-overlapping or only slightly overlapping temperature ranges. Continuous weight loss could result from a single reaction or from multiple reactions which produce measurable yields within overlapping temperature ranges.

Complete reaction of the NH_4HSO_4 in any mixture by means of reaction 1a or 1c should result in a 30.4% weight loss (equivalent to complete loss of the available NH_3 and H_2O). Complete reaction in any mixture by means of reactions 1a and 1b combined or by means of reactions 1c and 1d combined should result in 100% weight loss (equivalent to complete loss of the available NH_3 , H_2O and SO_3). If reactions 1a and 1b occur sequentially (as required), then the thermograph should show a single discontinuity (or plateau) at 30% weight loss. The same would be true for the sequential occurrence of reactions 1c and 1d. A schematic representation of the type of thermograph expected for the sequential occurrence of two reaction steps is shown in Figure A-1. Each experimental thermograph was judged against this criterion. Typical results are presented in Figure A-2 and Figure A-3.

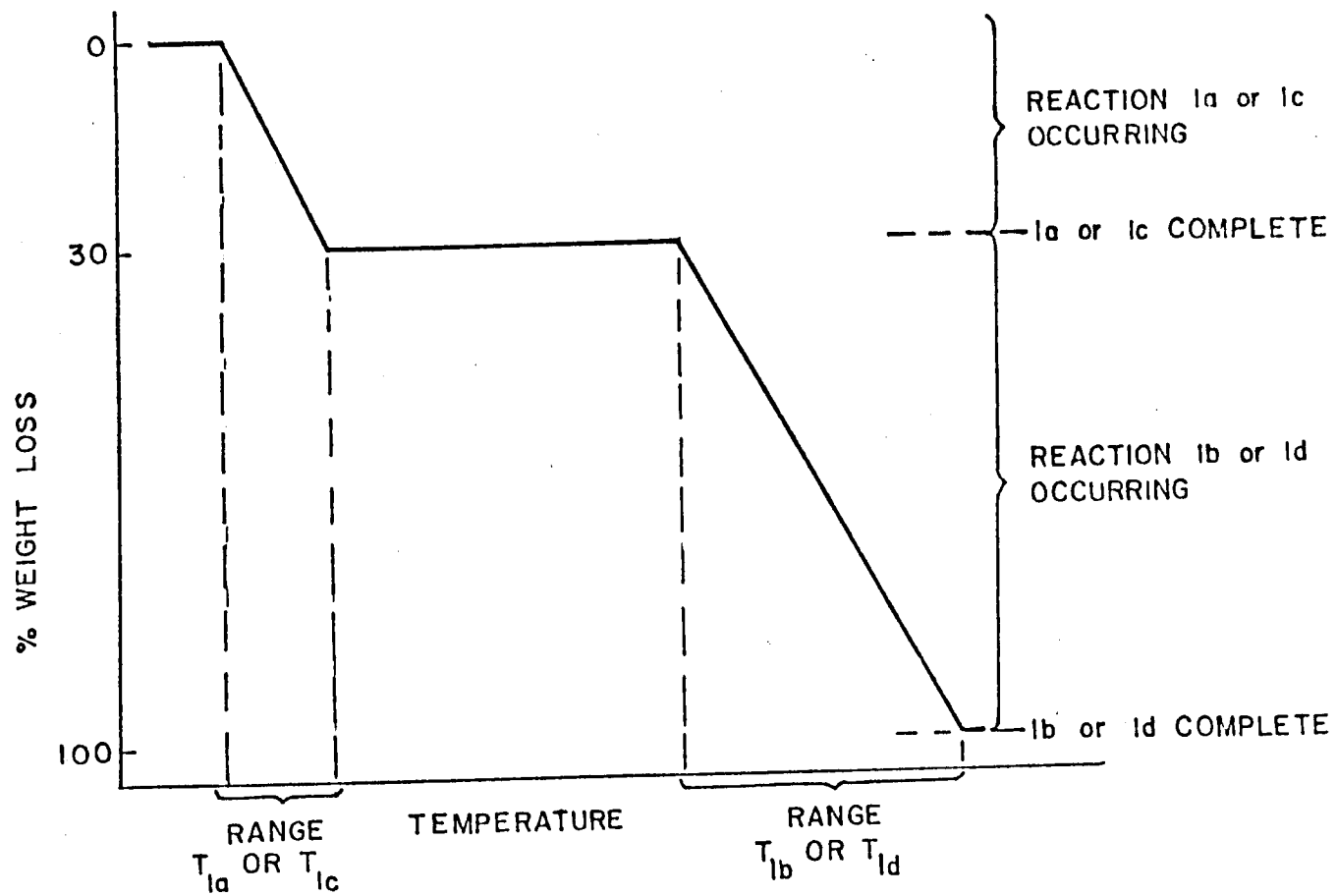


FIGURE A-1. Schematic representation of thermograph for mixture of NH_4HSO_4 with an intermediate former (metal sulfate or metal oxide) which decomposes in two sequential steps.

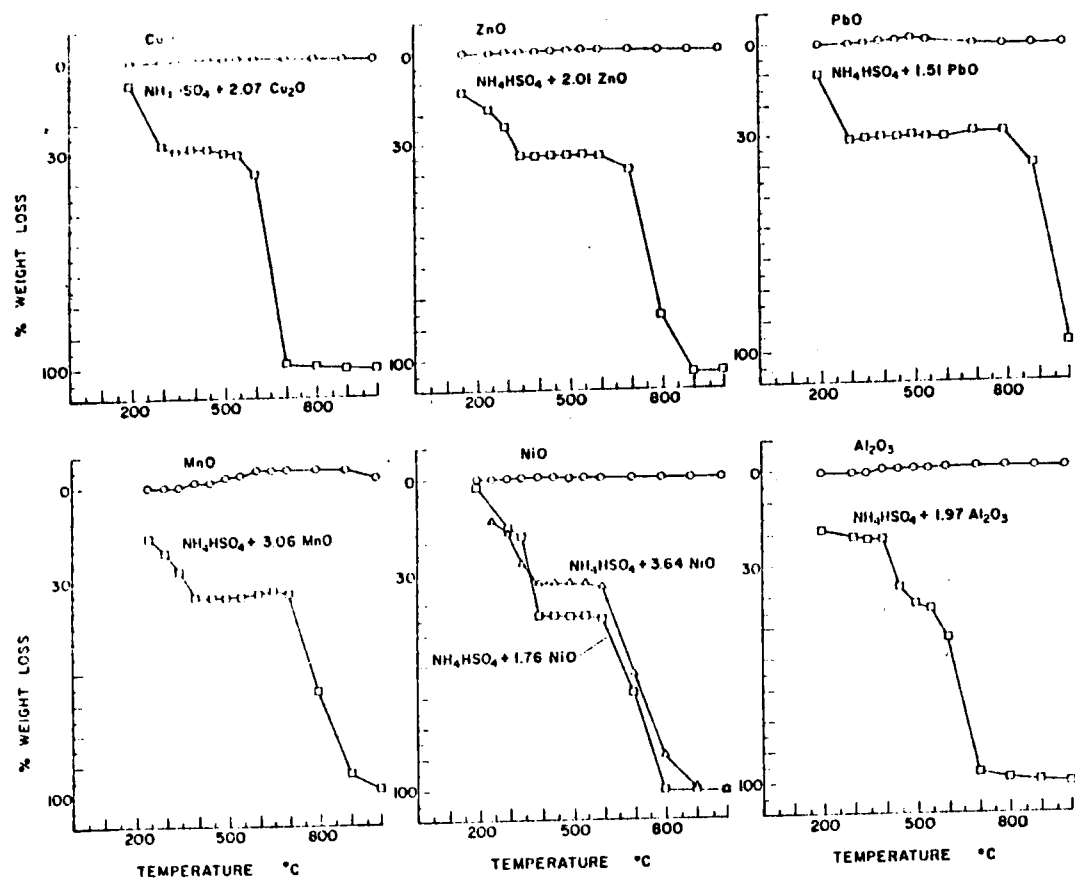


FIGURE A-3. TGA thermographs for selected transition metal oxides (circles) and for mixtures of nominally pure NH_4HSO_4 (Allied Chemical) with each metal oxide (squares) in the mole ratio indicated. For the pure metal oxides, weight loss is expressed as a percent of the NH_4HSO_4 weight in the sample before heating. Samples were heated at each set point temperature for 2 hours and cooled in a dessicator before weighing between each heating period.

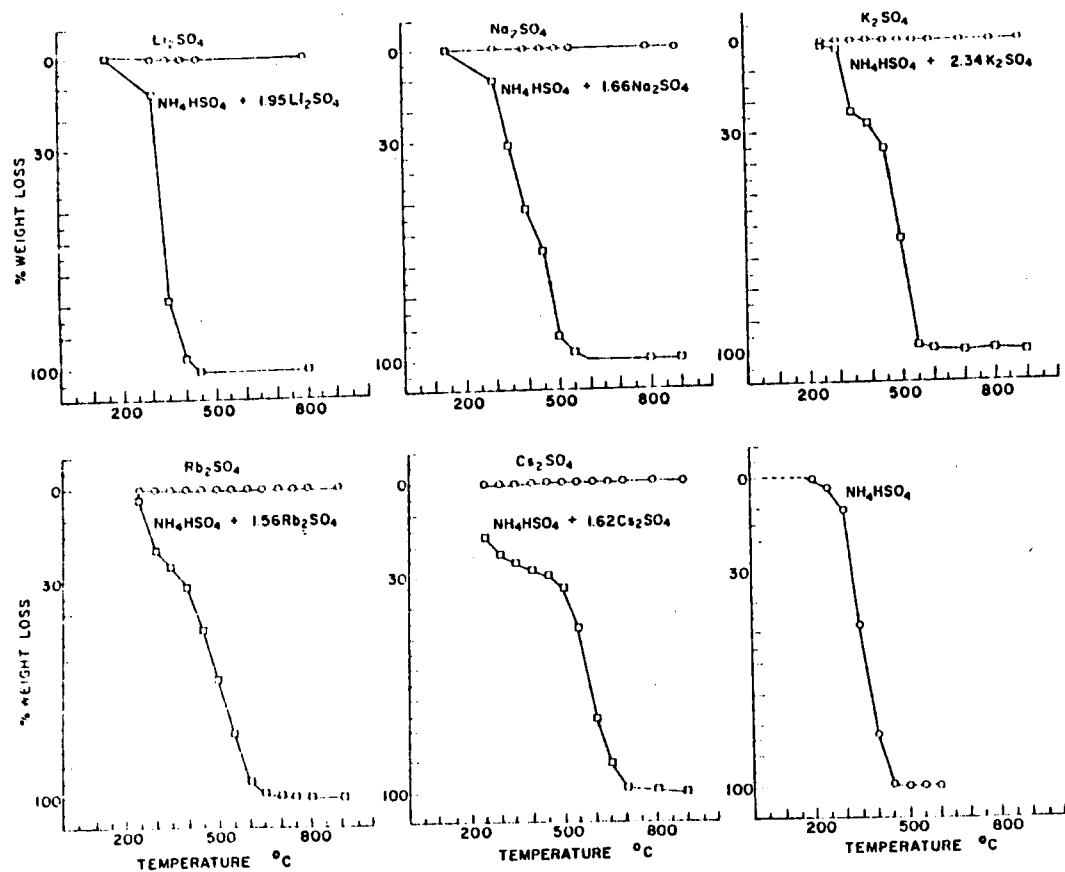


FIGURE A-2. TGA thermographs for the alkali metal sulfates (circles) and for mixtures of nominally pure NH_4HSO_4 (Allied Chemical) with each metal sulfate (squares) in the mole ratio indicated. For the pure metal sulfates, weight loss is expressed as a percent of the total sample weight before heating. For the mixtures, weight loss is expressed as a percent of the NH_4HSO_4 weight in the sample before heating. Samples were heated at each set point temperature for 2 hours and cooled in a dessicator before weighting between each heating period.

APPENDIX B

ANALYTICAL PROCEDURE USED FOR THE STUDY OF THE FIRST STEP IN DECOMPOSITION OF $\text{NH}_4\text{HSO}_4/\text{M}_2\text{SO}_4$ MIXTURES

The apparatus used to measure $\text{NH}_3(\text{g})$ and $\text{SO}_3(\text{g})$ yields from the first step (reaction 1a) of Mechanism I is shown schematically in Figure B-1. The heated portions of the reactor tube were quartz glass and the remainder was pyrex. In these experiments separate reaction mixtures were heated for various lengths of time and at different temperatures. Helium was used to entrain volatile products formed by the decomposition of the reaction mixture. Any $\text{NH}_3(\text{g})$ and $\text{SO}_3(\text{g})$ were dissolved from the carrier gas and at the conclusion of the heating period the resulting solution was analyzed according to the procedures discussed below. At the conclusion of an experiment, the apparatus was disassembled and the reactor and transfer line rinsed with water to dissolve any condensed solids. This solution was also analyzed. Finally the reaction mixture residue was dissolved in water and this solution analyzed. The analyses required are summarized on Table B-1. In principle each of the analyses (a,b,c,d,e,f) can be done by potentiometric titration of the aqueous or dilute acid solution in which analytes are dissolved. Other methods were also used as appropriate to analyze the solutions. These methods are discussed below.

Titration Method for Ammonia and Sulfur Oxide Analysis-

In analyses a and b the $\text{NH}_3(\text{g})$ and $\text{SO}_3(\text{g})$ to be measured are dissolved in dilute sulfuric acid (H_2SO_4). The H^+ ion concentration in the test solution as it is titrated with dilute sodium hydroxide (NaOH) can be approximated by the equation:

$$(\text{H}^+)^2 + \{[\text{NaOH}] - 2[\text{H}_2\text{SO}_4]\}(\text{H}^+) - K_w = 0 \quad (4-1)$$

where brackets indicate molar concentrations of the species enclosed when they

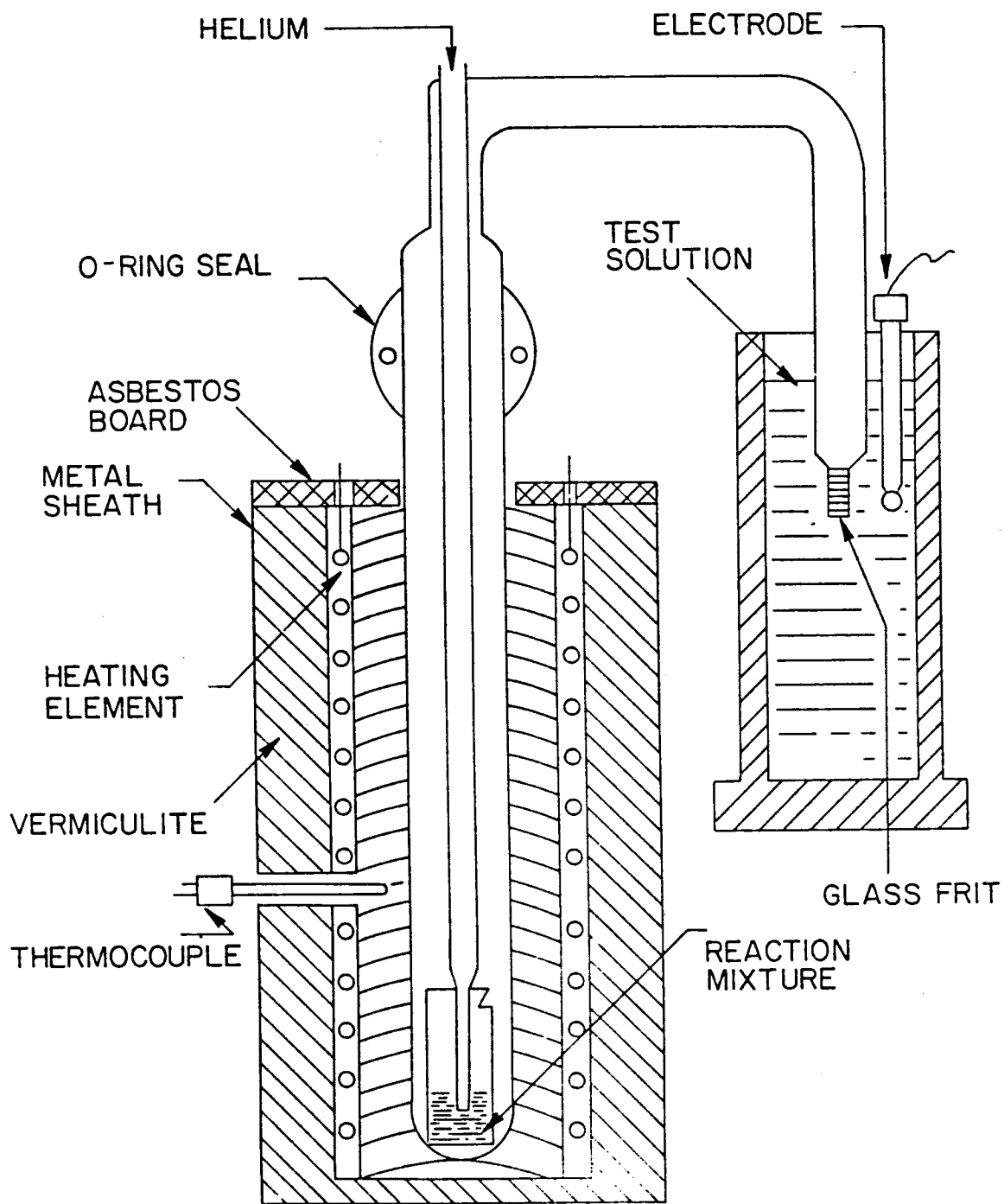
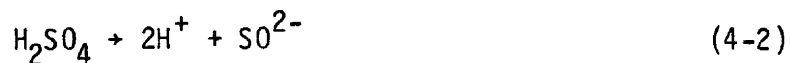


FIG. B-1. Apparatus used for quantitative chemical analysis of NH_3 and SO_3 yields from mixtures of NH_4HSO_4 with selected metal sulfates and metal oxides.

TABLE B-1
SUMMARY OF ANALYSES USED TO STUDY STOICHIOMETRY OF MECHANISM I

<u>Origin of Analyte</u>	<u>Test Solution</u>	<u>Type</u>	<u>Analyzed For</u>	<u>Method</u>	<u>Accuracy</u>
Volatile products from first reaction in decomposition of $\text{NH}_4\text{HSO}_4/\text{M}_2\text{SO}_4$ mixtures	.04 M H_2SO_4 in which volatile products are dissolved	a	Dissolved NH_3 as NH_4^+ or Dissolved NH_3 as NH_3	Titration of NH_4^+ Specific ion electrode	(NH_3 content in mm) $\pm .05$ mm (NH_3 content in mm) $\pm .02$ (NH_3 content)
		b	Dissolved SO_3 as H^+ or Dissolved SO_3 as BaSO_4	Titration of H^+ Aliquot by turbidimetry	(SO_3 content in mm) $\pm .05$ mm (SO_4^{-2} content in mm) $\pm .02$ (SO_2^{-2} content)
		c	NH_3 from NH_4HSO_4 and $(\text{NH}_4)_2\text{SO}_4$ as NH_4^+ or NH_3 from NH_4HSO_4 and $(\text{NH}_4)_2\text{SO}_4$ as NH_3	Titration of NH_4^+	(NH_3 content in mm) $\pm .05$ mm
				Specific ion electrode	(NH_3 content in mm) $\pm .02$ (NH_3 content)
Solids condensed in transfer line during decomposition of $\text{NH}_4\text{HSO}_4/\text{M}_2\text{SO}_4$ mixtures	Water in which solids are dissolved	d	SO_3 from NH_4HSO_4 and $(\text{NH}_4)_2\text{SO}_4$ as BaSO_4 or SO_3 from NH_4HSO_4 and $(\text{NH}_4)_2\text{SO}_4$ as BaSO_4	Titration of H^+	(SO_3 content in mm) $\pm .05$ mm
				Aliquot by turbidimetry	(SO_3 content in mm) $\pm .02$ (SO_2^{-2} content)
		e	NH_3 from NH_4HSO_4 as NH_4^+ or NH_3 from NH_4HSO_4 as NH_3	Titration of NH_4^+	(NH_3 content in mm) $\pm .05$ mm
				Specific ion electrode	(NH_3 content in mm) $\pm .02$ (NH_3 content)
Residue from first reaction in decomposition of $\text{NH}_4\text{HSO}_4/\text{M}_2\text{SO}_4$ mixtures	Water in which unreacted NH_4HSO_4 , ZnSO_4 and $\text{ZnO} \cdot 2\text{ZnSO}_4$ are dissolved	f	SO_3 from NH_4HSO_4 as HSO_4^- and from $\text{M}_2\text{S}_2\text{O}_7$ as HSO_4^- or H^+	Titration of H^+ plus HSO_4^- in aliquot plus dissolved NH_4^+ divided by 2	(SO_3 content in mm) $\pm .02$ mm

are combined to form the solution, parentheses indicate molar concentrations of the species enclosed after the prepared solution reaches equilibrium, and K_w equals the ionization constant of water at the solution temperature. This equation is based on the assumptions that H_2SO_4 and NaOH are completely ionized in solution:



that the concentration of acidic species in solution during titration is determined solely by the equilibrium:



and that the activity coefficients of all species in solution are equal to one. Under these assumptions, the conservation equations which apply to this solution as it is titrated with NaOH are:

$$[H_2SO_4] = (SO_4^{2-}) \quad (4-5)$$

$$[NaOH] = (Na^+) \quad (4-6)$$

$$K_w = (H^+) (OH^-) \quad (4-7)$$

and the electroneutrality equation which applies is:

$$(H^+) + (Na^+) = (OH^-) + 2(SO_4^{2-}) \quad (4-8)$$

Equation 4-1 can be obtained by changing the variables in Equation 4-8 according to the relationships given by Equations 4-5, 4-6, and 4-7. For calculations, the following additional change of variables can be made:

$$[H_2SO_4] = \frac{V_{H_2SO_4} M_{H_2SO_4}}{V_{H_2SO_4} + V_{NaOH}} \quad (4-9)$$

$$[\text{NaOH}] = \frac{V_{\text{NaOH}} M_{\text{NaOH}}}{V_{\text{H}_2\text{SO}_4} + V_{\text{NaOH}}} \quad (4-10)$$

where V and M represent the volume and molarity respectively of the constituents subscripted. Introduction of these relationships into Equation 4-1 gives:

$$(\text{H}^+)^2 + \frac{V_{\text{NaOH}} M_{\text{NaOH}} - V_{\text{H}_2\text{SO}_4} M_{\text{H}_2\text{SO}_4}}{V_{\text{H}_2\text{SO}_4} + V_{\text{NaOH}}} (\text{H}^+) - K_w = 0 \quad (4-11)$$

which upon rearrangement gives:

$$V_{\text{NaOH}} = \frac{2V_{\text{H}_2\text{SO}_4} M_{\text{H}_2\text{SO}_4} (\text{H}^+) + K_w V_{\text{H}_2\text{SO}_4} - V_{\text{H}_2\text{SO}_4} (\text{H}^+)^2}{(\text{H}^+)^2 + M_{\text{NaOH}} (\text{H}^+) - K_w} \quad (4-12)$$

In a typical analysis:

$$\begin{aligned} V_{\text{H}_2\text{SO}_4} &= 0.100 \text{ l} \\ M_{\text{H}_2\text{SO}_4} &= 0.04 \text{ M} \\ M_{\text{NaOH}} &= 1.00 \text{ M} \\ K_w &= 1 \times 10^{-14} \text{ (at } 25^\circ\text{C)} \end{aligned}$$

These data may be used along with Equation (4-12) to calculate V_{NaOH} as a function of (H^+) or pH ($= -\log (\text{H}^+)$). A sample calculation is shown graphically as curve 1 in Figure B-2. This calculated titration curve shows a single equivalence point (a_1) at a pH = 7.0. This point corresponds to the condition under which:

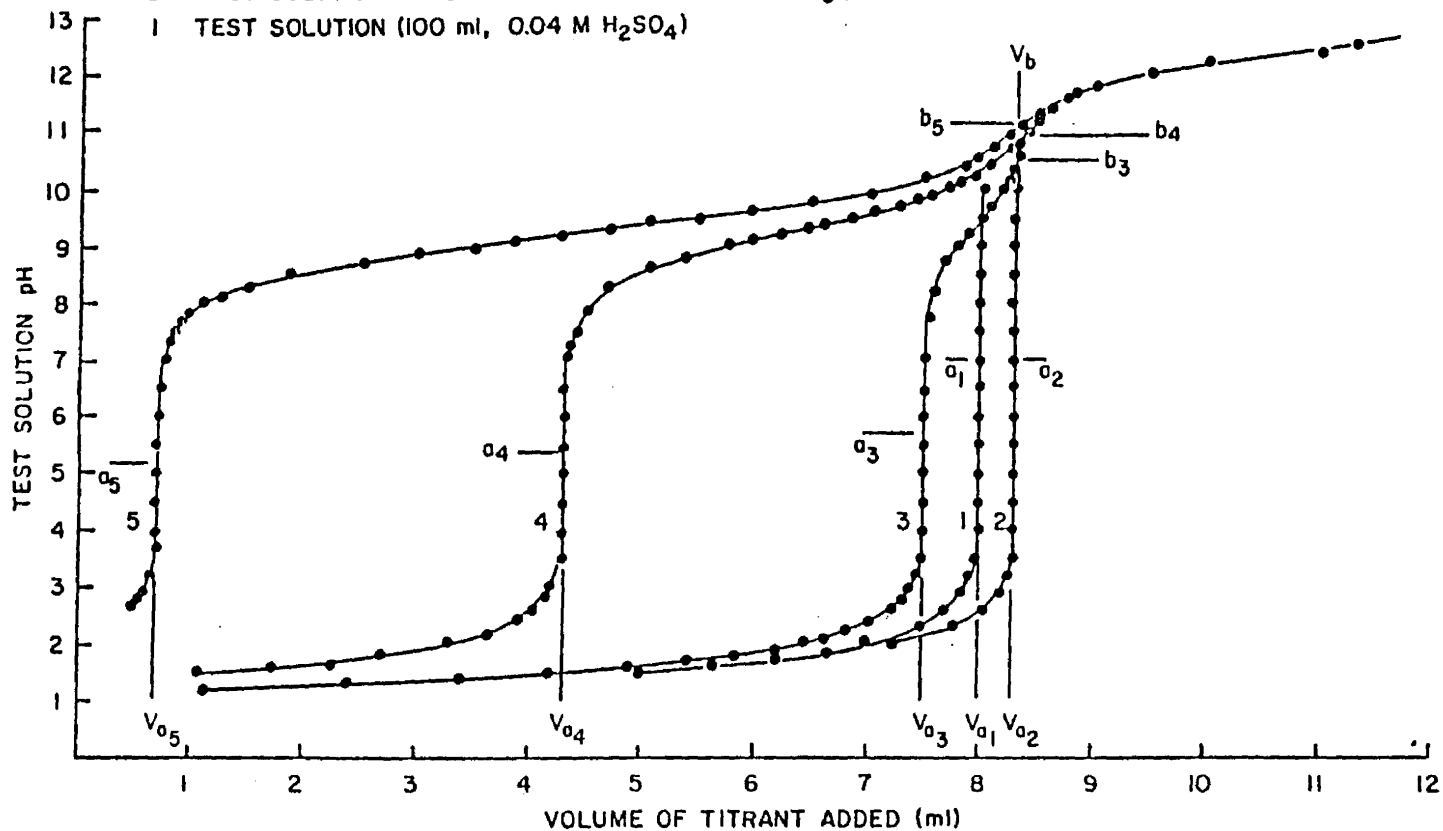
$$V_{a_1} M_{\text{NaOH}} = 2 V_{\text{H}_2\text{SO}_4} M_{\text{H}_2\text{SO}_4} = 2 n_{\text{H}_2\text{SO}_4} \quad (4-13)$$

Therefore the volume of titrant (V_{a_1}) required to reach equivalence point a_1 can be evaluated from an experimental titration curve and used to calculate the moles of H_2SO_4 ($n_{\text{H}_2\text{SO}_4}$) present in the test solution by means of the relationship:

FIGURE B-2

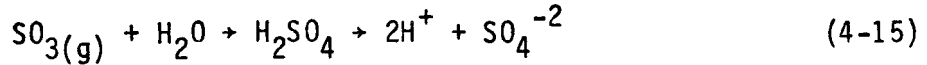
CALCULATED TITRATION CURVES FOR TYPICAL ANALYSES

- 5 TEST SOLUTION PLUS 1.6×10^{-4} MOLES TRAPPED $\text{SO}_3(\text{g})$ PLUS 7.6×10^{-3} MOLES TRAPPED $\text{NH}_3(\text{g})$
- 4 TEST SOLUTION PLUS 1.6×10^{-4} MOLES TRAPPED $\text{SO}_3(\text{g})$ PLUS 4.0×10^{-3} MOLES TRAPPED $\text{NH}_3(\text{g})$
- 3 TEST SOLUTION PLUS 1.6×10^{-4} MOLES TRAPPED $\text{SO}_3(\text{g})$ PLUS 8.0×10^{-4} MOLES TRAPPED $\text{NH}_3(\text{g})$
- 2 TEST SOLUTION PLUS 1.6×10^{-4} MOLES TRAPPED $\text{SO}_3(\text{g})$
- 1 TEST SOLUTION (100 ml, 0.04 M H_2SO_4)



$$\frac{V_{a1} M_{\text{NaOH}}}{2} = n_{\text{H}_2\text{SO}_4} \quad (4-14)$$

When $\text{SO}_3(\text{g})$ has been added to the H_2SO_4 test solution prior to titration the reaction of the dissolved gas may be represented as:



That is, the dissolved $\text{SO}_3(\text{g})$ forms H_2SO_4 which again is assumed to be completely ionized in solution and again the concentration of acidic species in solution during titration is determined solely by the equilibrium represented by Equation 4-4. The conservation equations which apply to this modified test solution as it is titrated with NaOH are:

$$[\text{H}_2\text{SO}_4] + [\text{SO}_3] = (\text{SO}_4^{2-}) \quad (4-16)$$

$$[\text{NaOH}] = (\text{Na}^+) \quad (4-17)$$

$$K_w = (\text{H}^+) (\text{OH}^-) \quad (4-18)$$

and the electroneutrality equation which applies is:

$$(\text{H}^+) + (\text{Na}^+) = (\text{OH}^-) + 2(\text{SO}_4^{2-}) \quad (4-19)$$

The following relationship:

$$[\text{SO}_3] = \frac{n_{\text{SO}_3(\text{g})}}{V_{\text{H}_2\text{SO}_4} + V_{\text{NaOH}}} \quad (4-20)$$

along with those given by Equations 4-16, 4-17, and 4-18 may be used to transform Equation 4-19 to:

$$(\text{H}^+)^2 + \frac{V_{\text{NaOH}} M_{\text{NaOH}} - 2V_{\text{H}_2\text{SO}_4} M_{\text{H}_2\text{SO}_4} - 2n_{\text{SO}_3(\text{g})}}{V_{\text{H}_2\text{SO}_4} + V_{\text{NaOH}}} (\text{H}^+) - K_w = 0 \quad (4-21)$$

which, for purposes of calculating a titration curve, can be rearranged to give:

$$V_{\text{NaOH}} = \frac{2V_{\text{H}_2\text{SO}_4} M_{\text{H}_2\text{SO}_4} (\text{H}^+) + 2n_{\text{SO}_3(\text{g})} (\text{H}^+) + K_w V_{\text{H}_2\text{SO}_4} - V_{\text{H}_2\text{SO}_4} (\text{H}^+)^2}{(\text{H}^+)^2 - M_{\text{NaOH}} (\text{H}^+) - K_w} \quad (4-22)$$

Substitution of typical values for the independent variables in this equation gives curve 2 in Figure B-2. Again, the titration curve shows a single equivalence point (a_2) at pH = 7.0, however, this equivalence point corresponds to the condition:

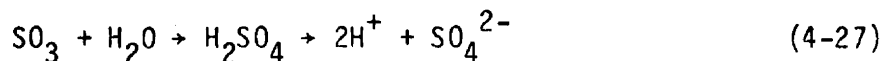
$$V_{a_2} M_{\text{NaOH}} = 2n_{\text{H}_2\text{SO}_4} + 2n_{\text{SO}_3(\text{g})} \quad (4-24)$$

The term $2n_{\text{H}_2\text{SO}_4}$ can be determined by a separate titration of the test solution alone as discussed above, and Equation 4-13 for this titration can be combined with Equation 4-24 to allow calculation of the term, $2n_{\text{SO}_3(\text{g})}$.

$$V_{a_2} M_{\text{NaOH}} - V_{a_1} M_{\text{NaOH}} = 2V_{\text{H}_2\text{SO}_4} M_{\text{H}_2\text{SO}_4} + 2n_{\text{SO}_3(\text{g})} - 2V_{\text{H}_2\text{SO}_4} M_{\text{H}_2\text{SO}_4} \quad (4-25)$$

$$(V_{a_2} - V_{a_1}) M_{\text{NaOH}} = 2n_{\text{SO}_3(\text{g})} \quad (4-26)$$

When both $\text{SO}_3(\text{g})$ and $\text{NH}_3(\text{g})$ have been added to the H_2SO_4 test solution prior to titration, as is done in analyses a and b (see Table B-1), the reactions of the dissolved gases may be represented as:



That is, the dissolved $\text{SO}_3(\text{g})$ is assumed to behave as discussed above, acting to increase the H^+ ion concentration in the test solution. The dissolved $\text{NH}_3(\text{g})$ acts as a base to reduce the H^+ ion concentration in the test solution by forming the conjugate acid NH_4^+ . This modified test solution thus contains not one but two acidic species, H^+ and NH_4^+ , and the concentration of acidic species during titration is determined by two simultaneous equilibria (Equations 4-4 and

4-29) rather than by a single equilibrium. The conservation equations which apply to this modified test solution as it is titrated with NaOH are:

$$[H_2SO_4] + [SO_3] = (SO_4^{2-}) \quad (4-30)$$

$$[NaOH] = (Na^+) \quad (4-31)$$

$$[NH_3] = (NH_3) + (NH_4^+) \quad (4-32)$$

$$K_w = (H^+) (OH^-) \quad (4-33)$$

$$K_{NH_3} = \frac{(NH_4^+) (OH^-)}{(NH_3)} \quad (4-34)$$

and the electroneutrality equation which applies is:

$$(H^+) + (Na^+) + (NH_4^+) = (OH^-) + 2(SO_4^{2-}) \quad (4-35)$$

The following relationship:

$$[NH_3] = \frac{n_{NH_3(g)}}{V_{H_2SO_4} + V_{NaOH}} \quad (4-36)$$

along with those given by Equations 4-20, 4-30, 4-31, 4-32, 4-33 and 4-34 may be used to transform Equation 4-35 to:

$$(H^+)^2 + \frac{K_{NH_3} n_{NH_3(g)} (H^+)^2}{\{K_w + K_{NH_3} (H^+)\} \{V_{H_2SO_4} + V_{NaOH}\}} \quad (4-37)$$

$$+ \frac{V_{NaOH} M_{NaOH} - 2V_{H_2SO_4} M_{H_2SO_4} - 2n_{SO_3(g)}}{V_{H_2SO_4} + V_{NaOH}} (H) - K_w = 0$$

which, for purposes of calculating a titration curve, can be rearranged to give:

$$V_{\text{NaOH}} = \frac{2V_{\text{H}_2\text{SO}_4} M_{\text{H}_2\text{SO}_4} (\text{H}^+) + 2n_{\text{SO}_3(\text{g})} (\text{H}^+) + K_w V_{\text{H}_2\text{SO}_4} - V_{\text{H}_2\text{SO}_4} (\text{H}^+)^2}{(\text{H}^+)^2 + M_{\text{NaOH}} (\text{H}^+) - K_w} \quad (4-38)$$

$$- \frac{K_{\text{NH}_3} n_{\text{NH}_3(\text{g})} (\text{H}^+)^2}{\{(\text{H}^+)^2 + M_{\text{NaOH}} (\text{H}^+) - K_w\} \{K_w + K_{\text{NH}_3} (\text{H}^+)\}}$$

Substitution of the following typical values for the independent variables in this equation:

$$\begin{aligned} V_{\text{H}_2\text{SO}_4} &= 0.100 \text{ l} \\ M_{\text{H}_2\text{SO}_4} &= 0.04 \text{ M} \\ M_{\text{NaOH}} &= 1.00 \text{ M} \\ K_w &= 1 \times 10^{-14} \text{ (at } 25^\circ\text{C)} \\ K_{\text{NH}_3} &= 1.8 \times 10^{-5} \text{ (at } 25^\circ\text{C)} \\ n_{\text{SO}_3(\text{g})} &= 1.6 \times 10^{-4} \text{ moles} \\ n_{\text{NH}_3(\text{g})} &= 7.6 \times 10^{-3} \text{ moles} \end{aligned}$$

gives curve 3 in Figure B-1. This curve shows two equivalence points, one (a_3) at pH = 5.7 and one (b_3) at pH = 10.5. The first (a_3) corresponds to the condition under which:

$$V_{a_3} M_{\text{NaOH}} = 2n_{\text{H}_2\text{SO}_4} + 2n_{\text{SO}_3} - n_{\text{NH}_4^+} \quad (4-39)$$

This is the equivalence point for the equilibrium represented by Equation 4-4. Equation 4-39 assumes that at the pH corresponding to a_3 virtually all the dissolved $\text{NH}_3(\text{g})$ exists as NH_4^+ ion. The second equivalence point (b_3) corresponds to the condition under which:

$$V_{b_3} M_{\text{NaOH}} = 2n_{\text{H}_2\text{SO}_4} + 2n_{\text{SO}_3(\text{g})} \quad (4-40)$$

This is the equivalence point for the equilibrium represented by Equation 4-29. Equation 4-40 assumes that at the pH corresponding to b_3 virtually all the

NH_4^+ ion has been converted to $\text{NH}_3(\text{aq})$. Equation 4-39 and 4-40 may be combined to give:

$$(V_{b_3} - V_{a_3})M_{\text{NaOH}} = N_{\text{NH}_4^+} = n_{\text{NH}_3(\text{g})} \quad (4-41)$$

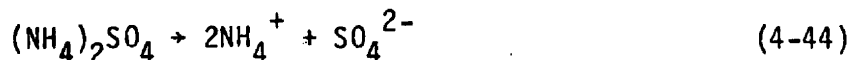
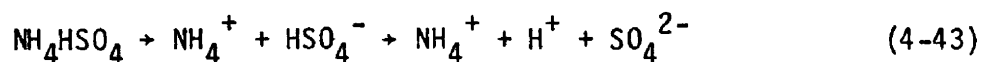
Equation 4-41 can also be combined with Equation 4-13 to give:

$$(V_{b_3} - V_{a_1})M_{\text{NaOH}} = 2n_{\text{SO}_3(\text{g})} \quad (4-42)$$

These last two equations illustrate how the yields of dissolved $\text{NH}_3(\text{g})$ and dissolved $\text{SO}_3(\text{g})$ can be obtained from two experimental titration curves similar to curves 1 and 3 in Figure B-1. One curve must be determined for the test solution alone, and a second curve for the test solution plus dissolved gases.

Curves 4 and 5 in Figure B-1 were calculated from Equation 4-36 using successively larger values of $n_{\text{NH}_3(\text{g})}$ corresponding to higher and higher yields of trapped $\text{NH}_3(\text{g})$. A comparison of curves 3, 4, and 5 illustrates the important points that: equivalence point "a" can be determined with good accuracy (± 0.02 millimoles) under all yield conditions encountered in these experiments; equivalence point "b" can be determined with somewhat lower accuracy (± 0.05 millimoles) under most yield conditions encountered in these experiments; equivalence point "b" is most difficult to determine accurately when the yield of dissolved $\text{NH}_3(\text{g})$ is large due to the overlap of equivalence point "b" with equivalence point "a". Fortunately, the uncertainty in equivalence point "b" is greatest at high $\text{NH}_3(\text{g})$ yields where it contributes the least total percent error.

In analyses c and d the solid to be analyzed for ammonia and sulfur oxide content is dissolved in water. The solid is assumed to be a mixture of NH_4HSO_4 and $(\text{NH}_4)_2\text{SO}_4$ formed by reactions between $\text{NH}_3(\text{g})$ and $\text{SO}_3(\text{g})$. These react when dissolved to form:



Again the solution contains two acidic species H^+ (from NH_4HSO_4) and NH_4^+ (from both NH_4HSO_4 and $(\text{NH}_4)_2\text{SO}_4$). The conservation equations which apply to this solution as it is titrated with NaOH are:

$$[\text{NH}_4\text{HSO}_4] + 2[(\text{NH}_4)_2\text{SO}_4] = (\text{NH}_4^+) + (\text{NH}_3) \quad (4-46)$$

$$[\text{NH}_4\text{HSO}_4] + [(\text{NH}_4)_2\text{SO}_4] = (\text{SO}_4^{2-}) \quad (4-47)$$

$$[\text{NaOH}] = (\text{Na}^+) \quad (4-48)$$

$$K_w = (\text{H}^+)(\text{OH}^-) \quad (4-49)$$

$$K_{\text{NH}_3} = \frac{(\text{NH}_4^+)(\text{OH}^-)}{(\text{NH}_3)} \quad (4-50)$$

and the electroneutrality equation which applies is:

$$(\text{H}^+) + (\text{Na}^+) + (\text{NH}_4^+) = (\text{OH}^-) + 2(\text{SO}_4^{2-}) \quad (4-51)$$

The following relationships:

$$[\text{NH}_4\text{HSO}_4] + 2[(\text{NH}_4)_2\text{SO}_4] = \frac{n_{\text{NH}_3(\text{g})}}{V_{\text{H}_2\text{O}} + V_{\text{NaOH}}} \quad (4-52)$$

$$[\text{NH}_4\text{HSO}_4] + [(\text{NH}_4)_2\text{SO}_4] = \frac{n_{\text{SO}_3(\text{g})}}{V_{\text{H}_2\text{O}} + V_{\text{NaOH}}} \quad (4-53)$$

$$[\text{NaOH}] = \frac{V_{\text{NaOH}} M_{\text{NaOH}}}{V_{\text{H}_2\text{O}} + V_{\text{NaOH}}} \quad (4-54)$$

along with those given by Equations 4-46, 4-47, 4-48, 4-49, and 4-50 may be used to transform Equation 4-15 to:

$$(H^+)^2 + \frac{K_{NH_3} n_{NH_3(g)} (H^+)^2}{\{K_w + K_{NH_3} (H^+)\} \{V_{H_2O} + V_{NaOH}\}} \quad (4-55)$$

$$+ \frac{\{V_{NaOH} M_{NaOH} - 2n_{SO_3(g)}\} (H^+)}{V_{H_2O} + V_{NaOH}} - K_w = 0$$

This equation is identical in form to Equation 4-37 and the calculated and experimental titration curves for this solution will be similar in shape to curves 3, 4, or 5 in Figure A-14. However, for this solution equivalence point "a" corresponds to the condition:

$$V_a M_{NaOH} = n_{NH_4HSO_4} \quad (4-56)$$

and equivalence point "b" to the condition:

$$V_b M_{NaOH} = n_{NH_4HSO_4} + n_{NH_4^+} \quad (4-57)$$

Equations 4-56 and 4-57 may be combined to give:

$$(V_b - V_a) M_{NaOH} = n_{NH_4^+} \quad (4-58)$$

and under the assumption that at equivalence point "b" virtually all the NH_4^+ ion has been converted to $NH_3(aq)$:

$$(V_b - V_a) M_{NaOH} = n_{NH_3} \quad (4-59)$$

which can be used directly to obtain from an experimental titration curve the yield of $NH_3(g)$ which must have reacted with $SO_3(g)$ to form the condensed solid.

Recalling that:

$$n_{NH_3(g)} = n_{NH_4HSO_4} + 2n_{(NH_4)_2SO_4} \quad (4-60)$$

$$n_{SO_3(g)} = n_{NH_4HSO_4} + 2n_{(NH_4)_2SO_4} \quad (4-61)$$

Equations 4-60 and 4-61 can be combined to give:

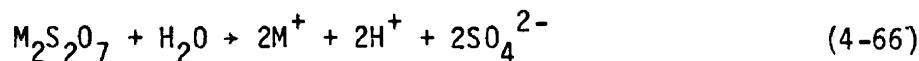
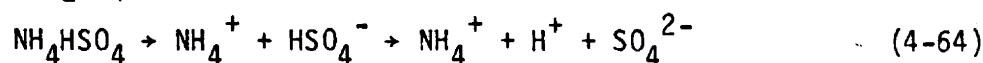
$$n_{\text{SO}_3(\text{g})} = n_{\text{NH}_4\text{HSO}_4} + \frac{n_{\text{NH}_3(\text{g})}}{2} - \frac{n_{\text{NH}_4\text{HSO}_4}}{2} = \frac{n_{\text{NH}_4\text{HSO}_4}}{2} + \frac{n_{\text{NH}_3(\text{g})}}{2} \quad (4-62)$$

Equation 4-62 can be transformed using the relationships given by Equations 4-56 and 4-59 to:

$$n_{\text{SO}_3(\text{g})} = \frac{V_a M_{\text{NaOH}}}{2} + \frac{(V_b - V_a) M_{\text{NaOH}}}{2} = \frac{V_b M_{\text{NaOH}}}{2} \quad (4-63)$$

which can be used directly to obtain from an experimental titration curve the yield of $\text{SO}_3(\text{g})$ which must have reacted with $\text{NH}_3(\text{g})$ to form the condensed solid.

In analyses e and f the solid residue to be analyzed for ammonia and sulfur oxide content is dissolved in water. The solid is assumed to be a mixture of NH_4HSO_4 , $\text{M}_2\text{S}_2\text{O}_7$, and M_2SO_4 . These react when dissolved to form:



Again the solution contains two acidic species H^+ and NH_4^+ . The conservation equations which apply to this solution as it is titrated with NaOH are:

$$[\text{NH}_4\text{HSO}_4] = (\text{NH}_4^+) + (\text{NH}_3) \quad (4-68)$$

$$[\text{NH}_4\text{HSO}_4] + [\text{M}_2\text{SO}_4] + 2[\text{M}_2\text{S}_2\text{O}_7] = (\text{SO}_4^{2-}) \quad (4-69)$$

$$2[\text{M}_2\text{SO}_4] + 2[\text{M}_2\text{S}_2\text{O}_7] = (\text{M}^+) \quad (4-70)$$

$$[\text{NaOH}] = (\text{Na}^+) \quad (4-71)$$

$$K_w = (\text{H}^+) (\text{OH}^-) \quad (4-72)$$

$$K_{\text{NH}_3} = \frac{(\text{NH}_4^+) (\text{OH}^-)}{(\text{NH}_3)} \quad (4-73)$$

and the electroneutrality equation which applies is:

$$(\text{H}^+) + (\text{Na}^+) + (\text{NH}_4^+) + (\text{M}^+) = (\text{OH}^-) + 2(\text{SO}_4^{2-}) \quad (4-74)$$

The following relationships:

$$[\text{NH}_4\text{HSO}_4] = \frac{n_{\text{NH}_4\text{HSO}_4}}{V_{\text{H}_2\text{O}} + V_{\text{NaOH}}} = \frac{n_{\text{NH}_3}}{V_{\text{H}_2\text{O}} + V_{\text{NaOH}}} \quad (4-75)$$

$$[\text{NH}_4\text{HSO}_4] + [\text{M}_2\text{SO}_4] + 2[\text{M}_2\text{S}_2\text{O}_7] = \frac{n_{\text{SO}_4^{2-}}}{V_{\text{H}_2\text{O}} + V_{\text{NaOH}}} \quad (4-76)$$

$$= \frac{n_{\text{SO}_3}}{V_{\text{H}_2\text{O}} + V_{\text{NaOH}}} + \frac{n_{\text{SO}_4}}{V_{\text{H}_2\text{O}} + V_{\text{NaOH}}}$$

$$2[\text{M}_2\text{S}_2\text{O}_7] + 2[\text{M}_2\text{SO}_4] = \frac{n_{\text{M}}}{V_{\text{H}_2\text{O}} + V_{\text{NaOH}}} \quad (4-77)$$

$$[\text{NaOH}] = \frac{V_{\text{NaOH}} M_{\text{NaOH}}}{V_{\text{H}_2\text{O}} + V_{\text{NaOH}}} \quad (4-78)$$

along with those given by Equation 4-68, 4-69, 4-70, 4-71, 4-72, and 4-73 may be used to transform Equation 4-74 to:

$$(\text{H}^+)^2 + \frac{K_{\text{NH}_3} n_{\text{NH}_3} (\text{H}^+)^2}{\{K_w + K_{\text{NH}_3} (\text{H}^+)\} \{V_{\text{H}_2\text{O}} + V_{\text{NaOH}}\}} \quad (4-79)$$

$$+ \frac{(V_{\text{NaOH}} M_{\text{NaOH}} + n_{\text{M}} - 2n_{\text{SO}_3} - 2n_{\text{SO}_4}) (\text{H}^+)}{V_{\text{H}_2\text{O}} + V_{\text{NaOH}}} - K_w = 0$$

In Equation 4-76 the term n_{SO_3} is equal to the number of moles of sulfur oxide initially present as NH_4HSO_4 before decomposition and present partly as unreacted NH_4HSO_4 and partly as $\text{M}_2\text{S}_2\text{O}_7$ in the residue. The term n_{SO_4} in Equation 4-76 represents the number moles of sulfur oxide initially present as M_2SO_4 before decomposition and present partly as unreacted M_2SO_4 and partly as $\text{M}_2\text{S}_2\text{O}_7$ in the residue. Therefore:

$$n_{SO_3} = n_{NH_4HSO_4} + n_{M_2S_2O_7} \quad (4-80)$$

$$n_{SO_4} = n_{M_2SO_4} + n_{M_2S_2O_7} \quad (4-81)$$

Only the term n_{SO_3} contributes to the formation of H^+ when the residue is dissolved, but both n_{SO_3} and n_{SO_4} contribute to the formation of SO_4^{2-} . Equation 4-79 is also identical in form to Equation 4-37 and the experimental titration curve for this solution will also be similar in shape to curves 3, 4, and 5 in Figure A-14. In this case, however, equivalence point "a" corresponds to the condition:

$$V_a M_{NaOH} = n_{NH_4HSO_4} + 2n_{M_2S_2O_7} \quad (4-82)$$

and equivalence point "b" to the condition:

$$V_b M_{NaOH} = n_{NH_4HSO_4} + 2n_{M_2S_2O_7} + n_{NH_4^+} \quad (4-83)$$

Equations 4-82 and 4-83 may be combined to give:

$$(V_b - V_a) M_{NaOH} = n_{NH_4^+} \quad (4-84)$$

and under the assumption that at equivalence point "b" virtually all the NH_4^+ ion has been converted to $NH_3(aq)$:

$$(V_b - V_a) M_{NaOH} = n_{NH_3} \quad (4-85)$$

which can be used directly to obtain, from an experimental titration curve, the yield of ammonia remaining in the residue as unreacted NH_4HSO_4 . Equation 4-82 can be used to transform Equation 4-80 to:

$$n_{SO_3} = n_{NH_4HSO_4} + \frac{V_a M_{NaOH} - n_{NH_4HSO_4}}{2} = \frac{n_{NH_4HSO_4}}{2} + \frac{V_a M_{NaOH}}{2} \quad (4-86)$$

Recalling that:

$$n_{\text{NH}_4\text{HSO}_4} = n_{\text{NH}_3} \quad (4-87)$$

Equation 4-87 and 4-85 can then be used to transform Equation 4-86 to:

$$n_{\text{SO}_3} = \frac{(V_b - V_a)M_{\text{NaOH}}}{2} + \frac{V_a M_{\text{NaOH}}}{2} = \frac{V_b M_{\text{NaOH}}}{2} \quad (4-88)$$

which can be used directly to obtain from an experimental titration curve the yield of sulfur oxide remaining in the residue either as unreacted NH_4HSO_4 or as $\text{M}_2\text{S}_2\text{O}_7$ ($= \text{M}_2\text{SO}_4 + \text{SO}_3$). Equation 4-88 does not include any sulfur oxide present as unreacted M_2SO_4 or that part of the $\text{M}_2\text{S}_2\text{O}_7$ which is due to the presence of M_2SO_4 .

In summary then, the solutions produced in the course of analyses a, b, c, d, e, f each when titrated with base (NaOH) give a titration curve having two equivalence points. The number of moles of each of the two analytes (SO_3 and NH_3) in the test solutions can be determine from these endpoints as follows:

For analyses a and b:

$$2n_{\text{SO}_3(\text{g})} = (V_{b_3} - V_{a_1})M_{\text{NaOH}}$$

$$n_{\text{NH}_3(\text{g})} = (V_{b_3} - V_{a_3})M_{\text{NaOH}}$$

For analyses c and d:

$$n_{\text{SO}_3(\text{g})} = \frac{V_b M_{\text{NaOH}}}{2}$$

$$n_{\text{NH}_3(\text{g})} = (V_b - V_a)M_{\text{NaOH}}$$

For analyses e and f:

$$n_{\text{NH}_3} = (V_b - V_a)M_{\text{NaOH}}$$

$$n_{\text{SO}_3} = \frac{V_b M_{\text{NaOH}}}{2}$$

Turbidimetric Method for Sulfur Oxide Analysis -

A well known turbidimetric technique exists for determining the SO_4^{-2} and HSO_4^- ion content of solutions by precipitation of these ions as BaSO_4 . Which can be quantified by measuring the optical attenuation of the solution after precipitation. The measured attenuation is compared to that produced in standard sulfate solutions of various concentrations. In principle this technique can be used for analyses b, d, f (see Table B-1) instead of potentiometric titration.

We have compared the two techniques. We find that the accuracy of the turbidimetric technique decreases as the SO_4^{-2} content to be measured increases. In particular, the accuracy of this analysis is given by:

$$(\text{SO}_4^{-2} \text{ content in millimoles}) \pm .02 (\text{SO}_4^{-2} \text{ content in millimoles})$$

We find that the accuracy of the pH titration technique remains essentially constant regardless of the H^+ , HSO_4^- and NH_4^+ content to be measured. In particular, when the calculation of sulfur oxide content involves only the titration of H^+ and HSO_4^- , the accuracy of this analysis is given by:

$$(\text{H}^+ + \text{HSO}_4^- \text{ content in millimoles}) \pm .02 \text{ millimoles}$$

When the calculation of sulfur oxide content involves titration of H^+ , HSO_4^- and NH_4^+ , the accuracy of the analysis is given by:

$$(\text{H}^+ + \text{HSO}_4^- + \text{NH}_4^+ \text{ content in millimoles}) \pm .05 \text{ millimoles}$$

When the calculation of sulfur oxide content involves titration of H^+ , HSO_4^- and NH_4^+ , the accuracy of the analysis is given by:

$$(\text{H}^+ + \text{HSO}_4^- + \text{NH}_4^+ \text{ content in millimoles}) \pm .05 \text{ millimoles}$$

Specific Ion Electrode Method for NH₃ Analysis -

Specific ion electrodes are commercially available for direct measurement of NH₃ or NH₄⁺ in solution. In principle such an electrode can be used for analyses a, c, e, (See Table B-1) instead of potentiometric titration.

We have compared the use of such an electrode (Orion #95-10) with the titration technique. We find that the accuracy of the specific ion electrode decreases as the NH₃ or NH₄⁺ content to be measured increases. In particular, the accuracy of this analysis is given by:

$$(\text{NH}_3 \text{ content in millimoles}) \pm .02 (\text{NH}_3 \text{ content in millimoles})$$

We find that the accuracy of the pH titration technique remains essentially constant regardless of the NH₄⁺ content to be measured. In particular, when the calculation of ammonia content involves only the titration of NH₄⁺, the accuracy of this analysis is given by:

$$(\text{NH}_4^+ \text{ content in millimoles}) \pm .05 \text{ millimoles}$$

Comparison of Analysis Methods -

A comparison of the accuracies of the three methods discussed above is given in Figure B-2. Several conclusions can be drawn from this figure.

- 1) When the ammonia content in a test solution is expected to be less than 2.5 millimoles total (this corresponds to ~30% of the 8 millimole sample of NH₄HSO₄ typically used in our experiments), then analysis for ammonia will be more accurate if done by specific ion electrode than if done by titration.
- 2) When the sulfur oxide content in a test solution is expected to be less than 1 millimole total (this corresponds to ~13% of the 8 millimole sample of NH₄HSO₄ typically used in our experiments), then analysis for sulfur oxide

will be more accurate if done by turbidimetry than if done by titration (if calculation involves only titration of H^+ and HSO_4^-).

- 3) When the sulfur oxide content in a test solution is expected to be less than 2.5 millimoles total (this corresponds to ~30% of the 8 millimole sample of NH_4HSO_4 typically used in our experiments), then analysis for sulfur oxide will be more accurate if done by turbidimetry than if done by titration (if calculation involves titration of H^+ , HSO_4^- and NH_4^+).

Analysis a generally involves measurement of a relatively large ammonia content (>30% of an 8 millimole sample of NH_4HSO_4). For this analysis, titration is the most suitable technique. Only when the ammonia yield is low (<30% of an 8 millimole sample of NH_4HSO_4) would analysis by specific ion electrode be more accurate.

Analysis b involves measurement of a relatively small sulfur oxide yield (<5% of an 8 millimole sample of NH_4HSO_4). If the test solution is dilute H_2SO_4 , the SO_4^{2-} content is high and titration allows the sulfur oxide yield to be distinguished from the SO_4^{2-} in the test solution by difference with a somewhat smaller error than turbidimetry, but neither method is very accurate for this analysis.

Analysis c involves measurement of a small ammonia content (<5% of an 8 millimole sample of NH_4HSO_4) in water solution. Use of the specific ion electrode was chosen for this analysis.

Analysis d involves measurement of a small sulfur oxide content (<5% of an 8 millimole sample of NH_4HSO_4) in water solution. Turbidimetry has been selected for this analysis.

Analysis e involves measurement of a relatively small ammonia content (<5% of an 8 millimole sample of NH_4HSO_4) in water solution. Use of the specific ion electrode was selected for this analysis.

Analysis f involves measurement of a relatively large sulfur oxide content (>90% of an 8 millimole sample of NH_4HSO_4 plus ~100% of the sulfur oxide from the added metal sulfate) in water solution. Titration was selected as the method for this analysis. This method detects only the sulfur oxide from NH_4HSO_4 . It does not detect the sulfur oxide from the added metal sulfate.

APPENDIX C

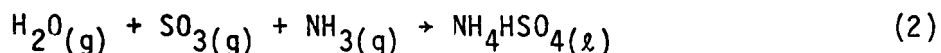
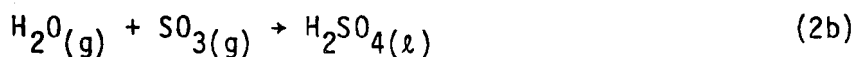
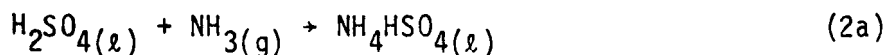
PROCEDURE FOR MEASURING THE SOLUBILITY OF ALKALI METAL SULFATES IN MOLTEN NH_4HSO_4

A weighed sample of NH_4HSO_4 was placed on a three neck pyrex flask. The flask was heated and equilibrated at a temperature above the melting point of NH_4HSO_4 . Temperature was measured with a mercury thermometer immersed in the melt. Weighed increments of metal sulfate were added to the melt, which was stirred continuously, and the mixture allowed to equilibrate. The addition of metal sulfate was repeated until solid metal sulfate persisted in the melt after equilibration. A measured volume (typically = 0.5g) of the melt was extracted and analyzed for NH_4^+ and HSO_4^- ion content by potentiometric titration (see Appendix B) with standard base. The sum of the measured NH_4^+ and HSO_4^- ion concentrations was divided by two to obtain the NH_4HSO_4 concentration in the extracted volume. This was multiplied by the extracted volume to obtain the weight of NH_4HSO_4 in the extracted sample. Subtraction of this weight from the total weight of the extracted sample gave the weight of metal sulfate dissolved. These weights were used to calculate the mole fraction of metal sulfate dissolved. The experiment was repeated to determine the solubility as a function of temperature.

APPENDIX D

PROCEDURE FOR CHLORIMETRIC MEASUREMENTS FOR REACTION 2

The heat of reaction for the energy storage step in the proposed cycle was determined by adiabatic calorimetry at atmospheric pressure. Since the quantitative determination of reaction heats of gaseous systems is difficult, the desired heat of reaction was not measured directly. Instead, only the heat of reaction 2a was actually measured. This experimental value was then combined with a literature [12] value for the heat of reaction 2b ($\Delta H = 42.05$ kcal/mole) to obtain the net heat of reaction 2:



A 250 ml dewar flask served as the calorimeter vessel. The heat capacity of this vessel was determined by measuring the adiabatic temperature change produced when a known weight of water of 100°C was poured into the flask. It is assumed that the heat capacity of the vessel is constant over the temperature range 25 to 100°C.

A weighed amount (typically 200g) of 98% sulfuric acid was placed in the dewar flask. Anhydrous ammonia was bubbled into the acid, and the temperature rise monitored. The extent of reaction was determined by removing small samples (~3g), which are weighed and analyzed by titration. The heat capacity of the reaction mixture was computed from the weighted sum of the known heat capacities for H_2SO_4 and H_2O which constitute most of the mass of the mixture. These heat capacities are known as a function of temperature [3].

In these experiments, the reaction was terminated when the temperature reached ~ 310°C (cf. a value of 405°C determined for complete reaction). The

experiment was repeated twice, giving experimental values of 35 kcal/mole and 32 kcal/mole for the heat of reaction 2a, and calculated values of 77 kcal/mole and 74 kcal/mole for the net regeneration reaction 2. These results are in good agreement with earlier measurements reported by Kelley et al. [3]. They measured a value of 75.5 kcal/mole for the heat of reaction 2 at 227°C. Using their value and known heat capacities, we calculate a value of 76 kcal/mole for the heat of reaction 2 at 310°C.

- [1] Handbook of Physics and Chemistry, 51st edition, R.C. Weast, ed., The Chemical Rubber Co., Cleveland, Ohio, pp. D61-D71, 1970-71.
- [2] D.D. Huxtable and D.R. Poole, "Thermal Energy Storage by the Sulfuric Acid Water System", in Proceedings of the 1976 Annual Meeting (published by the American Section of the International Solar Energy Society, Inc., American Technological University, Killeen, Texas, 1978).
- [3] Kelley et al. "Thermodynamic Properties of Ammonium and Potassium Alums and Related Substances with References to Extraction of Alumina from Clay and Anvite," U.S. Department of Interior, Technical Paper #688.

APPENDIX E

EVALUATION OF REACTOR CONSTRUCTION MATERIALS

Since the reaction mixtures involved in Mechanism I are potentially very corrosive, a series of experiments was done to determine what metals might be suitable for the construction of a large scale reactor. The test apparatus is shown in Figure E-1.

Test coupons of selected metals were each cleaned by placing in dilute HCl for 15 minutes, rinsed with acetone, and oven dried. Each coupon was weighed and placed in the quartz reaction tube. The bottom half of the test coupon was covered with a reaction mixture consisting of 5 $\text{K}_2\text{SO}_4 + \text{NH}_4\text{HSO}_4$. The top half of the coupon was not in contact with the reaction mixture. The same amount of reaction mixture (5.7097 g) was used with each coupon. The reactor was heated to 450°C (set point reached in ~ 1 hour) and held at this temperature for 24 hours. After allowing the reactor to cool to ambient temperature, the test coupon was removed, cleaned thoroughly with a soft brush to remove adhering solids, rinsed with acetone, dried, and reweighed. The weight loss per square centimeter of surface area for each coupon is given in Tabel E-1.

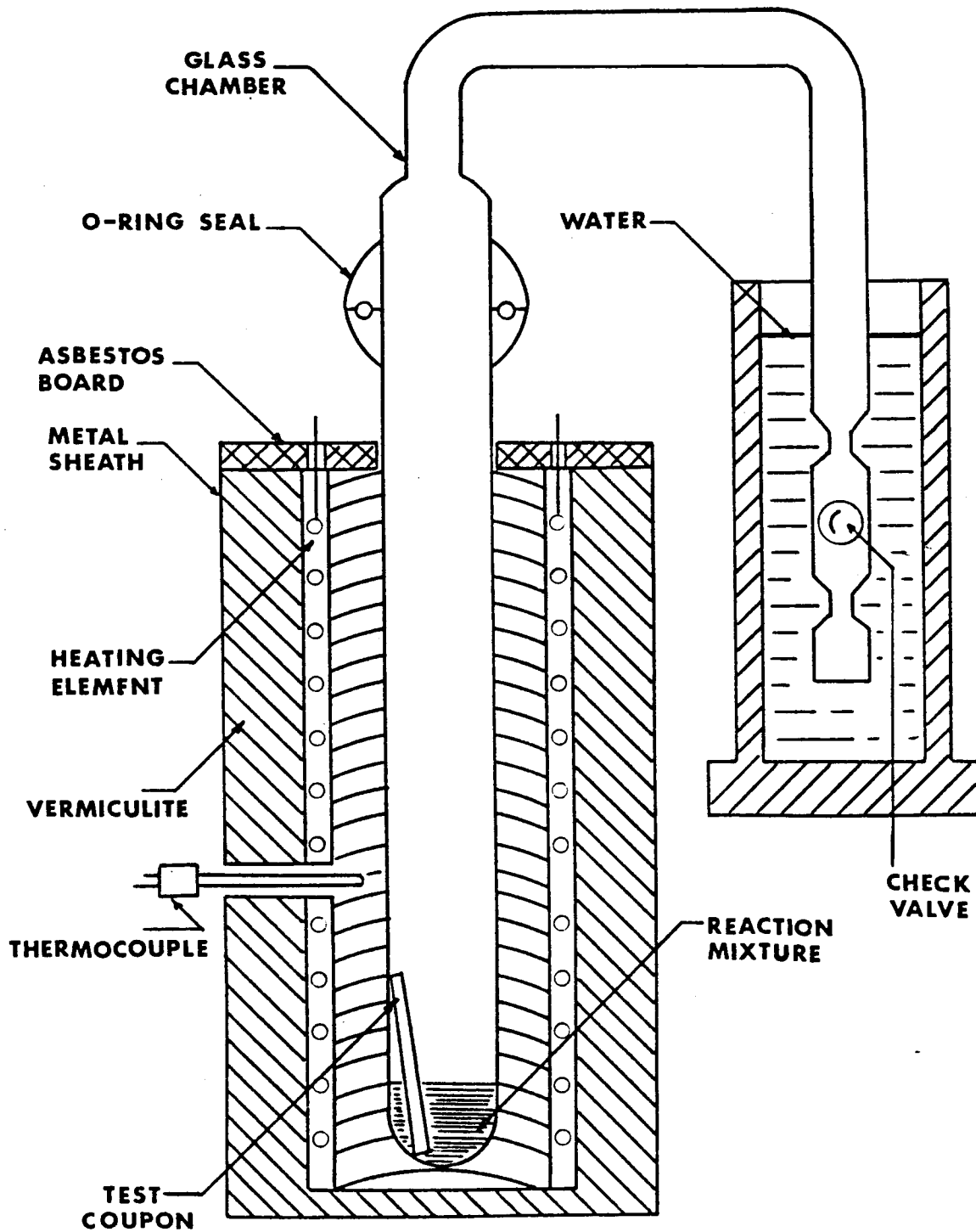


FIGURE E-1. Apparatus used to measure the corrosion effects on coupons of selected metals produced by exposure to molten reaction mixtures.

TABLE E-1

EVALUATION OF CORROSIVE EFFECT OF A TYPICAL
REACTION MIXTURE ON SELECTED CONSTRUCTION METALS

<u>Test Coupon in Reaction Mixture of $\text{NH}_4\text{HSO}_4 + 5 \text{K}_2\text{SO}_4$</u>	<u>Test Coupon Total Surface Area</u>	<u>Weight Loss per cm^2 of Surface Area after 24 hours at 450°C</u>
Stainless Steel 316	9.5 cm^2	.0055 g/cm^2
Inconel 617	6.8	.0081
Inconel 625	6.8	.0049
Inconel 671	8.4	.0058
Hastelloy C-4	8.4	.0075
Hastelloy C-276	9.2	.0056
Hastelloy G	8.4	.0050
Hastelloy X	8.4	.0026
Rene 41	12.8	.0030

APPENDIX F

ANALYTICAL PROCEDURES USED FOR THE STUDY OF FIRST STEP IN DECOMPOSITION OF $\text{NH}_4\text{HSO}_4/\text{ZnO}$ MIXTURES

The apparatus used to measure $\text{NH}_3(\text{g})$ and $\text{SO}_3(\text{g})$ yields from the first step (reaction 1c') of Mechanism II is shown schematically in Figure F-1. The heated portions of the reactor were quartz glass and the remainder was pyrex. In these experiments separate reaction mixtures were heated for various lengths of time and at different temperatures. Helium was used to entrain volatile products formed by decomposition of the reaction mixture. Any $\text{NH}_3(\text{g})$ or $\text{SO}_3(\text{g})$ was dissolved from the carrier gas and at the conclusion of the heating period the resulting solution was analyzed according to the procedures discussed below. At the conclusion of an experiment the apparatus was disassembled and the reactor and transfer line rinsed with water to dissolve any condensed solids. This solution was also analyzed. Finally the reaction mixture residue was dissolved in water and this solution analyzed. The analyses required are summarized in Table F-1. The methods used are discussed below.

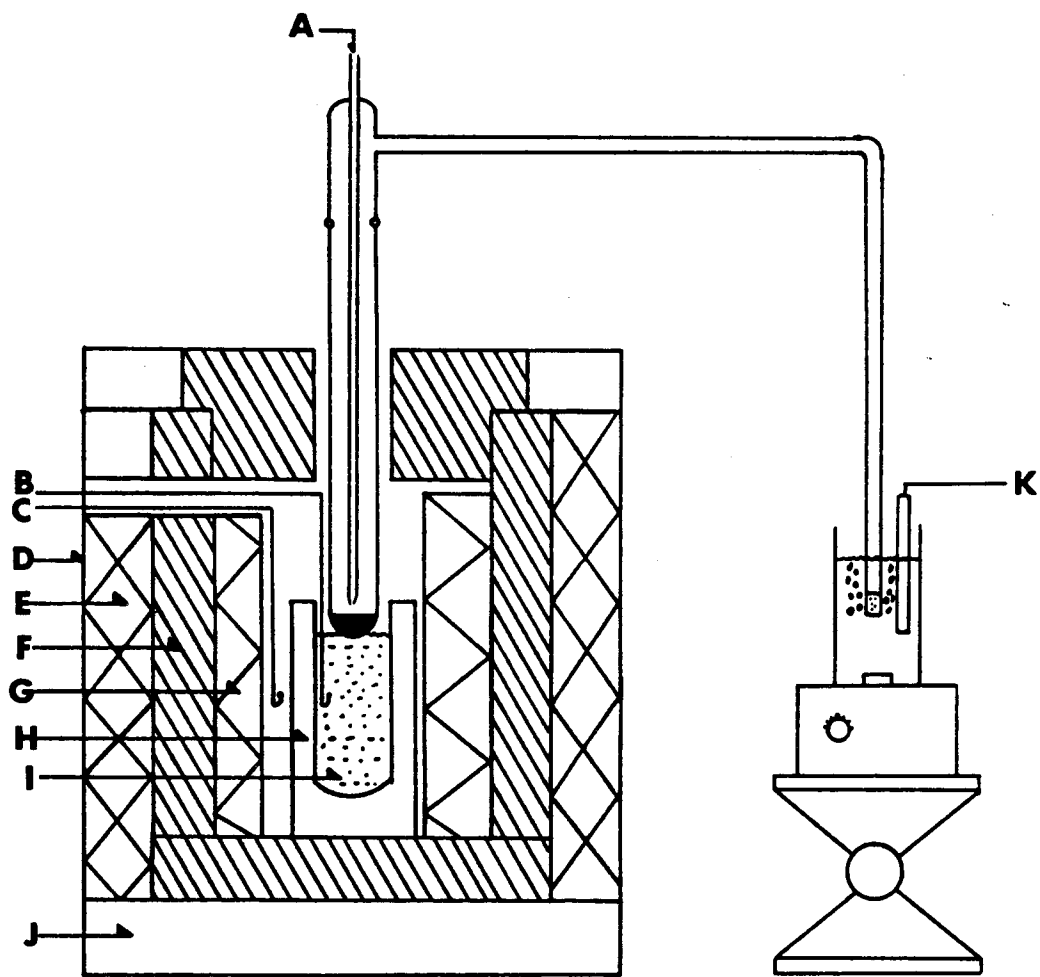
Titration Method For Ammonia and Sulfur Oxide Analysis-

The potentiometric titration used on these experiments is virtually the same as that described in Appendix B. In principle, this method could be applied to all the required analyses: a, b, c, d, e, f (see Table F-1).

Turbidimetric Method For Sulfur Oxide Analysis-

This method was identical to that described in Appendix B, and is applicable in principle to analyses b, d, f (See Table F-1).

FIGURE F-1. Apparatus used for quantitative chemical analysis of $\text{SO}_2(\text{g})$ and $\text{SO}_3(\text{g})$ yields from decomposition of $\text{NH}_4\text{HSO}_4/\text{ZnO}$ mixtures.



A. He Carrier Gas, B. Monitor Thermocouple, C. Control Thermocouple, D. Metal Tank, E. Vermiculite, F. Alumina Heat Shield, G. Heater Coils, H. Quartz Tube, I. Powered Alumina, J. Marionite, K. Conductivity Electrode.

TABLE F-1
SUMMARY OF ANALYSES USED TO STUDY STOICHIOMETRY OF MECHANISM II

<u>Origin of Analyte</u>	<u>Test Solution</u>	<u>Type</u>	<u>Analyzed For</u>	<u>Method</u>	<u>Accuracy</u>
Volatile products from first reaction in decomposition of $\text{NH}_4\text{HSO}_4/\text{ZnO}$ mixtures	0.1 M HCl in which volatile products dissolved	a	Dissolved NH_3 as NH_4^+	Titration of NH_4^+	(NH_3 content in mm) $\pm .05$ mm
			or Dissolved NH_3 as NH_3	Specific ion electrode	(NH_3 content in mm) $\pm .02$ (NH_3 content)
		b	Dissolved SO_3 as H^+	Titration of H^+	(SO_3 content in mm) $\pm .05$ mm
			or Dissolved SO_3 as BaSO_4	Aliquot by turbidimetry	(SO_4^{-2} content in mm) $\pm .02$ (SO_2^{-2} content)
Solids condensed in transfer line during decomposition of $\text{NH}_4\text{HSO}_4/\text{ZnO}$ mixtures	Water in which are dissolved	c	NH_3 from NH_4HSO_4 and $(\text{NH}_4)_2\text{SO}_4$ as NH_4^+	Titration of NH_4^+	(NH_3 content in mm) $\pm .05$ mm
			or NH_3 from NH_4HSO_4 and $(\text{NH}_4)_2\text{SO}_4$ as NH_3	Specific ion electrode	(NH_3 content in mm) $\pm .02$ (NH_3 content)
		d	SO_3 from NH_4HSO_4 and $(\text{NH}_4)_2\text{SO}_4$ as H^+	Titration of H^+	(SO_3 content in mm) $\pm .05$ mm
			or SO_3 from NH_4HSO_4 and $(\text{NH}_4)_2\text{SO}_4$ as BaSO_4	Aliquot by turbidimetry	(SO_3 content in mm) $\pm .02$ (SO_2^{-2} content)
Residue from first reaction in decomposition of $\text{NH}_4\text{HSO}_4/\text{ZnO}$ mixtures	Water in which unreacted NH_4HSO_4 , ZnSO_4 and $\text{ZnO} \cdot 2\text{ZnSO}_4$ dissolved	e	NH_3 from NH_4HSO_4	none	-
		f	SO_3 from NH_4HSO_4 as HSO_4^-	Turbidimetry or titration	-

Specific Ion Electrode Method for NH₃ Analysis-

This method was identical to that described in Appendix B, and is applicable in principle to analyses a, c, e (See Table F-1).

Comparison of Analysis Methods-

For analyses a and b the volatile NH₃(g) and SO₃(g) were dissolved in dilute HCl (rather than H₂SO₄ as discussed in Appendix B).

When the ammonia yield was expected to be less than 2.5 millimoles (~30% of the 8 millimole sample of NH₄HSO₄), analysis a was carried out with the specific ion electrode. For higher ammonia concentrations potentiometric titration was used.

For analysis b, turbidimetry was generally the method of choice.

For analysis c, analysis was by specific ion electrode.

For analysis d, either turbidimetry or potentiometric titration was used as dictated by the concentration level to be measured.

For analysis e, no method was found suitable. The residual ammonia was generally too low for analysis by potentiometric titration, and Zn²⁺ ion interfered with the function of the selected ion electrode.

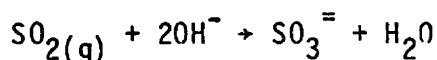
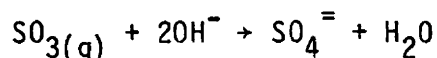
For analysis f, either turbidimetry or potentiometric titration was used as required.

APPENDIX G

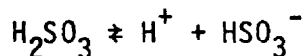
ANALYTICAL PROCEDURE USED FOR STUDY OF SECOND STEP IN DECOMPOSITION OF ZnO/NH₄HSO₄ MIXTURES

The apparatus used to measure SO₃(g) and SO₂(g) yields from the second step (reaction 1d) of Mechanism II was basically the same as shown in Appendix F (Figure F-1). In these experiments samples of the product from reaction 1c' were heated for various lengths of time and at different temperatures. Helium or in a few experiments air, was used to entrain the volatile products formed by the decomposition reaction. The system was modified by replacing the single trap used to dissolve volatile products from the carrier gas with a series of two traps. This was necessary to remove the relatively large amounts of SO₃(g) and SO₂(g) produced. Each trap was filled with an NaOH solution (1M). At the conclusion of an experiment the contents of the two traps were combined and analyzed by potentiometric titration with HNO₃(1M).

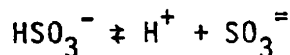
The resulting titration curve contains two endpoints. The product gases are assumed to react upon contact with NaOH as follows:



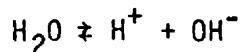
The resulting solution is assumed to involve the following equilibria:



$$K_{a1} = (\text{H}^+)(\text{HSO}_3^-)/(\text{H}_2\text{SO}_3) = 1.54 \times 10^{-2} \quad (1)$$



$$K'_{a2} = (\text{H}^+)(\text{SO}_3^{=})/(\text{HSO}_3^-) = 1.02 \times 10^{-7} \quad (2)$$



$$K_w = (\text{H}^+)(\text{OH}^-) = 1 \times 10^{-14} \quad (3)$$

Under the assumption that the activity coefficients for all species in solution are equal to one, the conservation equations which apply to the solution as it is titrated with HNO₃ are:

$$[SO_3(g)] = (SO_4^{=}) \quad (4)$$

$$[SO_2(g)] = (SO_3^{=}) + (HSO_3^{-}) \quad (5)$$

$$[NaOH] = (Na^{+}) \quad (6)$$

$$[HNO_3] = (NO_3^{-}) \quad (7)$$

Where brackets indicate molar concentrations of the species enclosed when they are first introduced into solution, and parentheses indicate molar concentrations of the species enclosed after the solution reaches equilibrium. Note that equation (1) is not considered in representing the conservation of $SO_2(g)$. Due to the relatively large ionization constant associated with this equation, protonation of HSO_4^{-} is negligible even during titration with HNO_3 . Likewise, protonation of $SO_4^{=}$ has been neglected.

The electroneutrality equation which applies to the solution as it is titrated with HNO_3 is:

$$(H^{+}) + (Na^{+}) = (HSO_3^{-}) + 2(SO_3^{=}) + (OH^{-}) + 2(SO_4^{=}) + (NO_3^{-}) \quad (8)$$

Equations (2) through (7) can be used to transform equation (8) to the following:

$$(H^{+}) + [NaOH] = [SO_2(g)] + \frac{[SO_2(g)]Ka_2}{(H^{+}) + Ka} + \frac{K_w}{(H^{+})} + 2[SO_2(g)] + [HNO_3] \quad (9)$$

Since wash water is added to the NaOH solution prior to titration, the following relationships apply during titration:

$$[NaOH] = \frac{V_{NaOH} M_{NaOH}}{V_{HNO_3} + V_{NaOH} + V_{H_2O}} \quad (10)$$

$$[\text{HNO}_3] = \frac{V_{\text{HNO}_3} M_{\text{HNO}_3}}{V_{\text{HNO}_3} + V_{\text{NaOH}} + V_{\text{H}_2\text{O}}} \quad (11)$$

$$[\text{SO}_3(\text{g})] = \frac{n_{\text{SO}_3(\text{g})}}{V_{\text{HNO}_3} + V_{\text{NaOH}} + V_{\text{H}_2\text{O}}} \quad (12)$$

$$[\text{SO}_2(\text{g})] = \frac{n_{\text{SO}_2(\text{g})}}{V_{\text{HNO}_3} + V_{\text{NaOH}} + V_{\text{H}_2\text{O}}} \quad (13)$$

For purposes of calculation, equations (10) through (13) can be used to transform equation (9) to:

$$V_{\text{HNO}_3} = \frac{n_{\text{SO}_2} \{(H^+)^2 + 2K_a'(H^+)\}}{\{K_{a2}' + (H^+)\} \{(H^+)^2 - M_{\text{HNO}_3}(H^+) - K_w\}} + \frac{2n_{\text{SO}_3}(H^+)}{\{(H^+)^2 - M_{\text{HNO}_3}(H^+) - K_w\}} + \frac{\{K_w - (H^+)^2\} \{V_{\text{NaOH}} + V_{\text{H}_2\text{O}}\}}{(H^+)^2 - M_{\text{HNO}_3}(H^+) - K_w} - \frac{V_{\text{NaOH}} M_{\text{NaOH}}(H^+)}{(H^+)^2 - M_{\text{HNO}_3}(H^+) - K_w} \quad (14)$$

Equation (14) has been used to calculate the titration curves shown in Figure G-1.

Each of the titration curves shows two endpoints as expected. The first at pH ~ 9 corresponds to the condition:

$$n_{\text{HNO}_3} = n_{\text{OH}^-} - 2n_{\text{SO}_3} - 2n_{\text{SO}_4}^{2-}$$

or

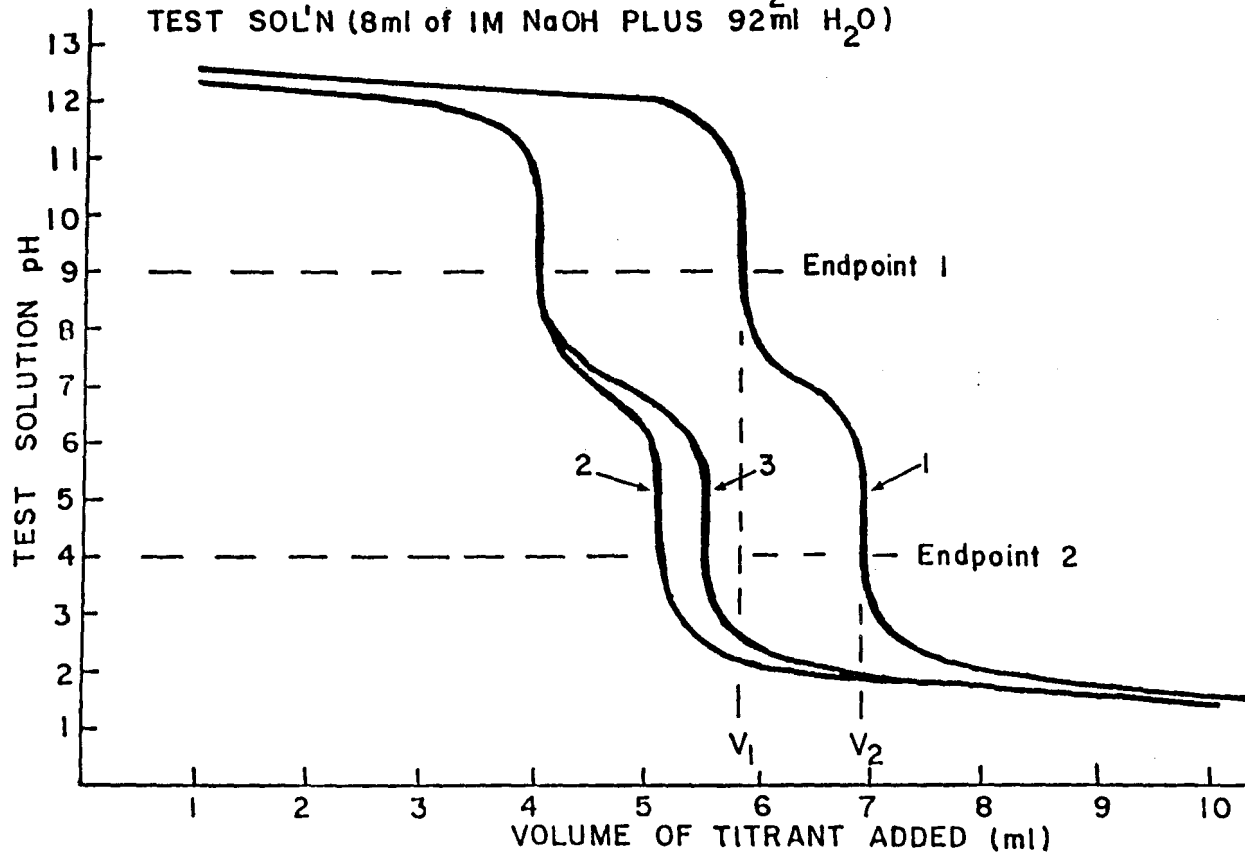
$$n_{\text{HNO}_3} = n_{\text{OH}^-} - 2n_{\text{SO}_2} - 2n_{\text{SO}_3}$$

which can be rearranged to

FIGURE G-1

CALCULATED TITRATION CURVES FOR TYPICAL ANALYSES

- 3 TEST SOL'N PLUS 2.7×10^{-3} MOLES SO_2 PLUS 5.0×10^{-4} MOLES SO_3
 - 2 TEST SOL'N PLUS 1.1×10^{-3} MOLES SO_2 PLUS 9.0×10^{-4} MOLES SO_3
 - 1 TEST SOL'N PLUS 1.1×10^{-3} MOLES SO_2
- TEST SOL'N (8ml of 1M NaOH PLUS 92ml H_2O)



$$2n_{\text{SO}_2} + 2n_{\text{SO}_3} = V_{\text{NaOH}} M_{\text{NaOH}} - V_1 M_{\text{HNO}_3} \quad (15)$$

from which we can calculate

$$\%(SO_2 + SO_3) = \left(\frac{V_{\text{NaOH}} M_{\text{NaOH}} - V_1 M_{\text{HNO}_3}}{2(\text{moles } NH_4HSO_4)} \right) 100 \quad (16)^*$$

The second endpoint, at pH ~ 4 corresponds to the condition:

$$n_{\text{HNO}_3} = n_{\text{OH}^-} - 2n_{\text{SO}_3^{2-}} - 2n_{\text{SO}_4^{2-}} + n_{\text{SO}_3^{2-}}$$

or

$$n_{\text{HNO}_3} = n_{\text{OH}^-} - 2n_{\text{SO}_2} - 2n_{\text{SO}_3} + n_{\text{SO}_2}$$

Which can be rearranged to

$$n_{\text{SO}_2} + 2n_{\text{SO}_3} = V_{\text{NaOH}} M_{\text{NaOH}} - V_2 M_{\text{HNO}_3} \quad (17)$$

The difference between the first and second endpoints, equation (15) minus equation (17), gives:

$$n_{\text{SO}_2} = (V_2 - V_1) M_{\text{HNO}_3}$$

from which we can calculate:

$$\%SO_2 = \left\{ \frac{(V_2 - V_1) M_{\text{HNO}_3}}{(\text{moles } NH_4HSO_4)} \right\} 100 \quad (18)^*$$

and

$$\%SO_3 = \%(SO_2 + SO_3) - \%SO_2 \quad (19)$$

Equations 16 and 18 were used for calculation of the $SO_3(g)$ and $SO_2(g)$ yields in these experiments.

* When this procedure is used to study the decomposition of pure $ZnSO_4$ rather than the product from reaction 1c' equation 16 is modified to:

$$\%(SO_2 + SO_3) = \left(\frac{V_{NaOH} M_{NaOH} - V_1 M_{HNO_3}}{2(\text{moles } ZnSO_4)} \right) 100 \quad (16a)$$

* When this procedure is used to study the decomposition of pure $ZnSO_4$ rather than the product from reaction 1c' equation 18 is modified to:

$$\%SO_2 = \left\{ \frac{(V_2 - V_1) M_{HNO_3}}{(\text{moles } ZnSO_4)} \right\} 100 \quad (18a)$$

APPENDIX H

METHODS EVALUATED FOR SIMULTANEOUS $\text{SO}_2(\text{g})$ AND $\text{SO}_3(\text{g})$ ANALYSIS

Many methods for the determination of $\text{SO}_2(\text{g})$ have been described in the literature, due primarily to the fact that $\text{SO}_2(\text{g})$ is a major air pollutant. Fewer methods have been published for the determination of $\text{SO}_3(\text{g})$. Chemical methods have generally been used when only one of the analytes is present in the matrix or when one of the two has been selectively removed from the matrix. These methods involve dissolving the analyte into a liquid and analyzing the resulting solution.

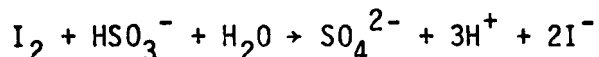
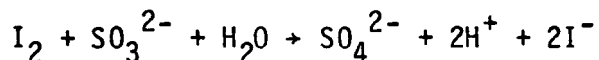
Absorbing liquids used for $\text{SO}_2(\text{g})$ include: aqueous NaOH solutions analyzed by titration of excess base; aqueous iodine/starch solutions analyzed by titration of excess iodine with thiosulfate (1); aqueous hydrogen peroxide/sulfuric acid solutions analyzed by measurement of electrical conductivity (2); aqueous hydrogen peroxide solutions analyzed by measurement of the SO_4^{2-} formed using titration with barium perchlorate (thorin indicator) (3-4), or with lead perchlorate (Sulfonazo indicator) (5-6), or turbidimetry (7), or by measurement of the H^+ formed using titration with NaOH (methyl red indicator) (8) (bromphenol blue indicator) (9); aqueous potassium or sodium tetrachloromercurate solutions analyzed colorimetrically after adding pararosaniline dye (10-13); aqueous formaldehyde solutions analyzed colorimetrically after adding pararosaniline dye (14).

Absorbing liquids used for $\text{SO}_3(\text{g})$ include: aqueous isopropanol solutions analyzed by measurement of the SO_4^{2-} formed using titration with lead perchlorate (Sulfonazo indicator) (6), or titration with barium perchlorate (thorin indicator) (15-17) (methyl blue indicator) (20) (alizerin red S indicator) (4), or photometrically using barium chloronilate (21), or spectrophotometrically

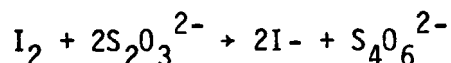
using barium chloroanilate (17-18, 22-23) or by turbidimetry (7, 24), or by measurement of the H^+ formed using titration with NaOH (bromphenol blue indicator) (9); aqueous isopropanol/acetone solutions analyzed by measurement of electrical conductivity (25).

In some cases these chemical methods have been combined to allow determination of both analytes in a common matrix. One technique involves a series of liquid absorbers. Generally, the matrix is passed first through an isopropanol solution which selectively dissolves $SO_3(g)$ and inhibits oxidation of $SO_2(g)$ and then through a hydrogen peroxide solution which dissolves the $SO_2(g)$ and oxidizes it to SO_4^{2-} (6, 7, 25). Each of the absorbing solutions is then analyzed separately by one of the methods stated above. A variation of this technique is to first condense the $SO_3(g)$ from the matrix and then absorb the $SO_2(g)$ from the matrix into a hydrogen peroxide solution (9). The $SO_3(g)$ condensate is dissolved in isopropanol and both solutions are analyzed.

We attempted to adapt three of these chemical methods to our experimental requirements. The first method tried involved dissolving the $SO_2(g)$ and $SO_3(g)$ from a nitrogen carrier gas into an aqueous iodine solution. The SO_2 should react with water to form SO_3^- and HSO_3^- . These ions would react as follows:



SO_3 reacts with water to form SO_4^{2-} which does not react with iodine. Two aliquots of the resulting solution were taken. One was titrated with $Na_2S_2O_3$ to measure I_2 .



The amount of SO_2 dissolved was obtained from the difference between the amount of I_2 present before and after adding the gas mixture to the solution. Tin(II)

chloride was added to the other aliquot to reduce the unreacted I_2 to I^- . Then, the clear sample was diluted and analyzed for total SO_4^{2-} by a standard turbidimetric method in which added Ba^{2+} causes precipitation of $BaSO_4$. Subtraction of the number of moles of SO_2 obtained by $Na_2S_2O_3$ titration from the total number of moles of SO_4^{2-} as measured by turbidimetry should give the number of moles of $SO_3(g)$ dissolved. The results indicated that the analysis for SO_2 was reliable and reproducible ($\pm 1\%$), but that the total SO_4^{2-} analysis was erratic and unreliable.

The second chemical method tried involved passing the $SO_2/SO_3/N_2$ gas mixture through a series of liquid solutions. The first was an aqueous isopropanol solution (80%) and the second was an aqueous H_2O_2 solution (3%). We were able to quantify the amount of $SO_2(g)$ dissolved on the H_2O_2 solution by measuring the electrical conductivity change produced when the SO_2 was oxidized to SO_4^{2-} , but found that the isopropanol retained SO_2 for an unacceptable length of time. Furthermore, SO_3 was not efficiently dissolved in the isopropanol at the flow rates (~ 160 cc/min) required for our experiments.

The third chemical method involved passing the $SO_2/SO_3/N_2$ gas mixture through a series of traps all containing dilute NaOH, and analyzing the resulting solution by potentiometric titration. This method gave reproducible and quantitative results. Both $SO_2(g)$ and $SO_3(g)$ were dissolved from the carrier gas at the required flow rates and oxidation of SO_2 to SO_3 was found to be slow with respect to analysis time. The potentiometric titration curve contains two endpoints which can readily be related to the amount of SO_2 and SO_3 dissolved (see Appendix G).

While this method proved useful for measurement of total $SO_2(g)$ and $SO_3(g)$ yields from a particular decomposition reaction, it could not be easily used for

measuring yield as a function of time. Sampling time is limited by the speed with which the absorbing solution can be switched and the repeated analysis of a large number of solutions is tedious. This is characteristic of most wet chemistry methods. For this reason we attempted to adapt some of the reported instrumental methods to our requirements.

For $\text{SO}_2(\text{g})$ these include: fluorescence (emission at 3940Å) (26-29); UV absorption (between 3200-1800Å) (30-31); IR absorption (bands at 518, 1151, and 1361 cm^{-1}) (32); mass spectrometry (33-35); Raman spectrometry (band at 1151 cm^{-1}) (36); gas chromatography (37-40). For $\text{SO}_3(\text{g})$: IR absorption (bands at 527, and 1391 cm^{-1}) (41); mass spectrometry (34-35, 42); Raman spectrometry (band at 1067 cm^{-1}) (36); gas chromatography (38) have been used.

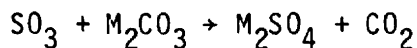
Attempts to adapt ultraviolet spectroscopy to the simultaneous measurement of SO_2 and SO_3 in a flowing carrier gas stream were unsuccessful. A number of problems were encountered. First, the molar extinction coefficient for SO_2 (at wavelengths between 260-310 nm) is from 2 to 4 orders of magnitude larger than that for SO_3 . Thus conditions, such as flow rate and optical path length, suitable for detection of one analyte are unsuitable for the other analyte. Second, SO_3 tended to condense on the inner surfaces of the optical cell even when the cell compartment was heated.

Although Raman spectrometry, gas chromatography and mass spectrometry have been used for simultaneous measurement of the two analytes, (34, 35, 36, 38) the extremely reactive nature of $\text{SO}_3(\text{g})$ makes it incompatible with the materials used in the construction of most commercial analytical instruments. In order to make use of the speed and convenience of instrumental analysis, we sought to find a reagent which would react quantitatively with $\text{SO}_3(\text{g})$ to produce a more stable and conveniently measured molecule.

We have tested a variety of reagents. Reaction with glycerine to form acrolein, and with 1,4-butanediol to form tetrahydrofuran were not quantitative. In general, the reactions of $\text{SO}_3(\text{g})$ with organic compounds appeared to be indiscriminate and unsatisfactory.

Certain alkali metal halides (eq. KCl) were reported to react to form addition compounds having the general formula $\text{M}(\text{SO}_3)_n\text{Cl}$ at $\sim 0^\circ\text{C}$ and some alkali metal sulfates (eq. K_2SO_4) were well known to react forming stable pyrosulfates, $\text{M}_2\text{S}_2\text{O}_7$. When SO_3 , from fuming sulfuric acid, was added to a flowing carrier gas and passed through tubes containing plugs of these reagents, the removal of SO_3 was found inefficient. Further, the resulting products are solids which cannot be conveniently quantified continuously in a flow system, but rather must be measured batchwise.

A thermodynamic analysis suggested that alkali and transition metal carbonates should react with both SO_2 and SO_3 to produce CO_2 as follows:



Although complete thermodynamic data for these reactions are not available, approximations lead to the conclusion that the ΔG° for reaction of SO_2 with a given metal carbonate is considerably less negative than the ΔG° for the reaction of SO_3 , though in general both reactions should be exoenergetic. Thus, preferential reaction with SO_3 would result only if the respective reactions have sufficiently different activation energies and dependence on temperature. A rather extensive series of experiments was done in an attempt to find a metal carbonate which would at some temperature react readily with SO_3 and negligibly with SO_2 . The carbonates tested included: Li_2CO_3 , Na_2CO_3 , K_2CO_3 , MgCO_3 and CaCO_3 . The product gases (SO_3 and SO_2) formed from the decomposition of

ZnSO₄ were passed through a tube containing each carbonate and the amount of CO₂ and SO₂ in the emerging gas mixture measured. The solid carbonates were either simply mixed with glass beads or in some experiments coated onto the beads by precipitation from an aqueous solution. The temperature of each carbonate was varied systematically. In no case was it possible to achieve selective reproducible and quantitative reaction with SO₃.

Both oxalic acid³⁷ and calcium oxalate⁴³ have been reported to react with SO₃ to produce CO₂. Calcium oxalate was tested in experiments similar to those used for the evaluation of metal carbonates. Its reaction with both SO_{3(g)} and SO_{2(g)} was measured systematically as a function of temperature and it was found to react selectively with SO₃ at temperatures between 300-375°C. This reagent was tested extensively and a method developed by which it could be used to quantitatively convert SO₃ to CO₂ in a flowing carrier containing both SO₃ and SO₂. This method is described in detail in Appendix I. It allows the amounts of SO₃ (as CO₂) and SO₂ to be measured continuously so that reaction rate as well as reaction yield information can be obtained conveniently. To date this method has been applied only to the study of the thermal decomposition of ZnSO₄, but it will undoubtedly find more extensive application. The conversion of SO₃ to CO₂ allows the SO₃ concentration in a gas stream to be monitored by any of a variety of instrumental methods. We selected infrared spectrometry as a matter of convenience.

APPENDIX I

Analytical Procedure Used For The Study Of $\text{SO}_3(\text{g})$ and $\text{SO}_2(\text{g})$

Yields From Decomposition Of ZnSO_4

The apparatus used is shown schematically in Figure I-1. A quartz reactor tube served to confine the evolved product gases. This tube is enclosed in a three zone split furnace and is heated over a length of 30 cm. Electrical power to each of the three furnace heaters was independently adjusted using a controller so as to provide a region of constant temperature ($\pm 2^\circ\text{C}$) extending from ~ 2 cm in either direction along the furnace axis from its midpoint.

To one end of the reactor tube is attached a stainless steel manifold. This manifold includes a carrier gas entrance port, a septum sealed syringe injection port, and an o-ring sealed thermocouple probe port. An inconel sheathed thermocouple passes through the probe port and extends along the reactor tube axis onto the furnace. Attached to the end of the probe is a quartz sample boat. The probe is mounted on an indexed slide mechanism which is used to reproducibly position the sample boat. Sample temperature is read with a digital thermometer connected to the probe.

The other end of the quartz reactor tube is connected to a pyrex tube. This pyrex tube is enclosed in a furnace and maintained at a temperature of 325°C . A plug of $\text{CaC}_2\text{O}_4 \cdot \text{H}_2\text{O}$ mixed with glass beads was placed in the center of the pyrex tube and held in place with pyrex wool. The plug was 1-2 inches long and $\sim 3/8$ inch in diameter. The ratio of $\text{CaC}_2\text{O}_4 \cdot \text{H}_2\text{O}$ to glass beads was arbitrarily adjusted to allow the desired carrier gas (He) flow. The $\text{CaC}_2\text{O}_4 \cdot \text{H}_2\text{O}$ was dehydrated in situ with carrier gas flowing.

Teflon tubing is used to conduct the carrier gas flow from the pyrex tube to each of two optical cells in series and thence to a soap bubble flow meter.

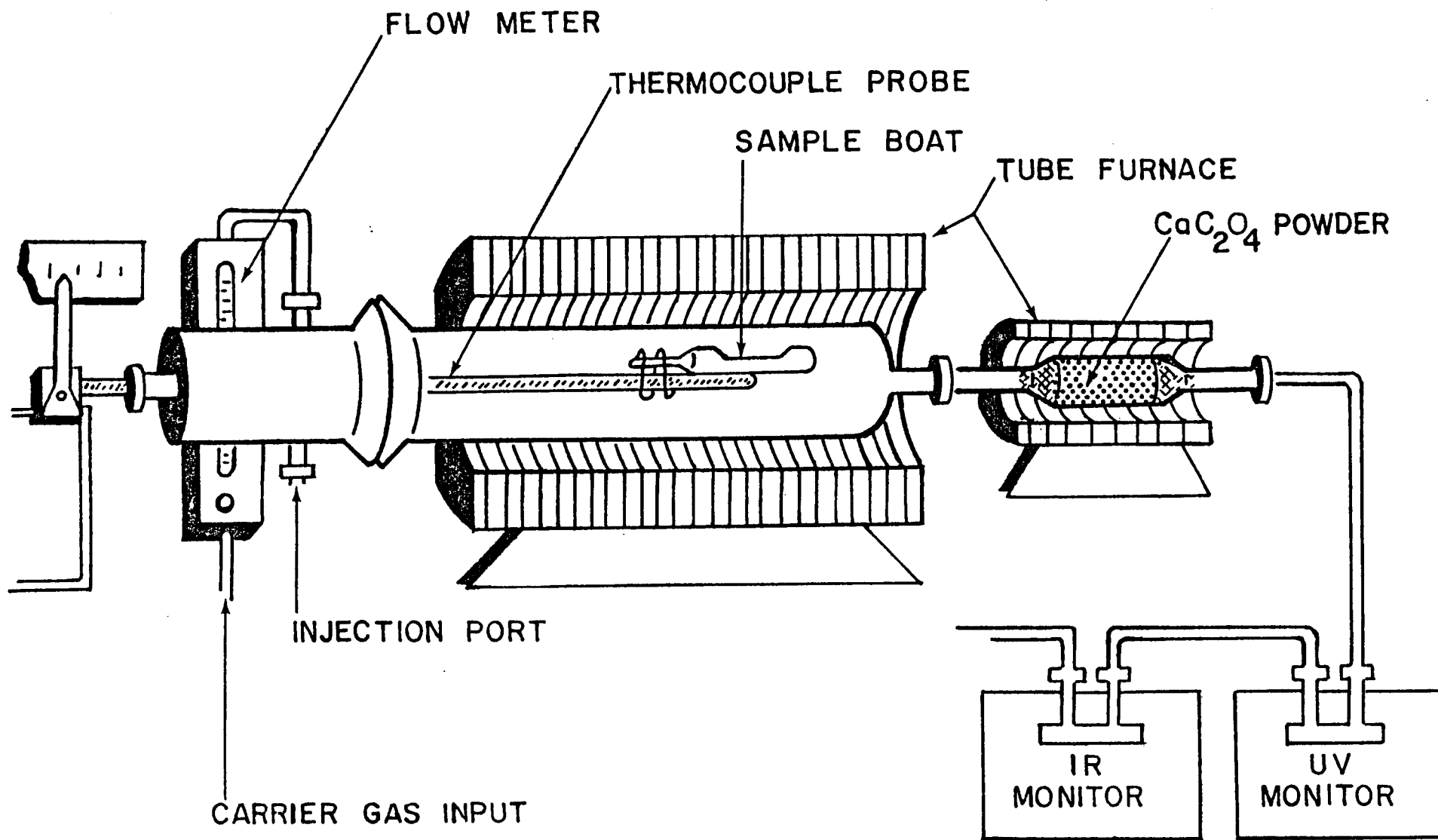
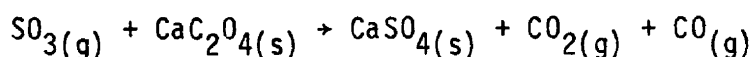


FIGURE I-1. Apparatus used to measure rate of $\text{SO}_2(\text{g})$ and $\text{SO}_3(\text{g})$ production from thermal decomposition of ZnSO_4 and ZnSO_4 mixtures.

Carrier gas flow rate was adjusted with a flow controller placed upstream from the manifold.

The CaC_2O_4 served to convert any $\text{SO}_3(\text{g})$ present in the carrier gas to $\text{CO}_2(\text{g})$ presumably by the reaction:



$\text{SO}_2(\text{g})$ was measured at the first optical cell which was part of a nondispersive ultraviolet monitor set to measure SO_2 absorption. CO_2 was measured at the second optical cell which was part of a nondispersive infrared monitor set to measure CO_2 absorption. UV and IR absorbances were recorded continuously on a dual pen integrating recorder. The response of each monitor was calibrated by injecting samples of $\text{SO}_2(\text{g})$ and $\text{CO}_2(\text{g})$ into the carrier gas with a syringe. The area under each respective absorbance curve was directly proportional to the amount of gas injected.

Although the reaction of $\text{SO}_3(\text{g})$ with $\text{CaC}_2\text{O}_4(\text{s})$ has not been investigated in detail, there is no doubt that SO_3 reacts quantitatively to give CO_2 under the conditions used in these experiments (Flow rate = 150-300 cc/min, CaC_2O_4 temperature = 325°C). This conclusion is based on the fact that it was possible to consistently obtain mole yields of $\text{CO}_2(\text{g})$ and $\text{SO}_2(\text{g})$ from the decomposition of a measured amount of ZnSO_4 that were equal in sum to the theoretical mole yield expected for complete conversion of the available sulfur to a mixture of $\text{SO}_2(\text{g})$ and $\text{SO}_3(\text{g})$. Direct injection of samples of $\text{SO}_2(\text{g})$ into the carrier stream verified that, at the flow rates used, SO_2 does not react with CaC_2O_4 at temperatures less than 375°C. At higher temperatures reaction becomes significant. When the CaC_2O_4 temperature was less than 300°C, the measured mole yields of CO_2 and SO_2 were less in sum than the theoretical yield and the deficiency was obviously due to a low CO_2 yield indicating incomplete reaction of SO_3 with CaC_2O_4 .

In view of these facts all experimental results were obtained with the CaC_2O_4 between 325-350°C and the IR absorption observed taken as indirect measure of the SO_3 present in the carrier.

In a typical experiment a weighed sample of ZnSO_4 was loaded into the sample boat and the manifold connected to the reactor tube. Carrier gas flow rate was adjusted and the furnace equilibrated at the desired set point temperature with the sample boat inside the manifold. A series of $\text{SO}_2(\text{g})$ and $\text{CO}_2(\text{g})$ samples were injected through the septum port to calibrate the optical detectors. The sample boat was then moved to a point just inside the furnace and allowed to equilibrate at a temperature between 350° and 450°C. This preheating was done to bring the sample temperature closer to the set point temperature and thus minimize the time required for the sample to reach its final temperature. Then the sample boat was moved to the center of the furnace and its decomposition monitored.

APPENDIX J

COPIES OF JOURNAL PUBLICATIONS RESULTING FROM THIS PROJECT

1. Study Of The Reaction Of NH_4HSO_4 With ZnO As A Part Of An Energy Storage Cycle, Rev. Int. Hautes Temper. Refract. (accepted).
2. Kinetics Of The Thermal Decomposition Of Zinc Sulfate, Rev. Int. Hautes Temper. Refract. (accepted).
3. Method For The Simultaneous Determination Of $\text{SO}_2(\text{g})$ and $\text{SO}_3(\text{g})$ In A Flowing Carrier Gas, Anal. Chem. (in Preparation).
4. The Thermal Decomposition of Zinc Sulfate, J. Phys. Chem. (in preparation).

	1. SERI Report No. SERI/TP-253-4279	2. NTIS Accession No. DE91002144	3. Recipient's Accession No.
4. Title and Subtitle Thermochemical Cycles for Energy Storage: Thermal Decomposition of ZnSO ₄ Systems: Final Topical Report, Jan. 1, 1992 - Dec. 1, 1984	5. Publication Date April 1992		6.
	7. Author(s) W.E. Wentworth		8. Performing Organization Rept. No.
9. Performing Organization Name and Address University of Houston 4800 Calhoun Houston, Texas 77004	10. Project/Task/Work Unit No.		11. Contract (C) or Grant (G) No. (C) DE-AC03-815F11557 (G)
	12. Sponsoring Organization Name and Address Solar Energy Research Institute 1617 Cole Boulevard Golden, Colorado 80401-3393		13. Type of Report & Period Covered Technical Report
15. Supplementary Notes SERI Technical Monitor: R. Gerald Nix, (303)231-1757			14.
16. Abstract (Limit: 200 words) Development of thermochemical cycles used for energy storage is the objective of this research. Each reaction of a ammonium hydrogen sulfate (NH ₄ SO ₄) cycle was examined. It was shown that when NH ₄ HSO ₄ is mixed with ZnO and decomposed, the resulting products can be released stepwise and separated by controlling the reaction temperature. Thermodynamic, kinetic, and other reaction parameters were measured for the steps of the reaction. A detailed investigation of one reaction--thermal decomposition of zinc sulfate (ZnSO ₄)--was completed. It proceeded rapidly at temperatures greater than 850 degrees C. This reaction can be accelerated and the temperature required reduced by adding an excess of ZnO, V ₂ O ₅ , and possibly other metal oxides. It was shown that zinc sulfate can be decomposed from a liquid mixture of ZnSO ₄ and LiSO ₄ , and that this decomposition can be catalyzed by V ₂ O ₅ , aluminum silicate, and possibly other metal oxides.			
17. Document Analysis a. Descriptors Thermochemical cycles; energy storage; thermal decomposition; zinc sulfate; ammonium hydrogen sulfate b. Identifiers/Open-Ended Terms c. UC Categories 202			
18. Availability Statement National Technical Information Service U.S. Department of Commerce 5285 Port Royal Road Springfield, VA 22161		19. No. of Pages 123	
		20. Price AO6	